THE DYNAMIC RESPONSE OF BILINEAR HYSTERETIC SYSTEMS

Thesis by

Wilfred Dean Iwan

In Partial Fulfillment of the Requirements

for the Degree of

Doctor of Philosophy

California Institute of Technology

Pasadena, California

1961

ACKNOWLEDGEMENTS

The author wishes to express his sincere appreciation to Professor T. K. Caughey for his guidance and many helpful suggestions in the preparation of this work and to Professor D. E. Hudson for his constant interest and encouragement.

The author is further indebted to the Shell Oil Company, the Bendix Aviation Corporation, and the Francis J. Cole Trust for fellowships granted during the course of this investigation.

ABSTRACT

A study is made of the dynamic response of one and two degree of freedom systems having a bilinear hysteretic restoring force. In the case of the one degree of freedom system exact steady state solutions are obtained for both square wave and trigonometric excitation. It is thereby shown that the system exhibits a soft type resonance and that there exists a critical level of excitation above which the system displays unbounded resonance. An approximate steady state theory for the one degree of freedom system is investigated and on the basis of this theory it is found that the system is stable and possesses a single locus of vertical tangency. The results of the exact and approximate steady state theories are supplemented by electric analog studies of both the harmonic and ultraharmonic response.

The response of the one degree of freedom system to transient excitation of finite duration is also examined and it is noted that certain rather general conclusions may be made about the final state of the system without reference to the specific time history of the excitation.

A first order approximate theory for the steady state response of the two degree of freedom system is formulated and it is shown that there are two critical levels of excitation for unbounded resonance. The existence of loci of vertical tangency is demonstrated and the stability problem is treated in limiting cases. Direct numerical integration of the equations of motion is carried out for a number of specific cases as a check of the approximate theory.

TABLE OF CONTENTS

I. INTRODUCTION

The present investigation deals with the dynamic behavior of systems having a hysteretic restoring force (or moment) which may be represented as a piece-wise linear function of the type shown schematically in Fig. 1. Because of the twofold slope character of this function, a system which possesses a restoring force of this type is referred to as a bilinear hysteretic system. It will be noted that for the limiting case in which the slope of the extreme upper and lower portions of the restoring force approaches zero, the system reduces to the well known elasto-plastic system.

Examples of physical systems which exhibit some form of hysteresis are numerous and in many cases the hysteretic behavior may be adequately described by the general bilinear characteristic. This is particularly true of systems which possess Coulomb damping and systems which contain one or more elasto-plastic elements. Systems of the first type include most built-up structures of riveted, bolted, or clamped construction in which the combined effect of friction and elastic forces may easily result in a bilinear hysteretic restoring force. On the other hand, systems of the second type occur whenever use is made of structural materials for which the elasto-plastic engineering approximation to "yielding" is satisfactory; i.e. some steels, masonry in shear, etc. Therefore, the results of any study of bilinear hysteresis will be applicable to a rather wide range of engineering problems.

Within the past few years there has been considerable interest in the dynamic response of both the general bilinear hysteresic system and the limiting elasto-plastic system. Among the earliest treatments of the subject is that due

to L. S. Jacobsen[1, 2, 3] who investigated the transient response of the general system by means of graphical techniques and also did work in developing a mechanical analog capable of representing hysteretic behavior. More recently, L. E. Goodman and J. H. Klumpp[4, 5] have done both analytic and experimental work on the dynamic properties of a laminated beam with a slip interface which is an example of a system having the general bilinear hysteretic character. The response of the limiting elasto-plastic system was considered graphically for transient pulses and square wave excitation by R. Tanabashi[6] and later, the same author[7] studied the transient response of the general system using graphical techniques and an electric analog. A similar investigation was also made by W. T. Thompson[8] who employed electric analog methods to solve for the response of the general system to a unidirectional force excitation. J. E. Ruzicka[9] has used both an approximate analytic theory and electric analog techniques to study the dynamic properties of a vibration absorber which has the general bilinear hysteresis characteristic, and the transient response of structures which contain one or more elasto-plastic elements has been considered by G. V. Berg[10] and by T. Kobori and R. Minai[11].

The stability of the steady state motion of the general system has only recently been demonstrated analytically by N. Ando[12]. Also, this same author has formulated an exact analytic solution for the steady state response of the limiting elasto-plastic system and has made extensive analytic studies of the transient response of both the one and two degree of freedom systems of the general type.

The behavior of the general bilinear hysteretic system has been studied quite thoroughly using approximate analytic techniques in a series of three papers

by T. K. Caughey[13, 14, 15]. In these papers the author successfully investigates the response of the one degree of freedom system to both trigonometric and random excitation and further treats the problem of the forced oscillation of a semi-infinite rod exhibiting weak bilinear hysteresis. For the case of the one degree of freedom system which is subjected to trigonometric excitation, electric analog studies were also made.

The objective of the present investigation is to both complement and extend the efforts of earlier workers. To this end, the response of the one and two degree of freedom bilinear hysteretic systems will be studied using graphical constructions, exact and approximate analytic techniques, and electric analog methods. It is hoped that this work will result in a more complete understanding of the dynamic behavior of such systems and that it will at the same time stimulate further study of the subject.

II. ONE DEGREE OF FREEDOM SYSTEM

A. General Considerations

Before beginning a detailed investigation into the behavior of the bilinear hysteretic system, it is important to formulate the problem as clearly as possible. For this reason, the next three subsections will be devoted to development of a simple and concise representation of the system equation of motion along with a discussion of the general nature of the steady state problem.

Explicit Statement of the Differential Equation of Motion

As a result of the assumed piece-wise linear character of the restoring force, the differential equation of motion may be expressed in terms of a set of linear differential equations each having a certain restricted region of validity. Let the parameters of the hysteresis loop be defined as shown in Fig. 1 with equivalent spring constants k_1 and $k_2 (k_2 < k_1)$, and a nominal "yield" force F_n. Then, in the regions of restoring force constant k_1, the differential equation of motion becomes,

$$m \frac{d^2y}{d\tau^2} + k_1 y + \left(\operatorname{sgn} \frac{dy}{d\tau}\right) (k_1 |y_m| - F_n)(k_1 - k_2)/k_1 = P(\tau) \qquad (2.1a)$$

and in the regions of restoring force constant k_2, the corresponding equation will be

$$m \frac{d^2y}{d\tau^2} + k_2 y + \left(\operatorname{sgn} \frac{dy}{d\tau}\right) F_n(k_1 - k_2)/k_1 = P(\tau) \qquad (2.1b)$$

where $P(\tau)$ is an exciting force which is applied to the mass.

The hysteresis loop of Fig. 1 has been drawn symmetrically with respect to the coordinate axes as would be the case for certain classes of steady state oscillation with k_2 finite. It may, however, be desired to investigate cases in which this symmetry does not exist as, for example, in the solution of transient motion. In such cases, equations (2.1a) and (2.1b) may still be employed provided only that the most recent maxima of the displacement is used for y_m. More will be said regarding this in a later section.

Introduction of Dimensionless Variables

The two equations (2.1a) and (2.1b) are sufficient for analyzing any motion of the generalized bilinear hysteretic system but their use is complicated by the necessity of separately specifying each individual system parameter for every solution. Thus, one seeks to express these equations in terms of certain dimensionless variables which contain only ratios of the various system parameters. This not only leads to considerable simplification in the statement of the equations themselves, but also enables investigation of an entire family of systems by means of a single quantitative solution.

Define a pair of dimensionless displacement and time variables by means of the relations,

$$x = \frac{k_1}{F_n} y$$
$$t = \sqrt{k_1/m}\, \tau. \tag{2.2}$$

Then, these new variables may be introduced into equations (2.1a) and (2.1b) to

obtain the dimensionless equations of motion,

$$\ddot{x} + x + (\operatorname{sgn} \dot{x})(|x_m| - 1)(1-\alpha) = p(t); \quad (|x_m| - 2) < -(\operatorname{sgn} \dot{x})\, x < |x_m| \qquad (2.3a)$$

$$\ddot{x} + \alpha x + (\operatorname{sgn} \dot{x})(1-\alpha) = p(t) \quad ; \quad -(\operatorname{sgn} \dot{x})\, x < (|x_m| - 2). \qquad (2.3b)$$

In these equations, the dot implies differentiation with respect to t, α is the ratio of k_2 to k_1 $(0 < \alpha < 1)$, x_m is the dimensionless maxima of displacement, and $p(t)$ is the ratio of the actual exciting force $P(\tau)$ to the nominal yield force F_n.

For much of the later work it will be convenient to express the two equations of motion (2.3a) and (2.3b) as a single differential equation

$$\ddot{x} + f(x, \dot{x}) = p(t) \qquad (2.4)$$

where it is apparent that

$$f(x, \dot{x}) = \begin{cases} x + (\operatorname{sgn} \dot{x})(|x_m| - 1)(1-\alpha) & ; \ (|x_m| - 2) < -(\operatorname{sgn} \dot{x})\, x < |x_m| \\ \alpha x + (\operatorname{sgn} \dot{x})(1-\alpha) & ; \ -(\operatorname{sgn} \dot{x})\, x < (|x_m| - 2). \end{cases} \qquad (2.5)$$

Then, $f(x, \dot{x})$ may be thought of as a normalized restoring force having the configuration shown in Fig. 2. Looked at in this way, the initial slope of the restoring force diagram and the force level at which a change in slope first occurs have both been normalized to unity and the slope of the second linear portion has become α. This concept of a normalized hysteresis loop will lead to considerable simplification in the application of both graphical and analytic methods of solution.

Orientation of the Steady State Hysteresis Loop

For the remainder of the present study, any analysis of steady state response will be restricted to cases where the periodic excitation has zero average value and can be expressed as a Fourier series which involves only odd functions of the

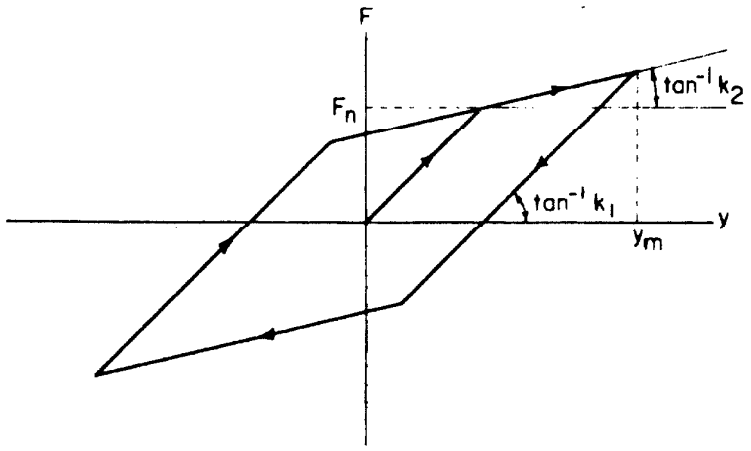

FIGURE 1. GENERAL BILINEAR HYSTERETIC RESTORING FORCE

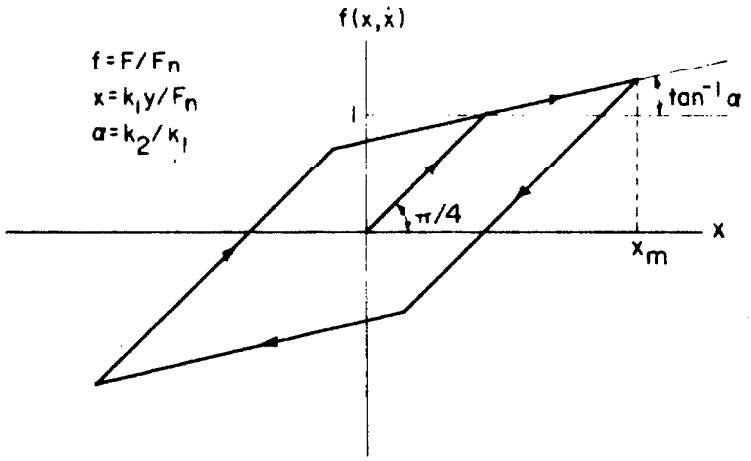

FIGURE 2. NORMALIZED BILINEAR HYSTERETIC RESTORING FORCE

time. Thus, if T is the period of the excitation, p(t) must satisfy the conditions

$$p(t) = -p(t + T/2) = p(t + T)$$
$$\int_t^{t+T} p(t)\,dt = 0. \tag{2.6}$$

Now, if one considers only those cases in which the displacement x is also a periodic function containing only odd order harmonics but having a possible average value different from zero, then this displacement may be written as

$$x = x_0 + \xi \tag{2.7}$$

where x_0 is a constant and

$$\xi(t) = -\xi(t + T/2) = \xi(t + T). \tag{2.8}$$

The inclusion of a constant term in the expression for x implies that the hysteresis loop for such oscillations is displaced from the origin as shown in Fig. 3. Thus, from (2.5) the restoring force may be written as a function of the new variable giving

$$f(x,\dot{x}) = \begin{matrix} \xi + (\operatorname{sgn}\dot{\xi})(|\xi_m| - 1)(1-\alpha) + \alpha x_0 \\ \alpha\xi + (\operatorname{sgn}\dot{\xi})(1-\alpha) + \alpha x_0 \end{matrix}$$
$$= f(\xi,\dot{\xi}) + \alpha x_0 \tag{2.9}$$

where due to the assumed nature of ξ,

$$\int_t^{t+T} f(\xi,\dot{\xi})\,dt = 0. \tag{2.10}$$

But now the differential equation of motion may be expressed as

$$\ddot{\xi} + f(\xi,\dot{\xi}) + \alpha x_0 = p(t), \tag{2.11}$$

where for periodic solutions $\ddot{\xi} = \ddot{x}$ must have a zero average value. Thus, averaging (2.11) term by term over one complete cycle and using relations (2.6)

and (2.10), one is forced to conclude that

$$\alpha x_0 = 0. \tag{2.12}$$

For the general case of finite α this result requires that x_0 be zero or equivalently that the hysteresis loop be symmetrical with respect to the force and displacement axes. However, if α is zero as in the limiting case of elasto-plastic behavior, equation (2.12) is satisfied for any arbitrary offset x_0, and the hysteresis loop need not be centered about the origin.

The above analysis although generally applicable to any excitation satisfying conditions (2.6) has been somewhat severely restricted by conditions (2.7) and (2.8) on the nature of the solution. To be sure, solutions satisfying these conditions do in fact exist and may be shown to be stable but this does not necessarily preclude the possibility of the existence of unsymmetrical solutions containing odd order harmonics. Whether or not such odd harmonic solutions actually exist in a particular instance depends on the detailed character of both the system and the excitation. Thus, formulation of any completely general criterion for the existence of these solutions becomes quite involved. However, for certain special cases of symmetric square wave excitation, it may be shown rather easily that for finite α all steady state oscillations regardless of their specific composition must correspond to a symmetric hysteresis loop configuration. These cases will now be discussed.

Let the hysteresis loop be displaced from the origin by an amount x_0 and consider the special case where the excitation changes sign from positive to negative while the system is in a state represented by some point on the upper linear segment of the restoring force diagram. This case is shown schematically

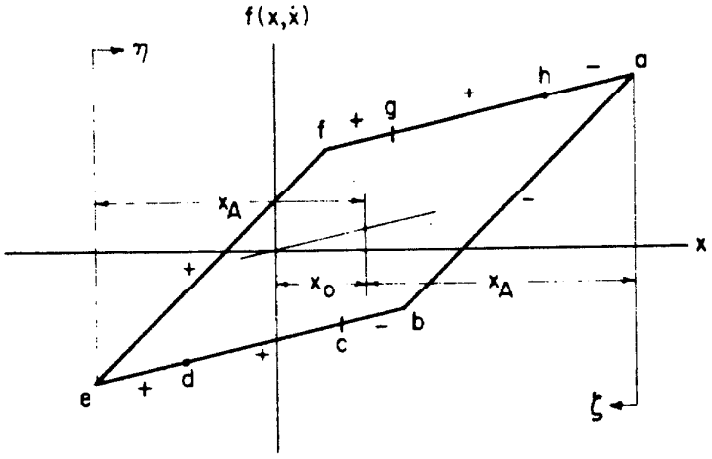

FIGURE 3. TYPICAL UNSYMMETRIC HYSTERESIS LOOP

in Fig. 3 where h and c denote the points at which the excitation changes from positive to negative and negative to positive respectively. The point h may be chosen arbitrarily but the point c will then be fixed by the periodicity requirement on the solution. In general, these two points will not be oriented symmetrically with respect to the hysteresis loop even though the time difference from point to point in each direction is exactly one half of the period of excitation. The reason for this will soon become apparent.

Also specified in Fig. 3 are the points d and g defined such that the distance b-c equals f-g and the distance d-e equals f-a. These points will be referred to later in the discussion.

For square wave excitation, the differential equation of motion (2.4) may be integrated directly over regions where the function p(t) has a constant value $\pm F$. Thus, referring to the figure, the velocity at any point on the linear segment a-b, a distance ζ from the point of maximum displacement, will be given by

$$\frac{1}{2} v_\zeta^2 = -\int_a^\zeta \left[f(x,\dot{x}) - p(t) \right] dx$$

$$= -\int_{x_0 + x_A}^{x_0 + x_A - \zeta} \left[x - (x_0 + x_A - 1)(1-\alpha) \right] dx - \int_{x_0 + x_A}^{x_0 + x_A - \zeta} F \, dx$$

$$= -\frac{(x_0 + x_A - \zeta)^2 - (x_0 + x_A)^2}{2} + \zeta(x_0 + x_A - 1)(1-\alpha) + F\zeta \qquad (2.13)$$

Similarly, the velocity at a point on the segment e-f, a distance η from the point

of minimum displacement, will be given by

$$\frac{1}{2} v_\eta^2 = -\int_{x_0 - x_A}^{x_0 - x_A + \eta} \left[x + (x_A - x_0 - 1)(1 - \alpha) \right] dx + \int_{x_0 - x_A}^{x_0 - x_A + \eta} F \, dx$$

$$= - \frac{(x_0 - x_A + \eta)^2 - (x_0 - x_A)^2}{2} + \eta(x_A - x_0 - 1)(1 - \alpha) + F\eta. \tag{2.14}$$

Therefore, for equal distances along the respective segments it is seen that

$$(v_\zeta^2 - v_\eta^2) \Big|_{\zeta = \eta} = 2\zeta x_0 \alpha, \tag{2.15}$$

or, stated more simply, if α is finite,

$$|v_\zeta| > |v_\eta| \tag{2.16}$$

for all $\zeta = \eta$ on the segments a-b and e-f.

If the equations of motion are further integrated along the segments b-e and f-a, it can likewise be shown that for finite α the velocity at every point on the lower segment is greater than the corresponding velocity on the upper segment so long as the excitation retains the same polarity. However, for periodic oscillations, the system must come to rest in the same absolute distance on both the upper and lower segments. Thus, since the energy absorbed internally is less and the velocity is greater on the lower segment, it is necessary that more energy be withdrawn externally on this segment than on the upper one. This may be accomplished only if the external force changes polarity from positive to negative at a point c on the lower segment such that the distance b-c is less than the distance f-h. (See Fig. 3)

Finally, if the equations of motion are integrated along the two segments h-a and d-e, it may readily be shown that for finite α the velocity at each point

on the former segment is greater than the velocity at the corresponding point on the latter segment.

Thus, in summary, it will be seen that the velocity at every point in the composite range h-c must be greater than that at each corresponding point in the composite range d-g. But for both ranges the absolute distance spanned is the same. Therefore, if $t_{h,c}$ denotes the time required for the system to move from the state represented by point h to that represented by point c and $t_{d,g}$ denotes a similar time related to points d and g, the above analysis implies that for periodic solutions with finite α and x_0

$$t_{h,c} < t_{d,g} . \tag{2.17}$$

Furthermore, since

$$t_{c,h} > t_{d,g} ,$$

it is apparent from (2.17) that

$$t_{h,c} < t_{c,h} . \tag{2.18}$$

Now the times $t_{h,c}$ and $t_{c,h}$ are determined solely by the external forcing function and if, as stated earlier, the discussion is restricted to excitations satisfying (2.6), these two times must be equal. Thus, (2.18) is a contradictory result and the assumptions upon which it is based must be either inconsistent or invalid. Since periodic solutions may be shown to exist throughout the entire range of consideration, this means that the assumption of a finite offset x_0 must in fact represent a physically unrealizable condition when α is greater than zero. Therefore, within the limits of the above analysis it may be concluded that all steady state hysteresis loops will be symmetric if α is finite. On the other hand,

if α equals zero, the arguments leading to (2.18) automatically become invalid as seen from the velocity difference expression (2.15). Indeed, in this limiting case it can be demonstrated that $t_{c,h}$ equals $t_{h,c}$ for all periodic solutions regardless of any finite offset x_0.

A second special case which can be treated by the same type of analysis is that in which the excitation changes from positive to negative at some point on the segment e-f and from negative to positive on the segment a-b of Fig. 3. Assuming both an initial offset x_0 and a finite α for this case, one is again led to an expression of the form of (2.18) and again it is concluded that for periodic solutions either x_0 or α must vanish. Thus, by means of a relatively simple analysis of two special cases it has been possible to demonstrate the symmetry of steady state hysteresis loops over the range of phase angles from 90° to almost 180°.

If one attempts to apply the above analysis to cases in which the phase angle is between 0° and 90° or very close to 180°, it will be found that a straight forward expression like (2.18) can no longer be obtained. Instead, it becomes necessary to make a more detailed study which depends, among other things, on the actual value of the amplitude of the excitation. In particular, for phase angles only slightly less than 90° it will be seen that the arguments on velocity difference seemingly breakdown most violently for large values of excitation. This, however, is also just the condition for which one would expect ultraharmonic response to be a factor. Thus, the analysis can become quite involved.

Throughout the remainder of the present work, the problem of unsymmetric hysteresis loops will be avoided by considering only those solutions which satisfy conditions (2.7) and (2.8). Under this restriction, it has then been shown

that all steady state solutions will correspond to symmetric hysteresis configurations so long as α is finite.

B. Steady State Phase Plane Solution

Graphical techniques are often employed as a starting point in the study of non-linear systems where the complexity of numerical or other techniques tends to obscure the general character of the solution. Used in this way, a graphical solution may many times point the way toward considerable simplification in the subsequent application of both exact and approximate analytic techniques. It is therefore quite reasonable that investigation of the bilinear hysteretic system should begin with a consideration of graphical solutions.

Description of the Method

In general, graphical methods are applied only when the system differential equation is autonomous. This, however, is usually the case only as a matter of convenience and not because of any inherent mathematical limitations. Thus, it is not surprising that L. S. Jacobsen[1, 2] has drawn together the ideas of numerous earlier workers in order to formulate a general graphical approach which is applicable to both autonomous and non-autonomous systems. Although this so called Phase-Plane Delta Method is of greatest value in obtaining the transient response of non-autonomous systems, it may with some additional effort be applied to the solution of the steady state response of systems subjected to periodic excitation. It is this latter application which will be considered below.

The dimensionless differential equations describing the behavior of the bilinear hysteretic system are equations (2.3a) and (2.3b) of the previous section. For purposes of clarity these equations are restated as follows:

$$\ddot{x} + x + (\operatorname{sgn} \dot{x})(|x_m| - 1)(1 - \alpha) = p(t) \; ; \; (|x_m| - 2) < -(\operatorname{sgn} \dot{x})\, x < |x_m| \qquad (2.19a)$$

$$\ddot{x} + \alpha x + (\operatorname{sgn} \dot{x})(1 - \alpha) = p(t) \; ; \; -(\operatorname{sgn} \dot{x})\, x < (|x_m| - 2). \qquad (2.19b)$$

Here, as before, the slope of the initial linear portion of the restoring force diagram has been normalized to unity, the slope of the second linear portion is α, and x_m is the maximum displacement.

For the present analysis, it is desirable to write equations (2.19a) and (2.19b) in the equivalent form,

$$\ddot{x} + x + (\operatorname{sgn} \dot{x})(|x_m| - 1)(1-\alpha) = p(t) \tag{2.20a}$$

$$\ddot{x} + \alpha x - (\operatorname{sgn} \dot{x})(|x| - 1)(1-\alpha) = p(t). \tag{2.20b}$$

Then, if the second time derivative of the displacement with respect to time is expressed as the product of the velocity and the first derivative of the velocity with respect to displacement, both of these equations may be written as

$$\frac{dv}{dx} = -\frac{x + \delta_{1,2}}{v} \tag{2.21}$$

where v is the velocity and

$$\delta_{1,2} = \begin{cases} +(\operatorname{sgn} \dot{x})(|x_m| - 1)(1-\alpha) - p(t), & \text{in the restoring force regime of slope 1} \\ -(\operatorname{sgn} \dot{x})(|x| - 1)(1-\alpha) - p(t), & \text{in the restoring force regime of slope } \alpha. \end{cases}$$

Equation (2.21) is now in a form which has a straight forward graphical and geometrical interpretation. Let $P(x_1, v_1, t_1)$ be that point in phase space which represents the state of the system at time t_1. Then, from (2.21) the phase plane contour passing through P will have a slope

$$\left.\frac{dv}{dx}\right|_P = -\frac{x_1 + \delta_{1,2}(x_1, t_1)}{v_1}.$$

Viewed geometrically, this is just the slope of a perpendicular to the line segment connecting P with the point $v = 0$, $x = -\delta(x_1, t_1)$; [See Fig. 4]. Therefore, the state of the system at some time only slightly greater than t_1 may be obtained

graphically by moving an incremental distance away from P in the direction of this perpendicular to a new point P $(x_1 + \Delta x_1,\ v_1 + \Delta v_1,\ t_1 + \Delta t_1)$. At this point a new slope may be constructed enabling advance to a new system point, and so on. By taking successive incremental steps in this manner the entire phase plane contour may be plotted.

It should be noted that the method of construction described above is quite similar to the well known Liénard construction. In the present case however, δ is a function of the displacement and time rather than of the velocity. This means that δ can not be obtained by a simple graphical procedure like that used in the Liénard method, but instead must be evaluated explicitly for each successive step along the phase contour. Thus, it now becomes necessary to know both the displacement and time corresponding to each new point of the construction. The displacement may be found directly from the coordinates of the system point but a slightly less direct procedure is required in order to evaluate the time.

Evaluation of the Time-Variable

Consider an infinitesimal variation along the phase contour as shown in Fig. 4. Then, if ρ is the length of the line segment connecting the system point P with the point $v = 0$, $x = -\delta$ and ds is the magnitude of the variation along the phase plane contour, the infinitesimal angle $d\theta$ through which ρ moves is given by

$$d\theta = ds/\rho \,. \tag{2.22}$$

Introducing the geometrical relations

$$ds = \sqrt{(dx)^2 + (dv)^2}$$

$$\rho = \sqrt{v^2 + (x + \delta)^2} \,,$$

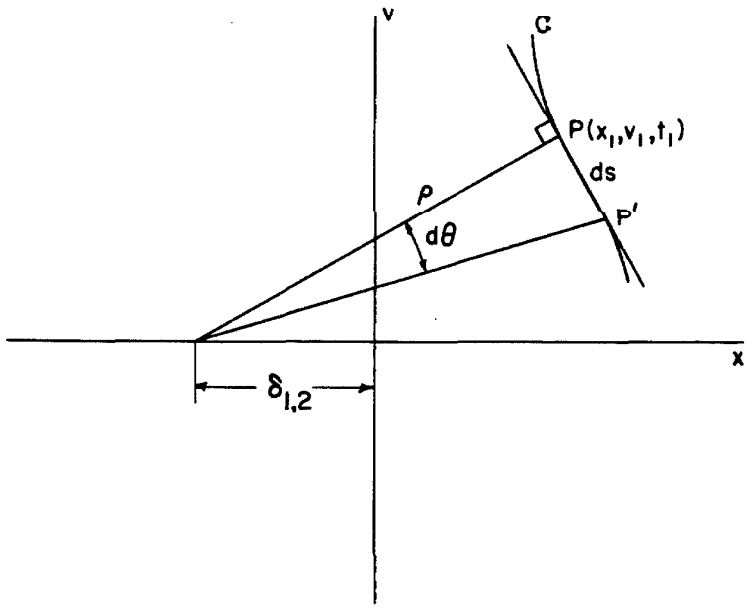

FIGURE 4. METHOD OF PHASE-PLANE CONSTRUCTION

expression (2.22) becomes;

$$d\theta = \frac{dx}{v} \cdot \sqrt{\frac{1 + (dv/dx)^2}{1 + (x + \delta)^2/v^2}} \quad . \tag{2.23}$$

But from (2.21) the two radicals appearing in (2.23) are identical. Thus

$$d\theta = \frac{dx}{v} = dt,$$

or, in incremental form

$$\Delta t = \Delta\theta. \tag{2.24}$$

Using equation (2.24), one may now calculate the incremental time difference corresponding to each successive step along the phase contour and thereby keep a cumulative tally of the total time t which may then be used in the evaluation of δ.

Application to Solution of Steady State Motion

When a damped system such as the bilinear hysteresis system is driven by a periodic force excitation, there exists in general one or more periodic solutions each of which is characterized by a closed contour in phase space. In the case of a stable steady state solution, this contour actually represents a limiting curve which will be approached arbitrarily closely by all contours having their origin within some definite region of convergence for the particular solution. An unstable solution, on the other hand, will have no such region of convergence and its corresponding closed contour may be obtained only by exact prescription of initial conditions and precise determination of the succeeding motion.

In practice, graphical techniques will usually be employed in the construction of the phase contour and the approximations introduced by this mechanism will make it impossible to obtain unstable steady state solutions. Therefore, if a graphically constructed phase contour approaches some limiting configuration for

large time, it may reasonably be assumed that this limiting contour represents one of the stable steady state solutions which exist for the system in question.

Results and Conclusions

Because of the nature of the method for determining t, the simplest form of periodic excitation which may be handled by the above technique is square wave excitation. In this case, p(t) will be constant except at discrete multiples of the half period of excitation and explicit evaluation of this function need not be made at every step along the phase contour.

The result of a typical graphical construction of the phase contour for a bilinear hysteretic system excited from rest by a square wave forcing function is shown in Fig. 5. At least three significant observations may be made from this phase plane diagram and these are discussed below.

First, it should be noted that a limiting phase contour most certainly exists in this case thereby implying the existence of at least one stable steady state solution for the particular frequency and magnitude of excitation considered here. Whether this steady state solution is the only one which exists cannot however be inferred from the figure and would have to be investigated by other means.

Secondly, convergence on the steady state solution is seen to be quite regular and also rather rapid. This same characteristic was observed in other constructions not shown here and is used later in the development of a method of exact solution for the steady state motion.

Finally it will be noted that except for a slight bulging along the displacement axis, the limiting phase contour has a general shape which is very nearly circular. Hence, it would appear that the solution wave forms for the displace-

ment and velocity may be almost harmonic in nature. This fact will be used later in establishing the validity of a set of assumptions which enable development of an approximate method of solution.

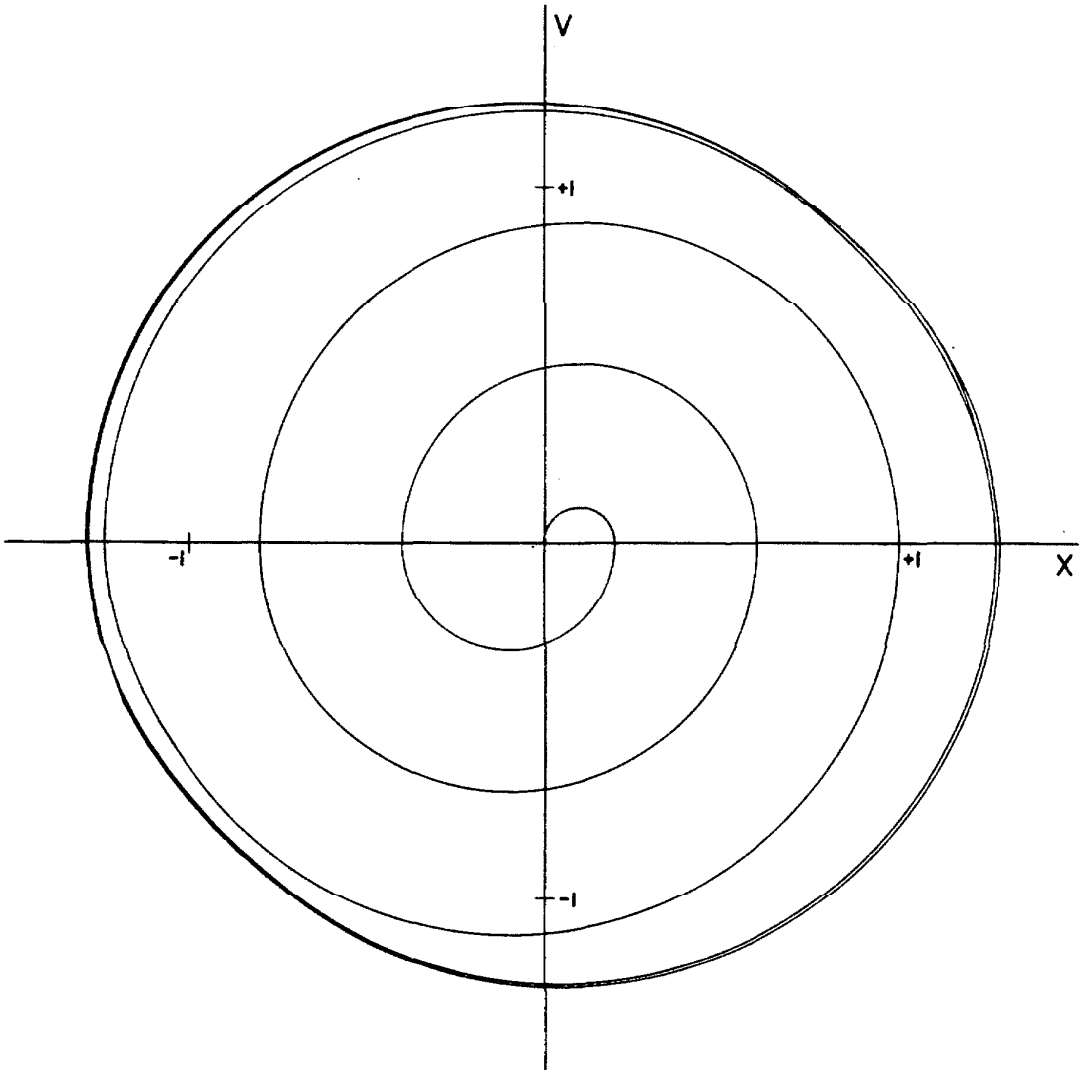

FIGURE 5. STEADY STATE PHASE-PLANE CONSTRUCTION
SQUARE WAVE EXCITATION — α=0.50, r=0.10

C. Exact Steady State Solution —— Square Wave Excitation

The form of excitation which is most easily analyzed mathematically is the square wave excitation employed in the previous section. Use of such a piece-wise constant forcing function leads to substantial simplification in the analytic form of the solution and thereby permits more detailed study of certain phenomena arising strictly from the non-linear or quasi-linear nature of the system. Furthermore, it will be seen later that the essential features of the steady state response are the same for both square wave and trigonometric excitation. Thus, the results of the square wave analysis may be used as guide posts in the treatment of the more complicated trigonometric case.

Equations Governing the Steady State Motion

For the purpose of formulating the equations governing the steady state motion, it will be necessary to divide the analysis into two separate parts; one pertaining to solutions in which the excitation changes sign while the system is at a point on a restoring force segment of slope α, and the other pertaining to solutions in which the excitation changes sign while the system is at a point on one of the segments of unity slope.

Case 1)- Excitation sign change on a segment of slope α.

Fig. 6 is a schematic representation of the hysteresis loop and displacement wave form for the case in which the external forcing function changes sign on one of the restoring force segments having a slope α. In the particular example shown, the sign change has been taken as positive to negative on the upper segment thereby corresponding to phase angles somewhat greater than 90^{o}. This,

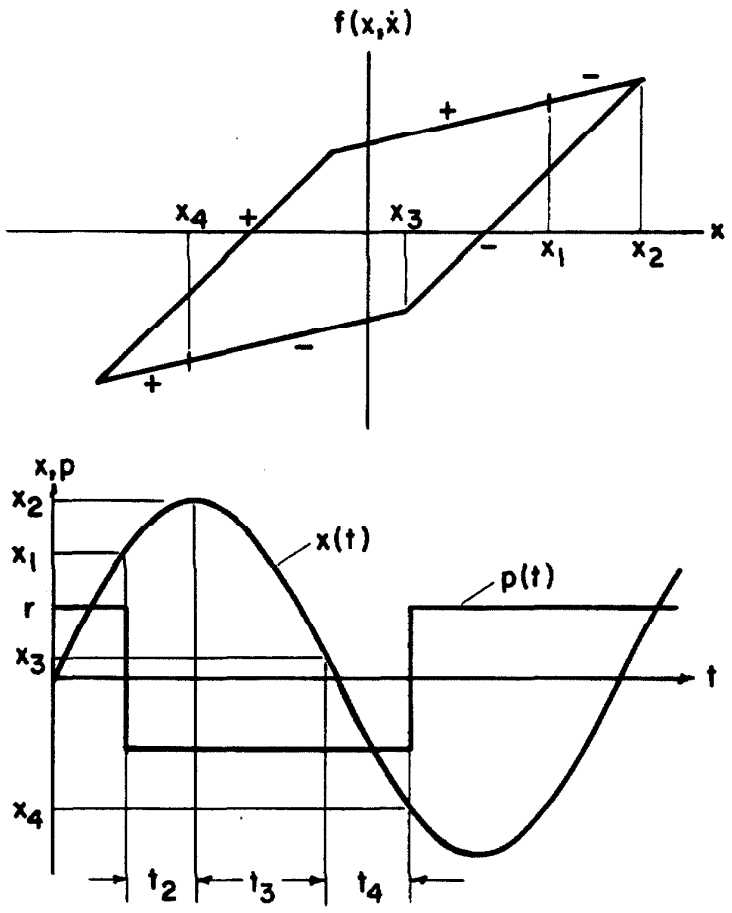

FIGURE 6. HYSTERESIS DIAGRAM AND DISPLACEMENT WAVE FORM - CASE 1)

however, does not restrict the generality of the following arguments since p(t) may be replaced by -p(t) at any stage in the analysis without changing the mathematics of the problem.

If the amplitude of excitation is denoted by r, then from (2.3b) the equation of motion along the upper most segment of the hysteresis loop will be

$$\ddot{x} + \alpha x = \pm r - (1-\alpha). \tag{2.25}$$

Taking as initial conditions the displacement x_1 and velocity $\dot{x}_1$ at which the sign of r becomes negative, the general solution of (2.25) may be written as

$$x = -\frac{(r+1-\alpha)}{\alpha}(1-\cos\sqrt{\alpha}\,t) + \frac{\dot{x}_1}{\sqrt{\alpha}}\sin\sqrt{\alpha}\,t + x_1\cos\sqrt{\alpha}\,t. \tag{2.26}$$

Now, after some time t_2, the system displacement will pass through a maximum x_2 and the velocity will become zero. Thus,

$$x_2 = -\frac{(r+1-\alpha)}{\alpha}(1-\cos\sqrt{\alpha}\,t_2) + \frac{\dot{x}_1}{\sqrt{\alpha}}\sin\sqrt{\alpha}\,t_2 + x_1\cos\sqrt{\alpha}\,t_2 \tag{2.27}$$

and

$$\dot{x}_2 = 0 = \dot{x}_1\cos\sqrt{\alpha}\,t_2 - \frac{1}{\sqrt{\alpha}}\left[(r+1-\alpha)+\alpha x_1\right]\sin\sqrt{\alpha}\,t_2. \tag{2.28}$$

But, from (2.28)

$$\tan\sqrt{\alpha}t_2 = \frac{\dot{x}_1\sqrt{\alpha}}{(r+1-\alpha)+\alpha x_1}. \tag{2.29}$$

Therefore, if $\sqrt{\alpha}\,t_2$ is less than π,

$$x_2 = -\frac{(r+1-\alpha)}{\alpha}\,\frac{1}{\alpha}\left[(r+1-\alpha+x_1\alpha)^2 + \dot{x}_1^2\alpha\right]^{1/2}. \tag{2.30}$$

For subsequent motion the velocity will be negative and from (2.3a) the governing equation becomes

$$\ddot{x} + x = -r + (x_2-1)(1-\alpha). \tag{2.31}$$

Specifying x_2 and $\dot{x}_2$ as initial conditions the general solution of this equation is

$$x = \left[(x_2-1)(1-\alpha) - r\right](1-\cos t) + x_2 \cos t. \tag{2.32}$$

Thus, if t_3 is the time required for the system to traverse the entire unity slope segment of the hysteresis loop, the displacement and velocity at the point where the slope again changes to α will be

$$x_3 = \left[(x_2-1)(1-\alpha) - r\right](1-\cos t_3) + x_2 \cos t_3 \tag{2.33}$$

and

$$\dot{x}_3 = -(\alpha x_2 + 1 - \alpha + r) \sin t_3. \tag{2.34}$$

But, due to the normalization of the hysteresis loop,

$$x_3 = x_2 - 2. \tag{2.35}$$

Therefore, from (2.33) it may be shown that

$$\cos t_3 = 1 - \frac{2}{(\alpha x_2 + 1 - \alpha + r)} \quad . \tag{2.36}$$

For r positive, this expression implies that $0 < t_3 < \pi$ for all $x_2 > 1$. However, in the case of r negative it will be seen that there is a possibility of obtaining values for $\cos t_3$ which are less than -1. Under these circumstances, the system velocity actually becomes zero before the displacement x_3 is reached and the hysteresis loop doubles back on itself. This is recognized as corresponding to a type of ultra-harmonic behavior which, in the case of square wave excitation, would be present even in a purely linear system. Thus, if the analysis of the present system is restricted to high enough frequencies (well above $\omega = 1/3$) such behavior should not be a factor. In this case then (2.36) may be used to eliminate t_3 from (2.34) giving

$$\dot{x}_3 = -2\,(\alpha x_2 - \alpha + r)^{1/2}. \tag{2.37}$$

As the system displacement continues to decrease beyond x_3, the equation of motion becomes

$$\ddot{x} + \alpha x = - r + (1- \alpha), \tag{2.38}$$

and taking x_3 and $\dot{x}_3$ as initial conditions, the general solution to this equation may be written as

$$x = \frac{1- \alpha -r}{\alpha} (1-\cos \sqrt{\alpha}\, t) + \frac{\dot{x}_3}{\sqrt{\alpha}} \sin \sqrt{\alpha}\, t + x_3 \cos \sqrt{\alpha}\, t. \tag{2.39}$$

Hence, if x_4 is the system displacement when the excitation next changes sign and t_4 is the time required for the system to move from x_3 to x_4,

$$x_4 = \frac{(1- \alpha -r)}{\alpha} + \left| x_2 - 1 - \frac{1-r}{\alpha} \right| \cos \sqrt{\alpha}\, t_4 - \frac{2(\alpha x_2 - \alpha + r)^{1/2}}{\sqrt{\alpha}} \sin \sqrt{\alpha}\, t_4 \tag{2.40}$$

and

$$\dot{x}_4 = - \sqrt{\alpha} \left| x_2 - 1 - \frac{1-r}{\alpha} \right| \sin \sqrt{\alpha}\, t_4 - 2(\alpha x_2 - \alpha + r)^{1/2} \cos \sqrt{\alpha}\, t_4. \tag{2.41}$$

But from the assumed nature of the excitation,

$$t_4 = \frac{\pi}{\omega} - t_2 - t_3$$

where ω is the frequency of the square wave forcing function. Thus, using equations (2.29) and (2.36),

$$t_4 = \frac{\pi}{\omega} - \frac{1}{\sqrt{\alpha}} \tan^{-1} \left[\frac{\dot{x}_1 \sqrt{\alpha}}{r + 1 - \alpha + x_1 \alpha} \right] - \cos^{-1} \left[1 - \frac{2}{(r + 1 - \alpha + x_1 \alpha)} \right] . \tag{2.42}$$

Since the analysis has been restricted to cases which give rise to symmetric hysteresis configurations, the periodicity conditions on the solution may now be

written as

$$x_4 = - x_1 \tag{2.43}$$

and

$$\dot{x}_4 = - \dot{x}_1. \tag{2.44}$$

Therefore, the problem of obtaining the steady state response has been reduced to one of solving the six equations (2.30), and (2.40) through (2.44) for the six unknowns x_1, $\dot{x}_1$, x_2, t_4, x_4 and $\dot{x}_4$. However, due to the transcendental character of these equations, direct solution is at best very difficult. Thus, it becomes advantageous to adopt the rather special techniques of solution which will be discussed shortly.

Case 2)- Excitation sign change on a segment of unity slope.

Fig. 7 is a schematic representation of the hysteresis loop and displacement wave form for the case in which the external forcing function changes sign on one of the unity slope segments of the restoring force diagram. For the particular case shown in the figure, this change has been taken as positive to negative but this again does not restrict the generality of the mathematical arguments which will follow.

Let the maximum positive displacement of the system be x_1 and denote the displacement when the excitation changes sign by x_2 such that the time difference between x_1 and x_2 is t_2. Then, the equation of motion in this range becomes

$$\ddot{x} + x = r + (x_1 - 1)(1 - \alpha) \tag{2.45}$$

and it is easily shown that

$$x_2 = \left[r + (x_1 - 1)(1 - \alpha) \right] + (1 - r - \alpha + \alpha x_1) \cos t_2 \tag{2.46}$$

and

$$\dot{x}_2 = - (1 - r - \alpha + \alpha x_1) \sin t_2. \tag{2.47}$$

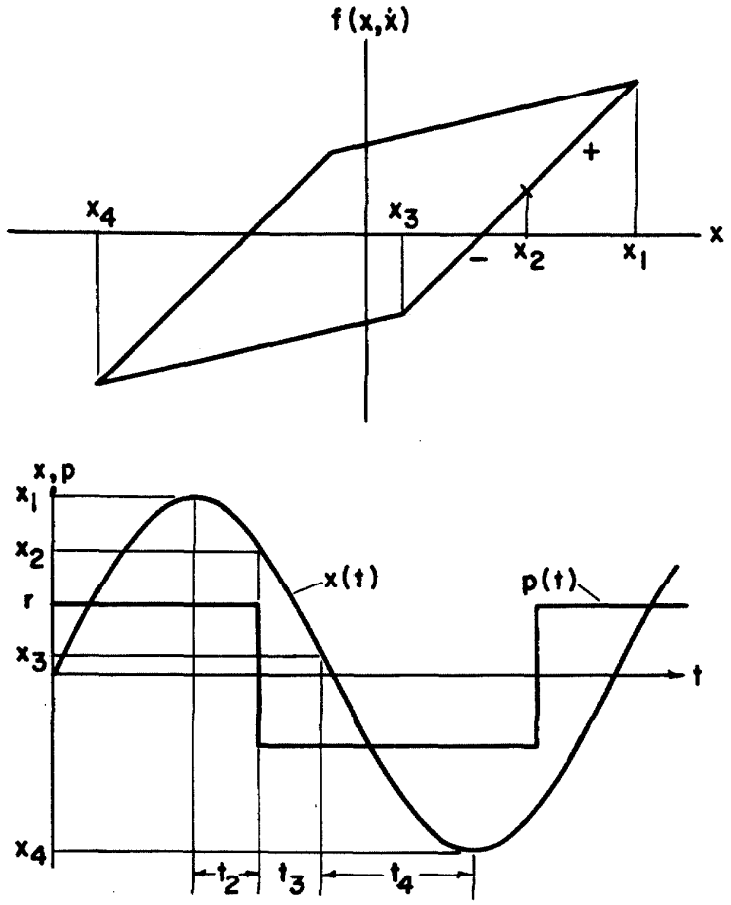

FIGURE 7. HYSTERESIS DIAGRAM AND DISPLACEMENT WAVE FORM - CASE 2)

For displacements less than x_2 the equation of motion will be identical to equation (2.45) except that r will be replaced by -r. Thus, if x_3 is the displacement at which the slope of the restoring force becomes α, and t_3 is the time required for the system to move from x_2 to x_3, it is apparent that

$$x_3 = \left[-r + (x_1-1)(1-\alpha)\right](1-\cos t_3) + x_2 \cos t_3 + \dot{x}_2 \sin t_3 \tag{2.48}$$

and

$$\dot{x}_3 = \left[-r + (x_1-1)(1-\alpha) - x_2\right] \sin t_3 + \dot{x}_2 \cos t_3. \tag{2.49}$$

However, due to the normalization of the hysteresis loop,

$$x_3 = x_1 - 2. \tag{2.50}$$

Therefore, from (2.48) it may be demonstrated that

$$t_3 = \cos^{-1} \frac{\left[x_1-2 + r-(x_1-1)(1-\alpha)\right]}{\left\{\left[x_2 + r-(x_1-1)(1-\alpha)\right]^2 + \dot{x}_2^2\right\}^{1/2}} - \tan^{-1} \frac{\dot{x}_2}{x_2 + r-(x_1-1)(1-\alpha)}, \tag{2.51}$$

where any ambiguity regarding the proper quadrant for t_3 must be resolved by a detailed analysis of (2.48).

As the displacement further decreases past x_3, the equation of motion takes the form

$$\ddot{x} + \alpha x = -r + (1-\alpha). \tag{2.52}$$

Thus, if x_4 is the minimum system displacement and t_4 is the time it takes for the system to come to rest from the displacement x_3,

$$x_4 = \frac{(1-\alpha-r)}{\alpha} + \frac{1}{\alpha}(\alpha x_3 + r + \alpha - 1) \cos \sqrt{\alpha}\, t_4 + \frac{\dot{x}_2}{\sqrt{\alpha}} \sin \sqrt{\alpha}\, t_4 \tag{2.53}$$

and

$$\dot{x}_4 = 0 = -\frac{1}{\sqrt{\alpha}}(\alpha x_3 + r + \alpha - 1) \sin \sqrt{\alpha}\, t_4 + \dot{x}_2 \cos \sqrt{\alpha}\, t_4. \tag{2.54}$$

But then from (2.54)

$$t_4 = \frac{1}{\sqrt{\alpha}} \tan^{-1} \frac{\sqrt{\alpha}\,\dot{x}_3}{(\alpha x_3 + r + \alpha - 1)}, \tag{2.55}$$

where in this case any ambiguity in the quadrant of t_4 requires detailed study of both (2.53) and (2.54).

Assuming that the steady state hysteresis loop is symmetric, the conditions for periodicity of the solution may now be stated as

$$x_1 = - x_4 \tag{2.56}$$

and

$$t_2 = \pi/\omega - t_3 - t_4. \tag{2.57}$$

Thus, the statement of the problem has once again been reduced to a set of highly transcendental simultaneous algebraic equations. In this case there are nine such equations [(2.46), (2.47), (2.48) through (2.51), (2.53), and (2.55) through (2.57)] and nine unknowns [x_1, x_2, $\dot{x}_2$, t_2, x_3, $\dot{x}_3$, t_3, x_4, and t_4]. An indirect approach for the solution of this set of equations will now be considered.

Method of Solution for Steady State Response

The method of solution outlined below is based in large measure on experience gained in the graphical construction of steady state phase plane contours. Indeed, it will be seen that the validity of the iterative approach formulated here is directly contingent upon the convergence of the graphical solutions discussed earlier.

Case 1)- Excitation sign change on a segment of slope α.

The method of solution in this case begins by arbitrary selection of initial

values for the two unknown variables x_1 and $\dot{x}_1$ (possibly guided by previous solutions in the neighborhood of the desired solution). Then, using equations (2.30) and (2.42) values may be calculated for x_2 and t_4 thereby enabling evaluation of x_4 and $\dot{x}_4$ from equations (2.40) and (2.41). Having determined x_4 and $\dot{x}_4$ in this manner, one may then solve for a new x_1 and $\dot{x}_1$ by means of relations (2.43) and (2.44). If these new values denoted by x_1^1 and $\dot{x}_1^1$ are equal to x_1 and $\dot{x}_1$, the steady state solution has been found. If, on the other hand, the two sets of parameters are unequal, the procedure is begun anew using x_1^1 and $\dot{x}_1^1$ in place of x_1 and $\dot{x}_1$. This iterative process is then continued until the new values calculated in any one cycle are identical or nearly identical to the initial values used to begin that cycle.

Convergence of the above procedure is difficult to demonstrate mathematically but may be inferred from the physical nature of the method itself. It will be noted that the present approach is essentially just a formalized mathematical way of constructing the system phase plane contour correspinding to periodic excitation from some arbitrary point in phase space. The only real difference between the method employed here and actual construction of the phase contour is that here only the end points of the contour are evaluated and this without the explicit determination of all intermediate points. Therefore, since the convergence of phase plane solutions has already been demonstrated in connection with the work on graphical techniques, it is entirely reasonable to conclude that the present method will likewise converge upon a stable steady state solution.

Case 2)- Excitation sign change on a segment of unity slope.

The method of solution in this case is very similar to that just described

except that now the analysis is begun by selection of the two unknown variables x_1 and t_2. This enables solution for x_2 and $\dot{x}_2$ from (2.46) and (2.47) which in turn defines x_3, $\dot{x}_3$, and t_3 from (2.49) through (2.51). Then, these values may be used in (2.53) and (2.55) to calculate x_4 and t_4. But, having determined all of the necessary parameters, one may use relations (2.56) and (2.57) to evaluate new estimates for x_1 and t_2. If these new values are equal to the initially selected values the problem is solved, if not the process of solution is begun again using the new values as a starting point. This procedure is continued until the initial and final values of x_1 and t_2 are equal over one complete cycle of calculations. Convergence of this scheme upon a steady state solution may be inferred from its similarity to a phase plane construction just as in the previous case.

Since solutions obtained by the above iterative procedures may theoretically be carried out to any desired degree of accuracy, it is therefore consistent to refer to them as exact steady state solutions. This term will be used throughout the remainder of the present work.

Discussion of Results

Figs. 8 and 9 show the results of typical digital computer solutions using the iterative procedures outlined above. The significant features of these results are discussed in the following paragraphs.

To begin with it will be noted that there is a definite tendency for the response peaks of this system to lean toward lower frequencies as is typical of soft systems (systems in which the effective restoring force constant decreases with amplitude). This results in a rather gentle slope on the high frequency side of the peak and a very steep slope on the low frequency side. Indeed, a careful

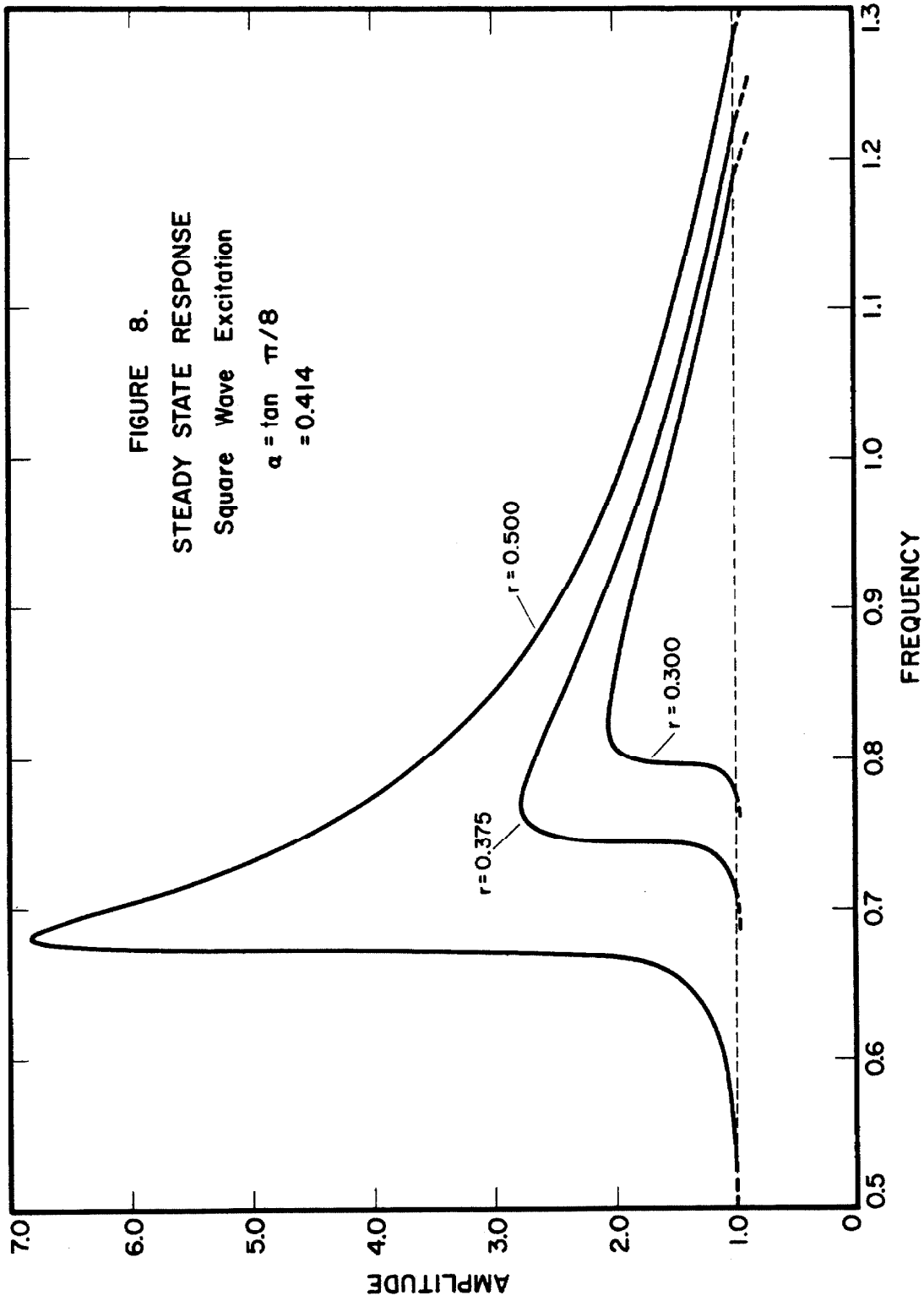
FIGURE 8.
STEADY STATE RESPONSE
Square Wave Excitation
α = tan π/8
=0.414
r = 0.500
r = 0.375
r = 0.300
AMPLITUDE
FREQUENCY
7.0
6.0
5.0
4.0
3.0
2.0
1.0
0
0.5
0.6
0.7
0.8
0.9
1.0
1.1
1.2
1.3

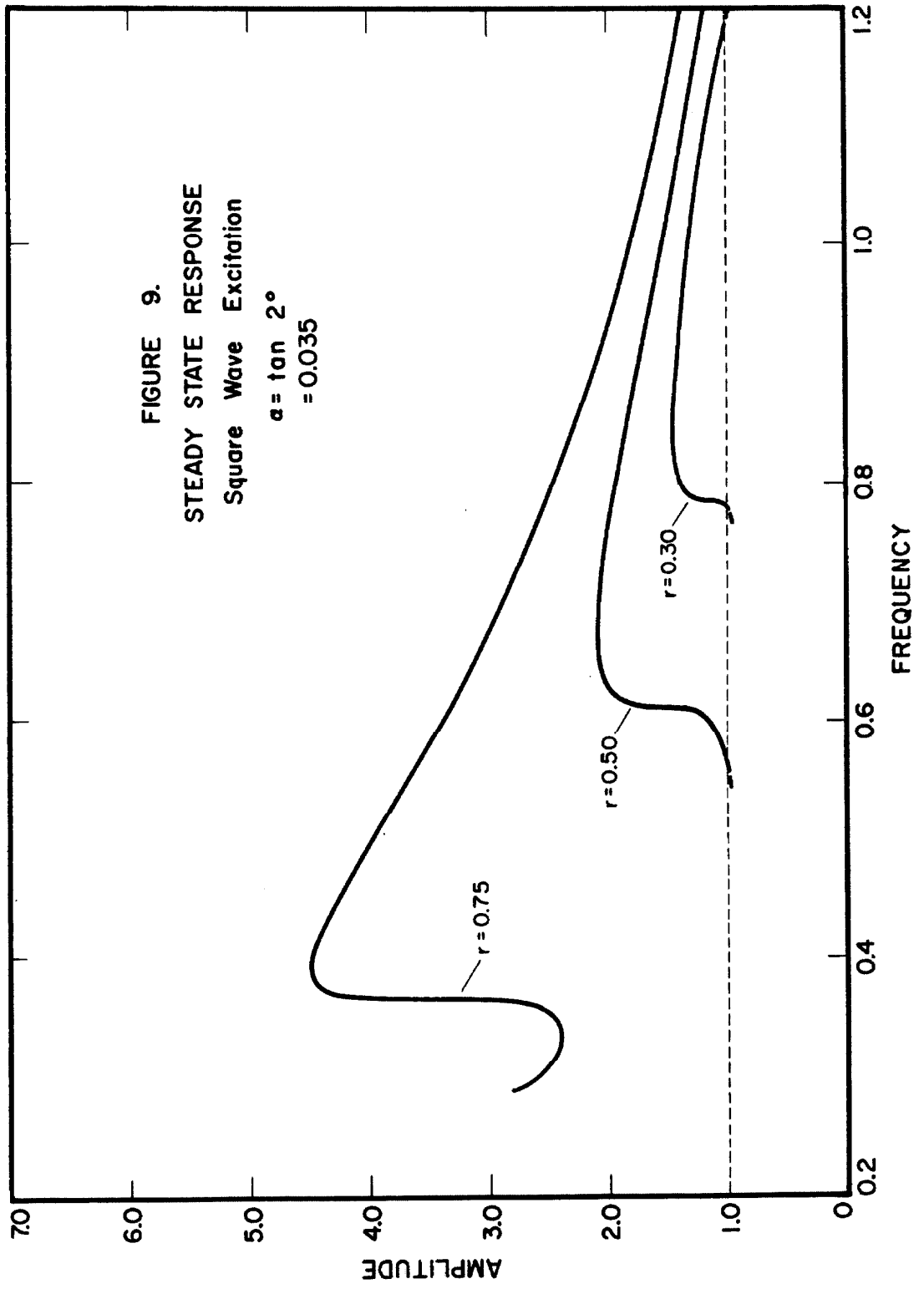
FIGURE 9.
STEADY STATE RESPONSE
Square Wave Excitation
α = tan 2°
= 0.035
r = 0.75
r = 0.50
r = 0.30
AMPLITUDE
FREQUENCY
0
1.0
2.0
3.0
4.0
5.0
6.0
7.0
0.2
0.4
0.6
0.8
1.0
1.2

examination of the plotted curves and the numerical data upon which they are based reveals that the low frequency side of the curve may well be vertical. However, within the accuracy of the numerical computations it is also seen that the slope on this low frequency side never becomes negative (i.e. the response curves all remain single valued). Thus, the so called "jumps" which often characterize soft systems do not appear to exist in the bilinear hysteresis system with square wave excitation.

For the particular case in which $\alpha = \tan 2^{\circ}$ and $r = 0.75$, it is seen that the response curve exhibits a somewhat peculiar second rise for low frequency. This takes place at a frequency of about 0.3 and may be attributed partly to the nature of the system nonlinearity and partly to the presence of a third harmonic term in the excitation. The role of the nonlinearity in producing ultraharmonic behavior will be considered in detail in a future section. Thus, it will be sufficient here to say only that for the specific case in question, the nonlinear effect is probably greatly overshadowed by that due to the nature of the excitation.

Unbounded Resonance Behavior

In order to understand more about the detailed behavior of the system, it is instructive to investigate the case in which the phase difference between the displacement and the excitation is 90°. In terms of the notation of Fig. 6, this condition on the phase angle may be expressed as

$$\dot{x}_1 = \dot{x}_2 = 0 \tag{2.58}$$

and

$$x_1 = x_2 = x_m \tag{2.59}$$

where x_m denotes the maximum system displacement for the case in question.

Using these relations along with the periodicity conditions (2.43) and (2.44), equations (2.40) and (2.41) become

$$-x_m = \frac{(1-\alpha-r)}{\alpha} + \left|x_m - 1 - \frac{1-r}{\alpha}\right| \cos\sqrt{\alpha}\,t_4 - \frac{2(\alpha x_m - \alpha + r)^{1/2}}{\sqrt{\alpha}} \sin\sqrt{\alpha}\,t_4 \tag{2.60}$$

and

$$0 = -\sqrt{\alpha}\left|x_m - 1 - \frac{1-r}{\alpha}\right| \sin\sqrt{\alpha}\,t_4 - 2(\alpha x_m - \alpha + r)^{1/2} \cos\sqrt{\alpha}\,t_4 \tag{2.61}$$

But, from (2.61),

$$\tan\sqrt{\alpha}\,t_4 = -\frac{2\sqrt{\alpha}(\alpha x_m - \alpha + r)^{1/2}}{(\alpha x_m - \alpha + r - 1)} . \tag{2.62}$$

Thus, the terms of (2.60) which contain $\sqrt{\alpha}\,t_4$ can be eliminated giving

$$(\alpha x_m - r - \alpha + 1)^2 = (\alpha x_m + r - \alpha - 1)^2 + 4\alpha(\alpha x_m + r - \alpha). \tag{2.63}$$

Solving this equation for x_m then yields

$$x_m = \frac{(1-\alpha)}{(1-\alpha) - r} . \tag{2.64}$$

From equation (2.64) it will be seen that the response amplitude x_m becomes infinite if r is equal to some critical value r_c defined by

$$r_c = (1-\alpha). \tag{2.65}$$

This then represents a type of amplitude and phase resonance which appears only under certain conditions of excitation. The frequency at the initial point of infinite response may be found from (2.42) and will be

$$\omega_c = \sqrt{\alpha}. \tag{2.66}$$

In the above analysis, x_m has been defined as the response amplitude which corresponds to a phase angle of 90^o and as such it is not necessarily equal to the peak amplitude of response in every case. However, for the limiting case of

infinite response, it may be shown that this 90^{o} phase angle amplitude is precisely the true peak amplitude of the system response. Thus, so far as the existence of a critical excitation level is concerned, equation (2.64) may be interpreted as applying to the peak response of the system.

Stability

It will be recalled that the iterative method of solution was contingent upon convergence to a steady state solution from some arbitrary initial point in phase space. Therefore, a solution obtained in this way should automatically satisfy the conditions for infinitesimal stability. Furthermore, the fact that the response curves appear to be single-valued would indicate that these solutions are probably the only stable solutions within the range of consideration.

D. Exact Steady State Solution —— Trigonometric Excitation

Having demonstrated the feasibility of obtaining an exact steady state solution for the case of square wave excitation, attention is now directed toward investigation of the system response under trigonometric excitation.

Equations Governing the Steady State Motion

Fig. 10 is a schematic representation of the hysteresis loop and displacement wave form for trigonometric excitation. Those values of displacement and time which are refered to explicitly in the following discussion have been noted in this figure.

Let x_1 be the maximum positive displacement of the hysteresis loop and let ϕ be the phase angle by which the displacement lags the excitation. Then, beginning at the point where the displacement is equal to x_1, the equation describing subsequent motion of the system will be

$$\ddot{x} + x = (x_1 - 1)(1 - \alpha) + r \cos(\omega t + \phi), \tag{2.67}$$

where ω and r are respectively the frequency and amplitude of the excitation, and where

$$\begin{aligned} x(0) &= x_1 \\ \dot{x}(0) &= 0. \end{aligned} \tag{2.68}$$

Equation (2.67) will remain valid until the displacement has decreased to some value x_2, at which point, the slope of the restoring force diagram changes to α. If t_2 is the time required for the system to move from displacement x_1 to x_2, then from (2.67) and (2.68) it will be seen that for $\omega \neq 1$

$$x_2 = \left[x_1 - (x_1 - 1)(1 - \alpha) - \frac{r}{1-\omega^2} \cos\phi\right] \cos t_2 + \frac{\omega r}{1-\omega^2} \sin\phi \sin t_2$$

$$+ (x_1 - 1)(1 - \alpha) + \frac{r}{1-\omega^2} \cos(\omega t_2 + \phi) \tag{2.69}$$

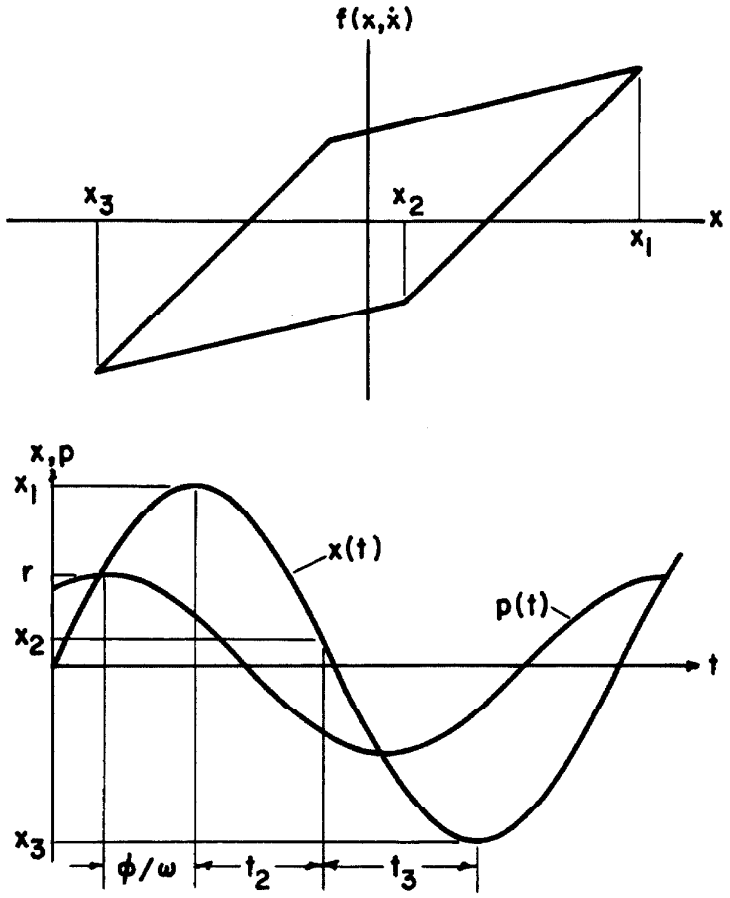

FIGURE 10. HYSTERESIS DIAGRAM AND DISPLACEMENT WAVE FORM

and

$$\dot{x}_2 = -\left[x_1 - (x_1-1)(1-\alpha) - \frac{r}{1-\omega^2}\cos\phi\right]\sin t_2 + \frac{\omega r}{1-\omega^2}\sin\phi\cos t_2$$

$$-\frac{r\omega}{1-\omega^2}\sin(\omega t_2+\phi). \qquad (2.70)$$

But, due to the assumed normalization of the hysteresis loop,

$$x_2 = x_1 - 2.$$

Thus, equation (2.69) may be rewritten as

$$0 = \left[x_1 - (x_1-1)(1-\alpha) - \frac{r}{1-\omega^2}\cos\phi\right]\cos t_2 + \frac{\omega r}{1-\omega^2}\sin\phi\sin t_2$$

$$+(1+\alpha-\alpha x_1) + \frac{r}{1-\omega^2}\cos(\omega t_2+\phi). \qquad (2.71)$$

Further motion of the system with negative velocity will take place along the lowermost restoring force branch of slope α. Therefore, the equation governing this motion may be expressed as

$$\ddot{x} + \alpha x = (1-\alpha) + r\cos\left[\omega(t+t_2)+\phi\right] \qquad (2.72)$$

where the initial conditions are now taken to be

$$x(0) = x_2 = x_1 - 2$$
$$\dot{x}(0) = \dot{x}_2 \qquad (2.73)$$

If the frequency and amplitude of excitation are such that the effects of ultraharmonics may be neglected, the hysteresis loop will have the configuration shown in Fig. 10 with no zeros of the velocity at other than the points of maximum and minimum displacement. In this case, if x_3 is the value of the minimum displacement and t_3 is the time required for the system to move from x_2 to x_3,

it will be seen from (2.72) and (2.73) that if $\omega^2 \neq \alpha$,

$$x_3 = \frac{1}{\sqrt{\alpha}}\left[\dot{x}_2 + \frac{\omega r}{\alpha-\omega^2}\sin(\omega t_2 + \phi)\right]\sin\sqrt{\alpha}\, t_3 + \frac{r}{\alpha-\omega^2}\cos\left[\omega(t_3 + t_2) + \phi\right]$$

$$+\left[x_1 - 2\,\frac{(1-\alpha)}{\alpha} - \frac{r}{\alpha-\omega^2}\cos(\omega t_2 + \phi)\right]\cos\sqrt{\alpha}\, t_3 + \frac{(1-\alpha)}{\alpha} \qquad (2.74)$$

and

$$\dot{x}_3 = 0 = \left[\dot{x}_2 + \frac{\omega r}{\alpha-\omega^2}\sin(\omega t_2 + \phi)\right]\cos\sqrt{\alpha}\, t_3 - \frac{r\omega}{\alpha-\omega^2}\sin\left[\omega(t_3 + t_2) + \phi\right]$$

$$-\sqrt{\alpha}\left[x_1 - 2 - \frac{(1-\alpha)}{\alpha} - \frac{r}{\alpha-\omega^2}\cos(\omega t_2 + \phi)\right]\sin\sqrt{\alpha}\, t_3. \qquad (2.75)$$

Before proceeding, it should be noted that for certain conditions of ultraharmonic response the system may actually have a pair of zeros of the velocity intermediate to the points x_2 and x_3. In this case, the system doubles back for a short distance on a segment of unity slope and then retraces its path to again follow the segment of slope α. This additional side excursion of the hysteresis loop makes it very difficult to include both harmonic and ultraharmonic behavior in a single general analytic solution. Therefore, the present discussion will be restricted to cases in which the response may be described by (2.74) and (2.75), and cases of predominantly ultraharmonic response will be considered separately in a later section.

If it is once again assumed that the hysteresis loop is symmetric, the periodicity conditions on the solution become

$$x_1 = -x_3 \qquad (2.76)$$

and

$$t_2 + t_3 = \pi/\omega. \qquad (2.77)$$

Thus, as in the case of square wave excitation, the problem has been reduced to the solution of a set of simultaneous transcendental equations. In this case there are six equations [equations (2.70), (2.71) and (2.74) through (2.77)] and six unknowns [x_1, ϕ, $\dot{x}_2$, t_2, x_3, and t_3].

For reasons which will soon become apparent, it is convenient to introduce a new variable ϕ' defined by

$$\phi' \equiv \phi + (t_2 + t_3 - \pi/\omega). \tag{2.78}$$

Then, in terms of this new variable the periodicity requirement (2.77) may be written in the equivalent form

$$\phi = \phi'. \tag{2.79}$$

Method of Solution for Steady State Response

Because of the highly transcendental character of the simultaneous equations governing the steady state behavior, direct solution by elimination of variables is impractical. Thus, guided by the results of graphical constructions and analytic solutions with square wave excitation, one again turns to an iterative method of solution as a means of making the problem more tractable.

The analysis in this case is begun by arbitrary selection of initial values for the two variables x_1 and ϕ. Then, using straight-forward algebraic or numerical techniques it is possible to progressively solve for t_2 from (2.71), $\dot{x}_2$ from (2.70), t_3 from (2.75), and finally x_3 and ϕ' from (2.74) and (2.78). Having thus determined all of the intermediate variables, equations (2.76) and (2.79) may then be used to calculate new values for x_1 and ϕ. If these new values are the same as the ones assumed initially, the problem is solved; if not, the

entire process is begun again using the new values as initial conditions. This procedure is continued until the initial and final values of x_1 and ϕ over a cycle of calculation are equal within some desired limit of accuracy.

The convergence of iterative procedures such as that just described was descussed in some detail with regard to the problem of square wave excitation. At that time it was noted that the iterative solution is really just a mathematical construction of the steady state phase contour and as such, the convergence of one type of solution should imply the convergence of the other. For the specific case of trigonometric excitation no actual constructions of the phase contour have been made. However, for square wave excitation it has been shown that both the phase plane and iterative solutions converge and, on the basis of this work there is no reason to believe that trigonometric excitation should behave any differently. Thus, it is reasonable to conclude that the iterative procedure outlined above will indeed converge.

Discussion of Results —— Fundamental Response Range

Figs. 11, 12, and 13 show the results of typical digital computer solutions in the range of parameters where ultraharmonic behavior is not a predominant factor. The overall resemblance of these figures to Figs. 8 and 9 for square wave excitation is immediately apparent and need not be elaborated upon. However, it is beneficial to once again point out the essential features associated with this type of steady state frequency response.

To begin with it will be seen that all of the curves exhibit a characteristic leaning toward low frequency which is typical of so called "soft" systems. This results in a somewhat gentle slope on the high frequency side of the response

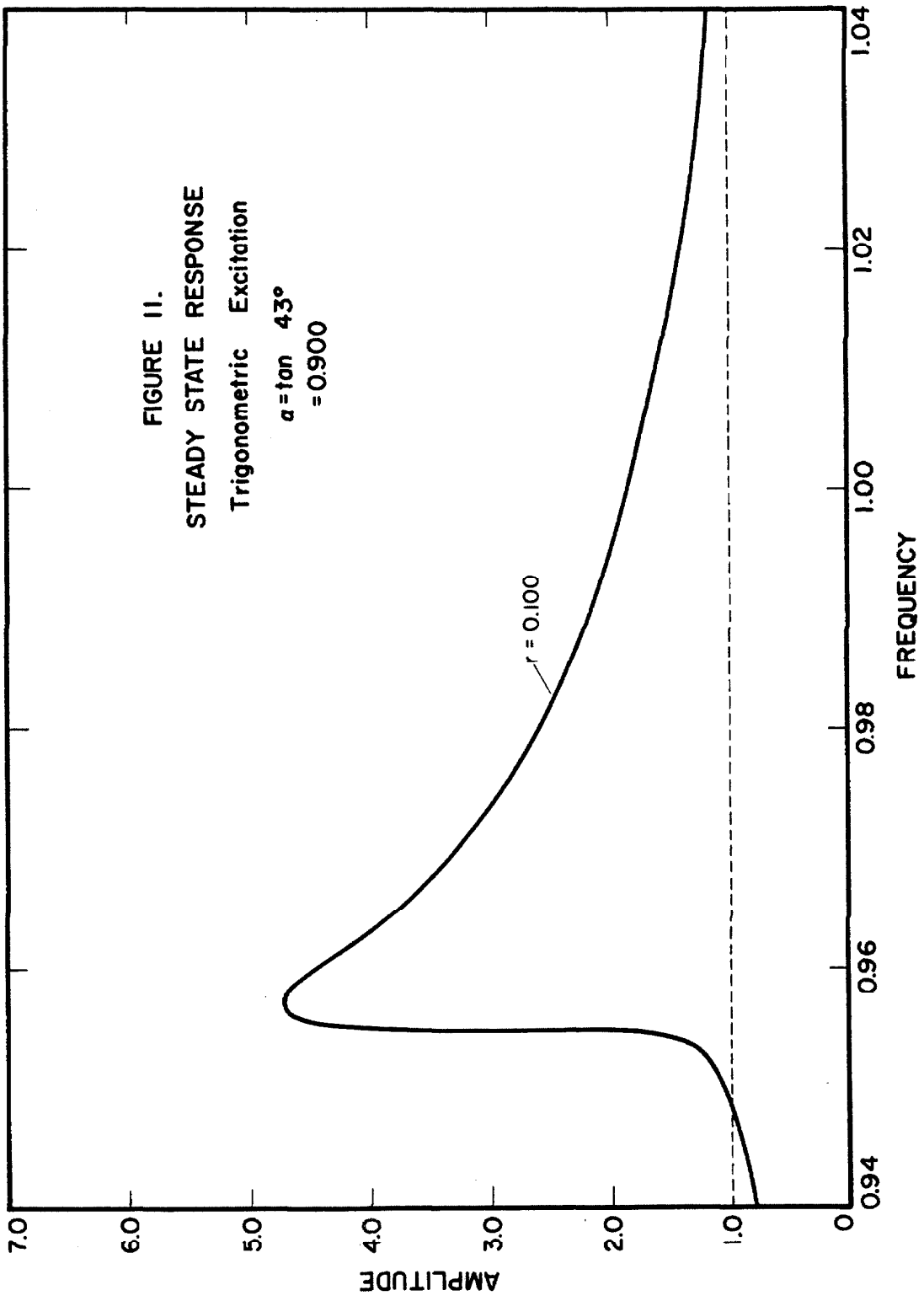
FIGURE 11.
STEADY STATE RESPONSE
Trigonometric Excitation
α = tan 43°
= 0.900
r = 0.100
AMPLITUDE
FREQUENCY
0
1.0
2.0
3.0
4.0
5.0
6.0
7.0
0.94
0.96
0.98
1.00
1.02
1.04

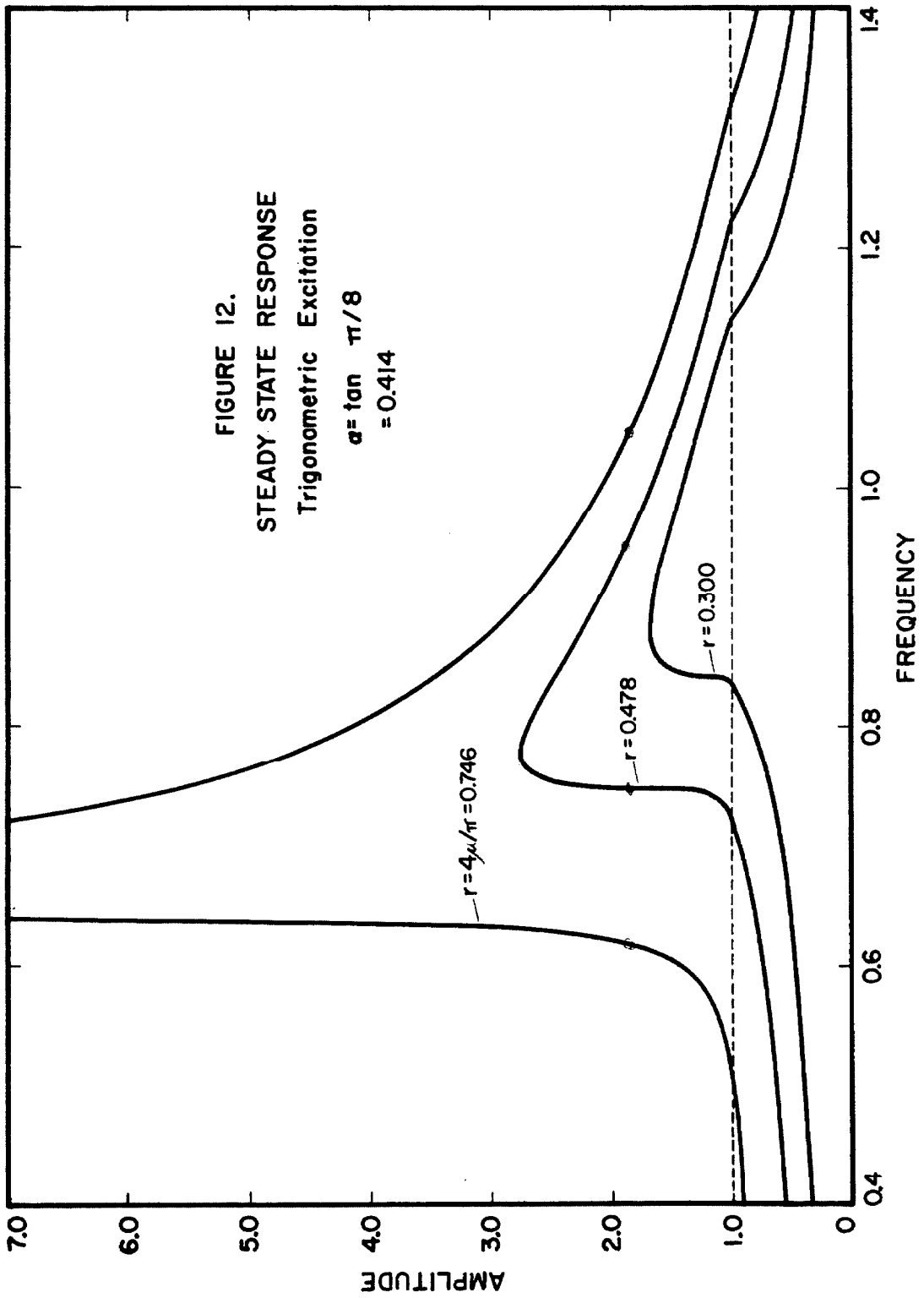
FIGURE 12.
STEADY STATE RESPONSE
Trigonometric Excitation
α = tan π/8
= 0.414
r = 4μ/π = 0.746
r = 0.478
r = 0.300
AMPLITUDE
FREQUENCY
7.0
6.0
5.0
4.0
3.0
2.0
1.0
0
0.4
0.6
0.8
1.0
1.2
1.4

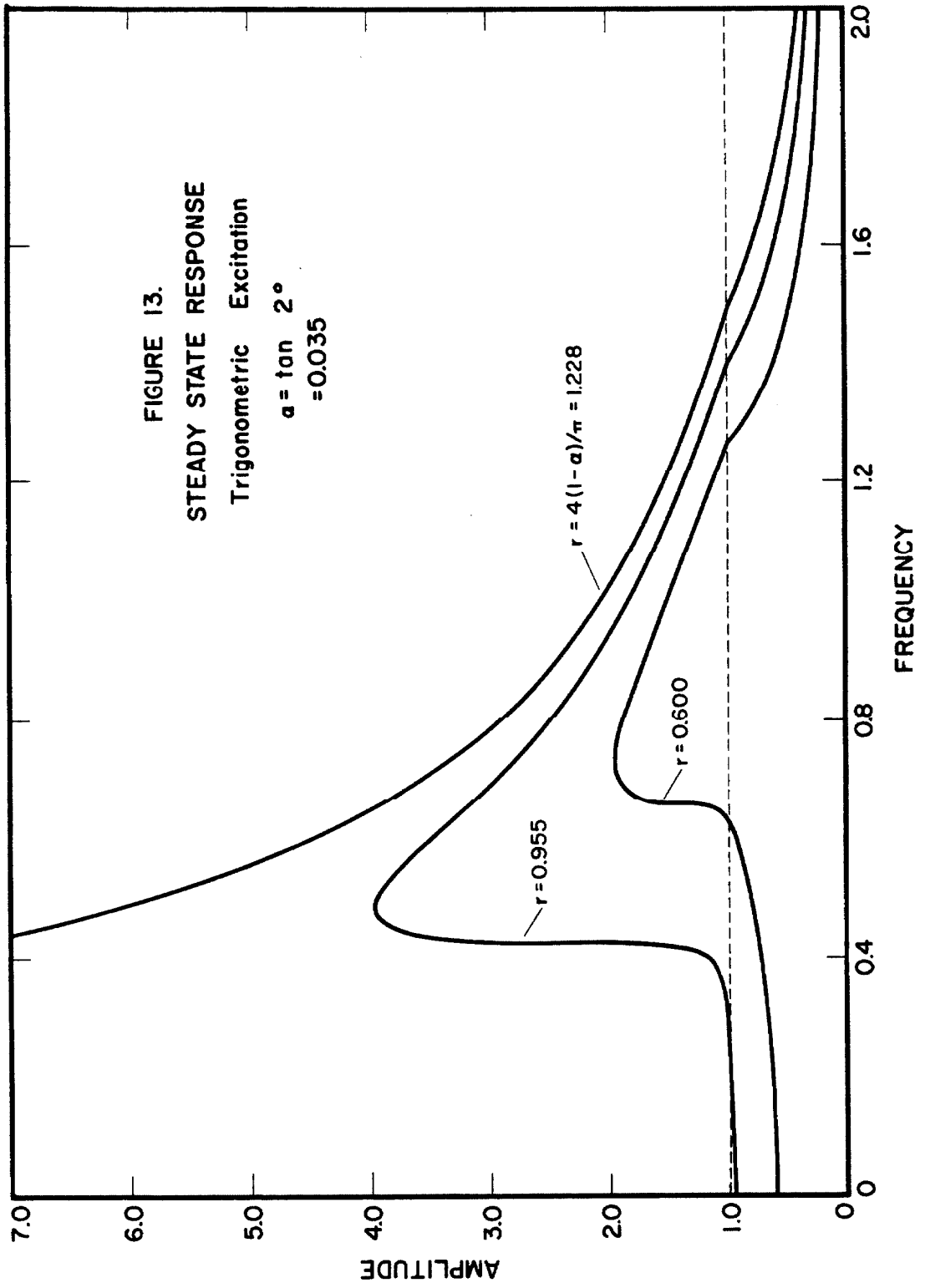
FIGURE 13.
STEADY STATE RESPONSE
Trigonometric Excitation
α = tan 2°
=0.035
r = 4(1-α)/π = 1.228
r = 0.600
r = 0.955
AMPLITUDE
FREQUENCY
7.0
6.0
5.0
4.0
3.0
2.0
1.0
0
0.4
0.8
1.2
1.6
2.0

curve and a very steep slope on the low frequency side. Numerous determinations of the response were made on the low frequency side of the curve and although convergence was extremely slow, it was possible to obtain sufficiently accurate results to indicate that ; 1) within the accuracy of the numerical computations the slope on the low frequency side is never negative, and 2) this slope may approach an infinite limit at its steepest point. Thus, on the basis of these observations it is concluded that there can be no more than one vertical tangency to a given response curve which in turn implies that the response curves are all single valued.

In those cases where a family of curves is plotted in the same figure, it will also be noted that the peak response occurs at a progressively lower frequency as the level of excitation is increased until, for a value of $r = 4(1-\alpha)/\pi$, the response does not close at all within the limits of the figure. This behavior is therefore very similar to the unbounded resonance behavior which was shown to exist in the case of square wave excitation. More will be said concerning this in the next subsection.

Unbounded Resonance Behavior

If r and ω are specified, it has been noted previously that the steady state response may be described by a set of six simultaneous equations in the six unknowns x_1, ϕ, $\dot{x}_2$, t_2, x_3, and t_3. Now, guided by the results of the square wave analysis performed earlier, one is led to consider the special case of the system response when

$$\omega = \sqrt{\alpha} \tag{2.80}$$

and

$$\phi = 0. \tag{2.81}$$

However, in specifying ϕ and ω it is no longer possible to concurrently specify

r. Thus, in this special case r must be looked upon as one of the variables of the problem and there are again six equations in six unknowns.

Equations (2.74) and (2.75) for x_3 and $\dot{x}_3$ were derived under the restriction that $\omega \neq \sqrt{\alpha}$. Thus, for the particular conditions specified by (2.80) and (2.81) these equations must be replaced by

$$x_3 = \left(\frac{\dot{x}_2}{\sqrt{\alpha}} - \frac{r}{2\alpha} \sin \sqrt{\alpha}\, t_2 \right) \sin \sqrt{\alpha}\, t_3 + \left[x_1 - 2 - \frac{(1-\alpha)}{\alpha} \right] \cos \sqrt{\alpha}\, t_3 + \frac{(1-\alpha)}{\alpha} + \frac{r}{2\sqrt{\alpha}}\, t_3 \cos \sqrt{\alpha}\, (t_3 + t_2). \tag{2.82}$$

and

$$\dot{x}_3 = 0 = \left(\dot{x}_2 - \frac{r}{2\sqrt{\alpha}} \sin \sqrt{\alpha}\, t_2 \right) \cos \sqrt{\alpha}\, t_3 - \sqrt{\alpha} \left[x_1 - 2 - \frac{(1-\alpha)}{\alpha} \right] \sin \sqrt{\alpha}\, t_3 + \frac{r}{2\sqrt{\alpha}} \cos \sqrt{\alpha}\, (t_3 + t_2) - \frac{r}{2}\, t_3 \sin \sqrt{\alpha}\, (t_3 + t_2). \tag{2.83}$$

These two equations along with equations (2.70), (2.71), (2.76) and (2.77) where $\phi = 0$ and $\omega = \sqrt{\alpha}$ are therefore the six equations which determine the system behavior.

Eliminating x_3 and t_3 by means of equations (2.76) and (2.77) the number of unknowns is reduced to four and the remaining equations become

$$x_m - 2 = \left[x_m - (x_m - 1)(1-\alpha) \right] \cos t_2 + \frac{\sqrt{\alpha}\, r}{1-\alpha} \sin t_2 + (x_m - 1)(1-\alpha) - \frac{r}{1-\alpha} \sin \sqrt{\alpha}\, t_2 \tag{2.84}$$

$$\dot{x}_2 = - \left[x_m - (x_m - 1)(1-\alpha) \right] \sin t_2 + \frac{\sqrt{\alpha}\, r}{1-\alpha} \cos t_2 - \frac{\sqrt{\alpha}\, r}{1-\alpha} \cos \sqrt{\alpha}\, t_2 \tag{2.85}$$

$$-x_m = \left(\frac{\dot{x}_2}{\sqrt{\alpha}} - \frac{r}{2\alpha} \cos \sqrt{\alpha}\, t_2 \right) \sin \sqrt{\alpha}\, t_2 - \left[x_m - 2 - \frac{(1-\alpha)}{\alpha} \right] \cos \sqrt{\alpha}\, t_2 + \frac{(1-\alpha)}{\alpha} - \frac{r}{2\sqrt{\alpha}} \left(\frac{\pi}{\sqrt{\alpha}} - t_2 \right) \tag{2.86}$$

$$0 = - \left(\dot{x}_2 - \frac{r}{2\sqrt{\alpha}} \cos \sqrt{\alpha}\, t_2 \right) \cos \sqrt{\alpha}\, t_2 - \sqrt{\alpha} \left[x_m - 2 - \frac{(1-\alpha)}{\alpha} \right] \sin \sqrt{\alpha}\, t_2 - \frac{r}{2\sqrt{\alpha}} \tag{2.87}$$

where the particular value of x_1 which corresponds to the conditions (2.80) and (2.81) has been denoted by x_m.

Equations (2.84) through (2.87) may be further reduced by using (2.85) to eliminate $\dot{x}_2$ from the remaining equations. Equation (2.84) will be unchanged by this process and equations (2.86) and (2.87) will become

$$-x_m = \frac{1}{\sqrt{\alpha}}\left\{-\left[x_m-(x_m-1)(1-\alpha)\right]\sin t_2 + \frac{\sqrt{\alpha}\,r}{1-\alpha}(\cos t_2 - \cos\sqrt{\alpha}\,t_2) - \frac{r}{2\sqrt{\alpha}}\cos\sqrt{\alpha}\,t_2\right\}$$

$$\sin\sqrt{\alpha}\,t_2 - \left[x_m - 2 - \frac{(1-\alpha)}{\alpha}\right]\cos\sqrt{\alpha}\,t_2 + \frac{(1-\alpha)}{\alpha} - \frac{r}{2\sqrt{\alpha}}\left(\frac{\pi}{\sqrt{\alpha}} - t_2\right) \qquad (2.88)$$

$$0 = -\left\{-\left[x_m-(x_m-1)(1-\alpha)\right]\sin t_2 + \frac{\sqrt{\alpha}\,r}{1-\alpha}(\cos t_2 - \cos\sqrt{\alpha}\,t_2) - \frac{r}{2\sqrt{\alpha}}\cos\sqrt{\alpha}\,t_2\right\}$$

$$\cos\sqrt{\alpha}\,t_2 - \sqrt{\alpha}\left[x_m - 2 - \frac{(1-\alpha)}{\alpha}\right]\sin\sqrt{\alpha}\,t_2 - \frac{r}{2\sqrt{\alpha}}. \qquad (2.89)$$

Then, solving equation (2.84) for x_m yields

$$x_m = \frac{(1-\alpha)\cos t_2 + \frac{r}{(1-\alpha)}(\sqrt{\alpha}\sin t_2 - \sin\sqrt{\alpha}\,t_2) + (1+\alpha)}{\alpha(1-\cos t_2)} \qquad (2.90)$$

and solving equation (2.88) for r gives

$$r = \frac{x_m(\cos\sqrt{\alpha}\,t_2 - 1) + \left[2 + \frac{(1-\alpha)}{\alpha}\right](\sin t_2 \sin\sqrt{\alpha}\,t_2 + \cos^2\sqrt{\alpha}\,t_2 + \frac{(1-\alpha)}{\alpha}\cos\sqrt{\alpha}\,t_2)}{\frac{1}{2\alpha}\sin\sqrt{\alpha}\,t_2 + \frac{1}{2\sqrt{\alpha}}\left(\frac{\pi}{\sqrt{\alpha}} - t_2\right)\cos\sqrt{\alpha}\,t_2} \qquad (2.91)$$

where equation (2.89) has been used to simplify the form of (2.91).

Formally equations (2.90) and (2.91) may now be used to solve for r and x_m in terms of t_2. These results in conjunction with (2.89) would then give one equation in the one unknown t_2. However, it is readily seen that this would lead to such a complicated expression that practically speaking the problem could not

be solved. Thus, the procedure followed here will be to select a reasonable value for t_2 and then demonstrate that this value along with the values it predicts for x_m and r are all consistent with the statements of equations (2.89) through (2.91).

Assume that the desired solution is $t_2 = 0$; or, to be more correct both physically and mathematically, assume that

$$t_2 \to 0. \tag{2.92}$$

Then, from (2.90) it may be shown that

$$\lim_{t_2 \to 0} (x_m) = \lim_{t_2 \to 0} \left[\frac{-(1-\alpha)\, t_2^2/2 - r\sqrt{\alpha}\, t_2^3/3! + 2 + 0(t_2^4)}{\alpha\, t_2^2/2 + 0(t_2^4)} \right]. \tag{2.93}$$

Assuming for the moment that r is no less than zeroeth order in t_2, (2.93) becomes

$$\lim_{t_2 \to 0} (x_m) = \lim_{t_2 \to 0} \left[4/\alpha t_2^2 + \alpha/3 + 0(t_2^2) \right]. \tag{2.94}$$

Therefore,

$$x_m \to \infty \text{ as } t_2 \to 0. \tag{2.95}$$

and it is immediately recognized that this is just the type of solution which was sought.

The assumption that r is no less than zeroeth order in t_2 may now be verified from equation (2.91). In this way it may be shown, after considerable manipulation, that

$$\lim_{t_2 \to 0} (r) = \lim_{t_2 \to 0} \left[4(1-\alpha)/\pi + 0(t_2) \right]. \tag{2.96}$$

Hence,

$$r \to 4(1-\alpha)/\pi \text{ as } t_2 \to 0. \tag{2.97}$$

and r is indeed zeroeth order as assumed.

It now remains only to show that the values of t_2, r, and x_m obtained above satisfy the third equation (2.89). Taking the limit of both sides of this equation it may be shown that the right hand side is of order t_2. Thus, as t_2 approaches zero, the equation is satisfied and the assumed values for t_2, r, and x_m must represent the true limiting solution of the problem.

Summarizing, it has been shown that the exact equations of the steady state motion predict an amplitude and phase resonance ($x_m \to \infty$, $\phi = 0$) which occurs with finite amplitude of excitation at a frequency $\omega = \sqrt{\alpha}$. The amplitude of excitation which yields this behavior may therefore be looked upon as a critical parameter for the particular system under consideration and will be denoted by

$$r_c = 4(1-\alpha)/\pi . \tag{2.98}$$

Stability

The validity of the iterative procedure used here has been based upon the premise that solutions begun at some arbitrary initial point in phase space will eventually converge to a steady state configuration if such exists. However, it will be recognized that this is precisely the way in which one usually defines a stable solution. Therefore, if in a particular case the iterative procedure actually does converge independently of the initial conditions, the solution obtained thereby should be stable.

All of the information relative to the response curves of Figs. 11, 12 and

13 was obtained by means of the iterative method with arbitrary initial conditions. Although convergence on the nearly vertical portions of these curves was very slow, a steady state solution was reached in every case considered. Thus, on the basis of this convergence it may be concluded that the solutions represented by these figures are in fact stable.

For the present case of trigonometric excitation the stability of the steady state solutions may also be treated purely mathematically. In order to do this, one assumes a small initial perturbation on the displacement and velocity at the beginning of one cycle and then, using the equations governing the steady state behavior, calculates the status of these perturbations at the beginning of each subsequent cycle. N. Ando[12] has carried out such an analysis and has thereby shown that solutions of the type shown in Figs. 11, 12, and 13 are stable in the sense that any initial perturbations will die out for large time.

Harmonic Content —— Fundamental Response Range

As a guide to the eventual formulation of approximate methods of solution, it is instructive to examine the harmonic content of the steady state displacement wave form.

Let the steady state solution be given by

$$x_s(t) = \sum_{n=1}^{\infty} (a_n \sin n\omega t + b_n \cos n\omega t), \tag{2.99}$$

where

$$a_n = \frac{1}{\pi}\int_0^{2\pi} x_s(t) \sin n\omega t \, d(\omega t) \tag{2.100}$$

and

$$b_n = \frac{1}{\pi}\int_0^{2\pi} x_s(t) \cos n\omega t \, d(\omega t). \tag{2.101}$$

Then, for the purposes of the present analysis the harmonic content of x_s may be defined as

$$\chi = \left[\frac{\sum_{n=2}^{\infty} (a_n^2 + b_n^2)}{(a_1^2 + b_1^2)} \right]^{1/2} . \tag{2.102}$$

In order to evaluate χ in practice it will be convenient to introduce the new quantity Δ defined by

$$\begin{aligned} \Delta &= \left[x_s(t) - (a_1 \sin\omega t + b_1 \cos\omega t) \right] \\ &= \sum_{n=2}^{\infty} (a_n \sin n\omega t + b_n \cos n\omega t) . \end{aligned} \tag{2.103}$$

Then, using the orthogonality properties of the trigonometric functions, it may be shown that

$$\chi^2 = \int_0^{2\pi} \Delta^2 \, d(\omega t)/\pi (a_1^2 + b_1^2). \tag{2.104}$$

But now Δ, a_1, and b_1 may all be determined directly from the nature of the displacement $x_s(t)$. Thus, if x_s is known either explicitly or numerically, it is conceptually a rather simple matter to calculate χ using equation (2.104). This has been done for two different cases. In one case the actual non-linearity is moderate ($\alpha = \tan \pi/8$) and in the other the non-linearity may be considered extreme ($\alpha = \tan 2^{\circ}$). For each case, the frequency of excitation was selected so that the amplitude of response would be in the medium value range where the effects of the non-linearity are maximized. The results of this analysis are presented in Table I.

TABLE I.

Case no.	α	r	ω	Fig. no. of response curve	Harmonic content, χ
1	tan $\pi/8$	0.746	0.80	12	0.008
2	tan 2^{o}	0.955	0.50	13	0.039

From Table I it is seen that even for the two relatively severe cases taken above, the actual harmonic content is very low. Indeed, for the case with α = tan $\pi/8$, the harmonic content might be considered negligible. Thus, within the range of predominantly fundamental response the displacement solution may be approximated quite well by its fundamental Fourier component.

Fig. 14 shows the displacement and velocity wave forms which correspond to the cases considered in Table I. Again it will be noted that the displacement wave forms are very nearly trigonometric. However, this same observation may not be applied too well to the velocity wave forms.

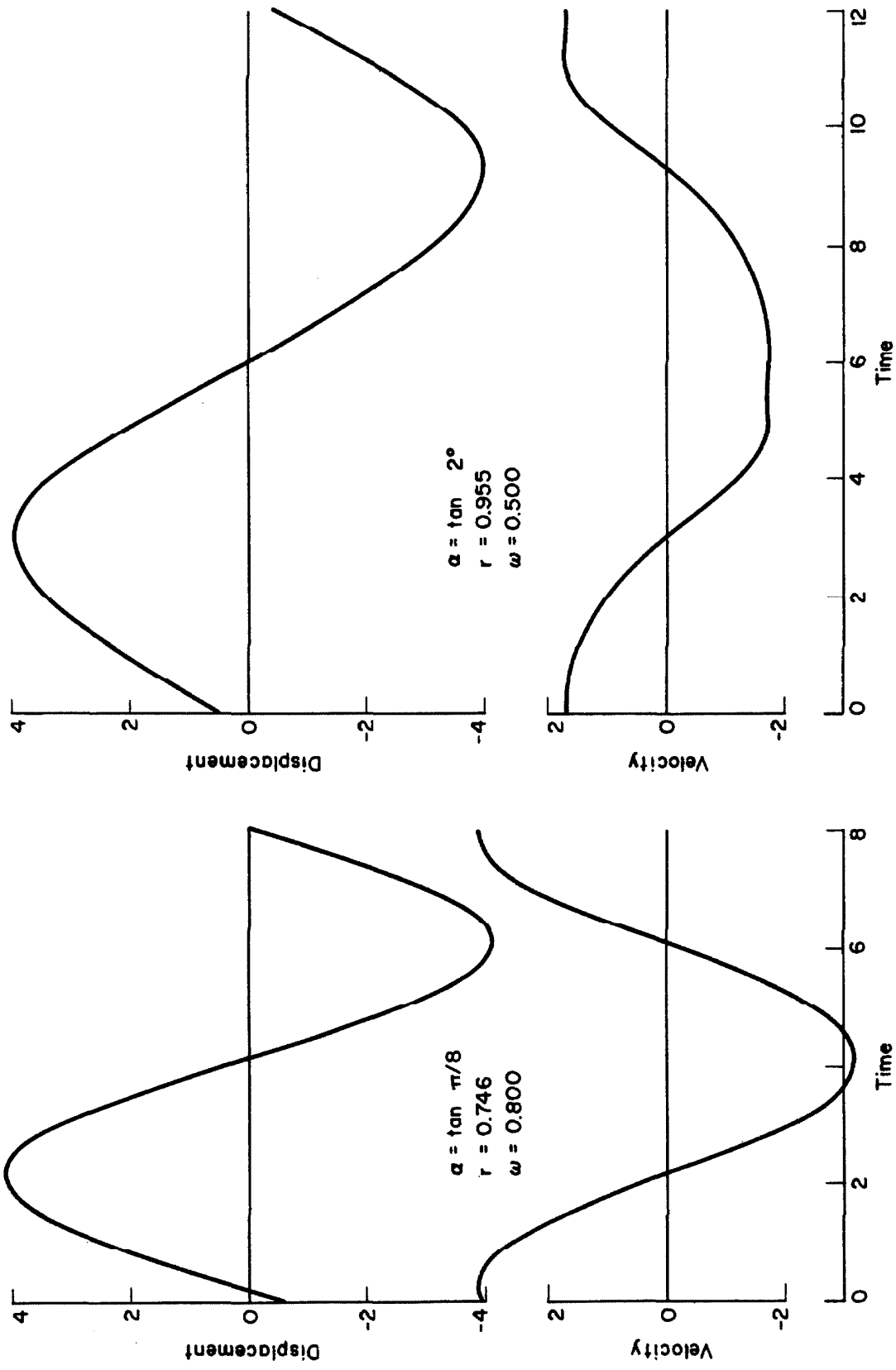

FIGURE 14. DISPLACEMENT AND VELOCITY WAVE FORMS

E. Approximate Steady State Theory

One of the earliest published attempts to formulate an approximate theory for the steady state oscillation of the bilinear hysteretic system was made by N. Ando[12]. In this treatment of the problem an equivalent linear damping coefficient was obtained by energy considerations and an equivalent linear spring constant was selected on the basis of a two point displacement collocation. Frequency response curves predicted by this procedure have somewhat the same shape as those for the exact solution, but in general the agreement is not as close as might be desired.

More recently, T. K. Caughey[13] has treated the problem very successfully by the method of slowly varying parameters. This method not only gives an extremely good approximation to the steady state response but also enables direct investigation of the stability of such motion. This approach will be considered later in connection with the addition of viscous damping.

The method of solution which will be employed in the present study is the so called method of equivalent linearization developed by Kryloff and Bogoliuboff (See Ref. 16). The biggest advantage in using this method is that it gives a very clear picture of the nature of the approximations involved and at the same time enables estimation of the magnitude of the errors which are introduced through the linearization process. It will be found that this method arrives at exactly the same steady state equations as the method of slowly varying parameters. Unfortunately, however, the present method gives no direct information about the stability of steady state solutions. Thus, it will be necessary to defer a full

consideration of this point to the investigation of the viscous damped hysteretic system where it may be treated as a limiting case.

Formulation of the Governing Equations

Let the differential equation of motion for trigonometric excitation be written in the form

$$\ddot{x} + \gamma\dot{x} + \kappa x + \varepsilon(x,\dot{x}) = r\cos\omega t. \tag{2.105}$$

where from (2.4) it will be seen that

$$\varepsilon(x,\dot{x}) = f(x,\dot{x}) - \gamma\dot{x} - \kappa x. \tag{2.106}$$

Then $\varepsilon(x,\dot{x})$ is, so to speak, the error which would be introduced into the equation of motion if the nonlinear system were approximated by a linear system with spring constant κ and damping coefficient γ. In seeking to linearize the problem, one must therefore select κ and γ so as to make ε (or, strictly speaking, the mean squared value of ε) a minimum. This will be accomplished if

$$\frac{\partial\overline{\varepsilon^2}}{\partial\kappa} = 0 \tag{2.107a}$$

and

$$\frac{\partial\overline{\varepsilon^2}}{\partial\gamma} = 0 \tag{2.107b}$$

where the bar denotes an average over one complete cycle of oscillation. Having thus made $\overline{\varepsilon^2}$ a minimum, the equation of motion may be linearized by neglecting ε in (2.105). This gives

$$\ddot{x} + \gamma\dot{x} + \kappa x = r\cos\omega t. \tag{2.108}$$

Equation (2.108) may now be used to solve for the fundamental steady state

motion in the usual manner by letting

$$x = A \cos \theta \tag{2.109}$$

where

$$\theta = \omega t - \phi. \tag{2.110}$$

Substituting (2.109) into (2.108) yields

$$-\omega^2 A \cos\theta + \kappa A \cos\theta - \omega\gamma A \sin\theta = r \cos(\theta + \phi)$$

Thus, collecting terms in $\cos\theta$ and $\sin\theta$, it will be seen that the two equations which determine A and ϕ become

$$-\omega^2 A + \kappa A = r \cos\phi \tag{2.111a}$$

$$-\omega\gamma A = -r \sin\phi, \tag{2.111b}$$

where for the linearized problem both κ and γ will in general be functions of A.

The values κ and γ which minimize $\overline{\varepsilon^2}$ may now be found directly from equations (2.107a and b) using the linearized solution (2.109). In this case

$$\overline{\varepsilon(x, \dot{x})^2} = \frac{1}{2\pi}\int_0^{2\pi}\left[f(A, \theta) - \kappa A \cos\theta + \omega\gamma A \sin\theta\right]^2 d\theta. \tag{2.112}$$

Therefore, making use of the orthogonality properties of the trigonometric functions,

$$\frac{\partial\overline{\varepsilon^2}}{\partial\kappa} = \kappa A^2 - \frac{A}{\pi}\int_0^{2\pi} f(A, \theta)\cos\theta \, d\theta \tag{2.113}$$

and

$$\frac{\partial\overline{\varepsilon^2}}{\partial\gamma} = \omega^2\gamma A^2 + \frac{A\omega}{\pi}\int_0^{2\pi} f(A, \theta)\sin\theta \, d\theta. \tag{2.114}$$

But from (2.107a and b), both partial derivatives must vanish. Thus,

$$\kappa = \frac{1}{A\pi}\int_0^{2\pi} f(A, \theta) \cos\theta \, d\theta \tag{2.115}$$

and

$$\gamma = -\frac{1}{A\omega\pi}\int_0^{2\pi} f(A, \theta) \sin\theta \, d\theta . \tag{2.116}$$

At this point it may be noted that $-A\omega\gamma\pi$ is just the total energy loss per cycle due to viscous damping. Therefore, equation (2.116) states that the energy loss per cycle due to viscous damping should be equal to that due to hysteresis where both losses are calculated on the basis of the linearized displacement.

Letting

$$C(A) = \frac{1}{\pi}\int_0^{2\pi} f(A, \theta) \cos\theta \, d\theta \tag{2.117a}$$

$$S(A) = \frac{1}{\pi}\int_0^{2\pi} f(A, \theta) \sin\theta \, d\theta , \tag{2.117b}$$

equations (2.111a and b) which govern the steady state response may then be written as

$$-\omega^2 A + C(A) = r\cos\phi \tag{2.118a}$$

$$S(A) = -r\sin\phi . \tag{2.118b}$$

Squaring and adding equations (2.118a and b), it is seen that

$$\left[-\omega^2 A + C(A)\right]^2 + \left[S(A)\right]^2 = r^2 . \tag{2.119}$$

Therefore, the equation for the frequency response becomes

$$\omega^2 = \frac{C(A)}{A} \pm \left\{\left[\frac{r}{A}\right]^2 - \left[\frac{S(A)}{A}\right]^2\right\}^{1/2} . \tag{2.120}$$

Evaluation of C(A) and S(A)

The functions C(A) and S(A) as defined by equations (2.117a and b) contain integrals over one complete cycle of oscillation. However, due to the assumed symmetry properties of the steady state hysteresis loop, these integrals may be replaced by twice the integral over a half cycle. From equation (2.5) it will be seen that for the half cycle of negative velocity,

$$f(A, \theta) = \begin{cases} A \cos\theta - (A-1)(1-\alpha) & ; \ (A-2)/A < \cos\theta < 1 \\ \alpha A \cos\theta - (1-\alpha) & ; \ \cos\theta < (A-2)/A. \end{cases} \tag{2.121}$$

Thus, defining the angle θ^* by

$$\theta^* = \cos^{-1}\frac{A-2}{A}, \tag{2.122}$$

the equations (2.117a and b) for C(A) and S(A) may be written as

$$C(A) = \frac{2}{\pi}\left\{\int_0^{\theta^*}\left[A\cos\theta - (A-1)(1-\alpha)\right]\cos\theta\, d\theta + \int_{\theta^*}^{\pi}\left[\alpha A\cos\theta - (1-\alpha)\right]\cos\theta\, d\theta\right\} \tag{2.123a}$$

and

$$S(A) = \frac{2}{\pi}\left\{\int_0^{\theta^*}\left[A\cos\theta - (A-1)(1-\alpha)\right]\sin\theta\, d\theta + \int_{\theta^*}^{\pi}\left[\alpha A\cos\theta - (1-\alpha)\right]\sin\theta\, d\theta\right\}. \tag{2.123b}$$

Carrying out the indicated integrations, it may then be shown that

$$C(A) = \begin{cases} \frac{A}{\pi}\left[(1-\alpha)\theta^* + \alpha\pi - \frac{(1-\alpha)}{2}\sin 2\theta^*\right] & ; \ A > 1 \\ A & ; \ A < 1 \end{cases} \tag{2.124a}$$

and

$$S(A) = \begin{cases} -\frac{A}{\pi}(1-\alpha)\sin^2\theta^* & ; \ A > 1 \\ 0 & ; \ A < 1 \ . \end{cases} \tag{2.124b}$$

Discussion of Steady State Results

Using equations (2.120) and (2.124a and b), it is possible to construct frequency response curves which correspond to the exact solutions of Figs. 11, 12, and 13. This has been done and the results are shown along with the exact solutions in Figs. 15, 16, and 17.

For the cases of small to moderate α in Figs. 15 and 16, it will be noted that the agreement between exact and approximate steady state solutions is quite good. This is in large measure due to the fact that the actual displacement wave forms for moderate α in the fundamental frequency range ($\omega \approx 1$) are very nearly harmonic as was shown in a previous section. In these cases then, the first order approximation presented here very nearly describes the true motion of the system.

For the extreme case of $\alpha = \tan 2^{\circ}$ shown in Fig. 17, agreement is likewise quite good so long as consideration is restricted to the frequency range where the behavior is predominantly fundamental in nature. However, for frequencies approaching $\omega = 1/3$, it is seen that the difference between exact and approximate solutions becomes rather large. This is for the most part due to the presence of ultraharmonics in the exact solution which have been neglected in the present single component approximation. More will be said concerning this matter in a later section.

Error Term

One reason for the closeness of agreement between the approximate and exact steady state theories may be seen from an analysis of the so called "error term" $\epsilon(x, \dot{x})$ which is defined by equation (2.106). Substituting for κ and γ in

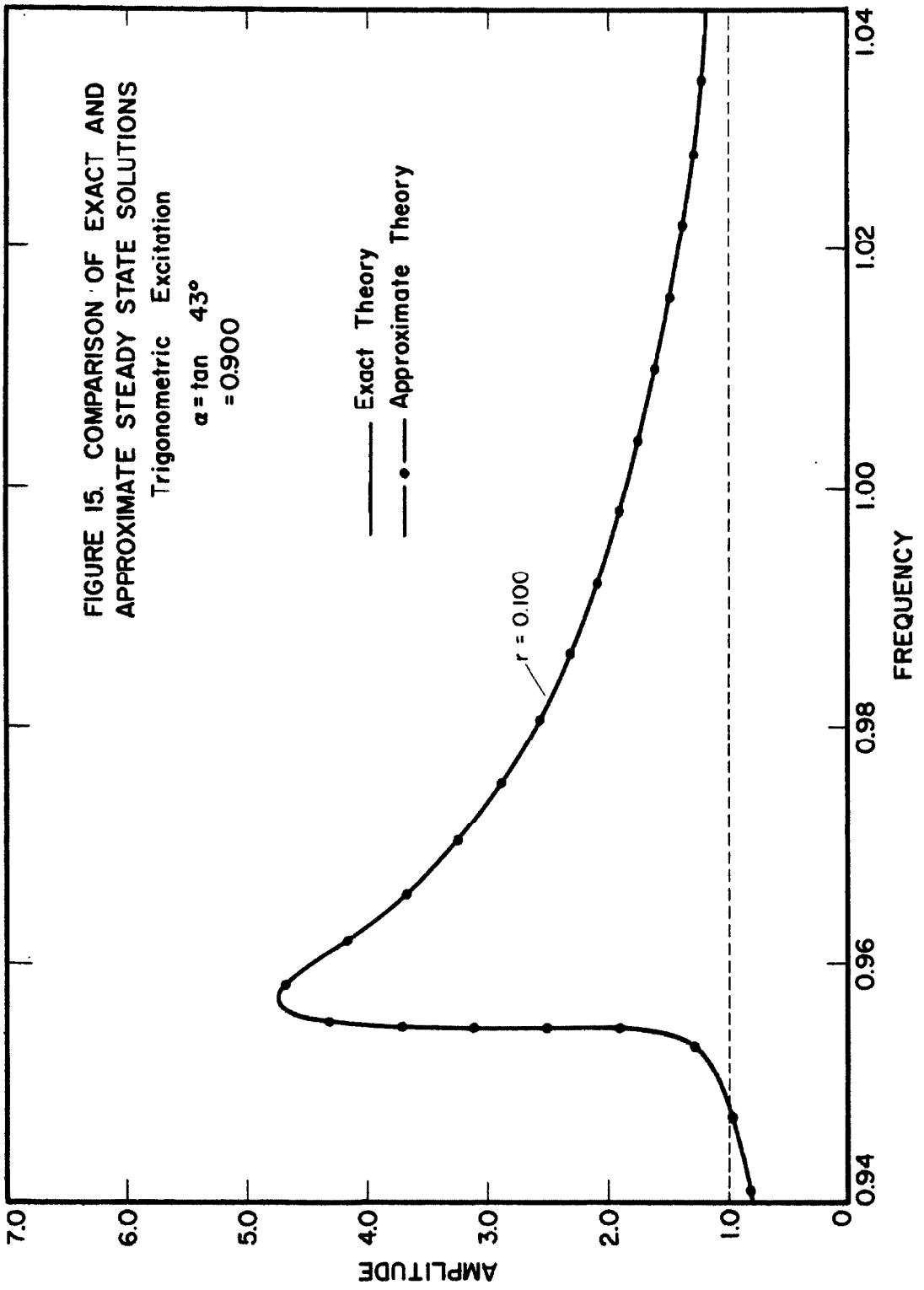
FIGURE 15. COMPARISON OF EXACT AND APPROXIMATE STEADY STATE SOLUTIONS
Trigonometric Excitation
α = tan 43°
= 0.900
Exact Theory
Approximate Theory
r = 0.100
AMPLITUDE
FREQUENCY
0
1.0
2.0
3.0
4.0
5.0
6.0
7.0
0.94
0.96
0.98
1.00
1.02
1.04

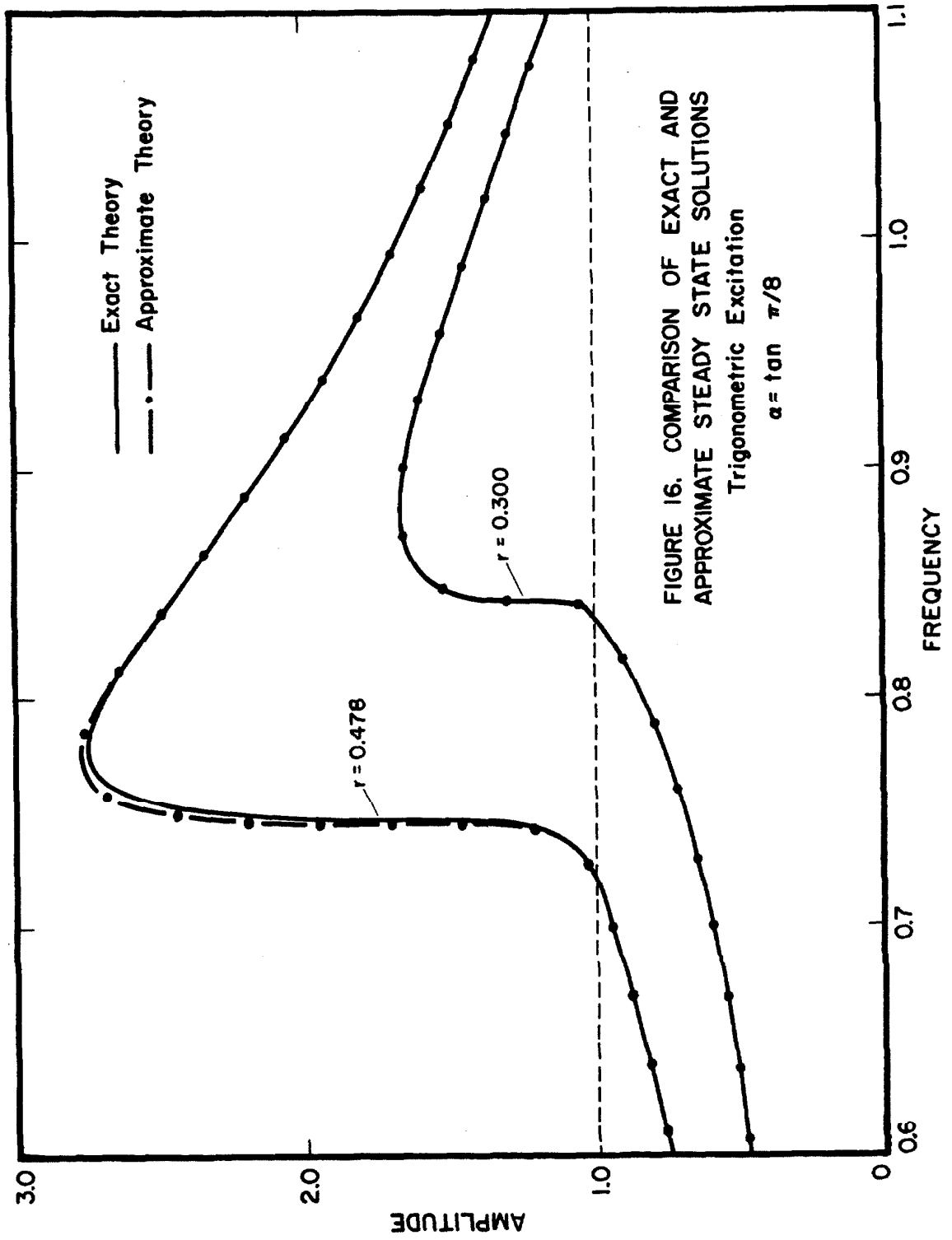

FIGURE 16. COMPARISON OF EXACT AND APPROXIMATE STEADY STATE SOLUTIONS
Trigonometric Excitation
$\alpha = \tan \pi/8$

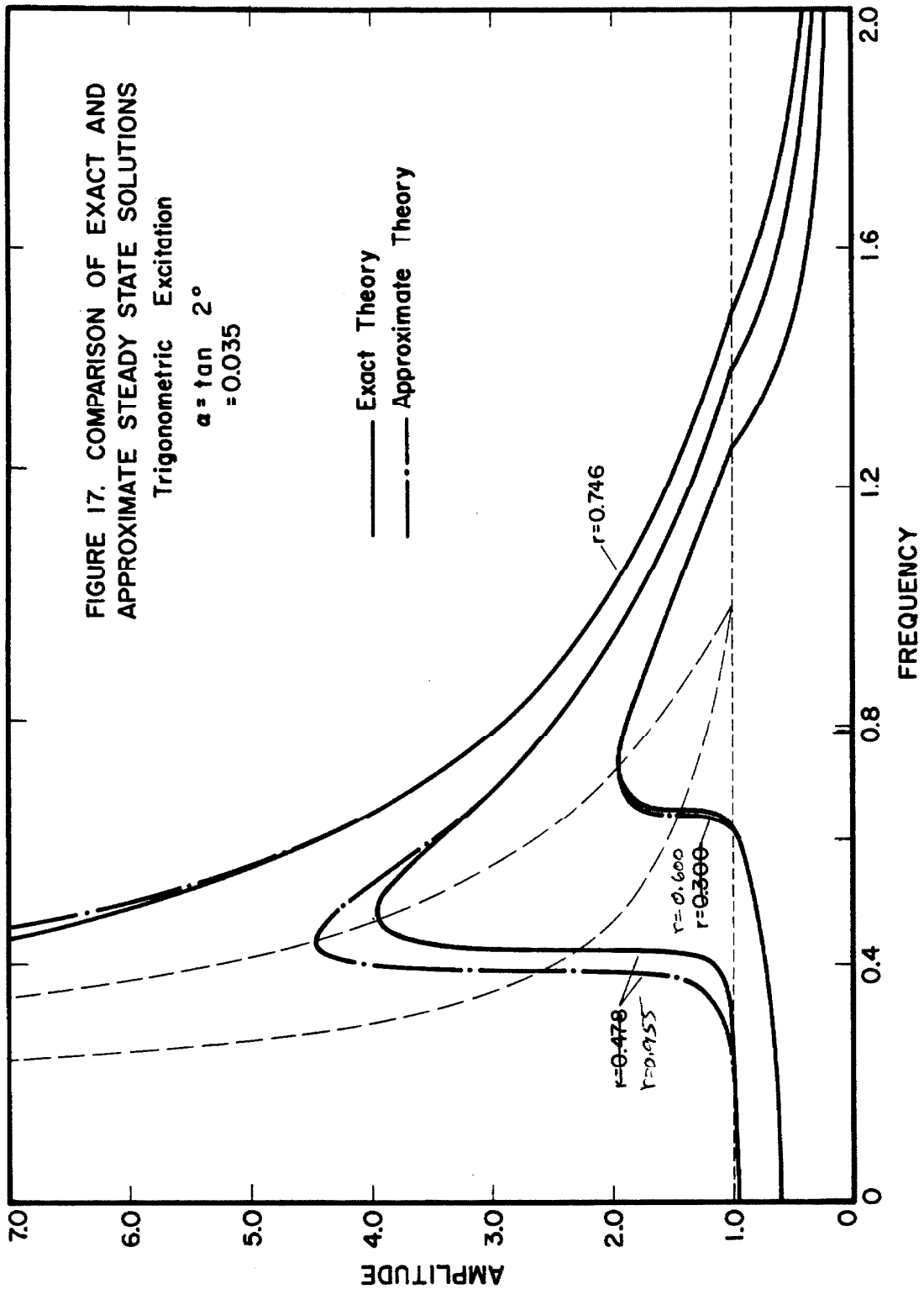
FIGURE 17. COMPARISON OF EXACT AND APPROXIMATE STEADY STATE SOLUTIONS
Trigonometric Excitation
α = tan 2°
=0.035
Exact Theory
Approximate Theory
r=0.746
r=0.600
r=0.300
r=0.478
r=0.955
AMPLITUDE
FREQUENCY
0
1.0
2.0
3.0
4.0
5.0
6.0
7.0
0.4
0.8
1.2
1.6
2.0

equation (2.112), it will be seen that

$$\overline{\varepsilon(x,\dot{x})^2} = \frac{1}{2\pi}\int_0^{2\pi}\left[f(A,\theta) - S(A)\sin\theta - C(A)\cos\theta\right]^2 d\theta. \qquad (2.125)$$

Integrating this expression and using the orthogonality properties of the trigonometric functions then gives

$$\overline{\varepsilon(x,\dot{x})^2} = \frac{1}{2\pi}\int_0^{2\pi}\left[f(A,\theta)\right]^2 d\theta - \frac{1}{2}\left[C^2(A) + S^2(A)\right]$$

$$= \overline{f^2}(A) - \frac{1}{2}\left[C^2(A) + S^2(A)\right]. \qquad (2.126)$$

All of the quantities appearing on the right hand side of equation (2.126) are known or may be calculated using equations (2.121) through (2.124). Thus, $\overline{\varepsilon^2}$ may be regarded as a known function of the amplitude A and the hysteresis loop parameter α. In particular, for the limiting case of $\alpha \approx 1$, it may easily be shown that ε is of order $(1-\alpha)$ for all A finite.

Assume that the true steady state displacement may be written as

$$x = A\cos(\omega t - \phi) + \xi \qquad (2.127)$$

where $A\cos(\omega t - \phi)$ satisfies the linearized equation of motion (2.108), and ξ is composed of terms in $3\omega t$ and higher multiples of the excitation frequency. Then, from the complete equation of motion (2.105) it is seen that ξ must satisfy a differential equation of the form

$$\ddot{\xi} + \gamma\dot{\xi} + \kappa\xi = \varepsilon(x,\dot{x},t) \qquad (2.128)$$

where the time dependence of ε has been noted explicitly. If ε is broken up into its Fourier components this equation may be solved directly. Thus, assuming that the largest contribution will come from the term in $3\omega t$, the magnitude of

the solution becomes approximately

$$|\xi| \approx \frac{|\varepsilon|}{\sqrt{(9\omega^2 - \kappa^2)^2 + (\gamma\omega)^2}} \tag{2.129}$$

But, in the range of frequencies where the motion is predominantly fundamental in character

$$\omega \approx 1$$

and, as a first approximation, κ may be taken as 1 and γ as 0. Hence for these conditions

$$|\xi| \approx |\varepsilon|/8. \tag{2.130}$$

A measure of the fractional amount by which the single component approximation misrepresents the actual system displacement may therefore be defined by

$$\Psi \equiv \frac{\left(\overline{\varepsilon^2}\right)^{1/2}}{8A/\sqrt{2}} \tag{2.131}$$

$$\approx \left(\frac{\overline{\xi^2}}{\overline{x^2}}\right)^{1/2} . \tag{2.132}$$

Values of this parameter have been calculated and are shown in Fig. 18. On the basis of this figure one would expect the closeness of agreement between approximate and exact solutions to be very good even for rather marked system nonlinearities so long as attention is limited to the region of validity of the present analysis ($\omega \approx 1$). Indeed, this is exactly what was observed in the calculated frequency response curves of Figs. 15, 16, and 17.

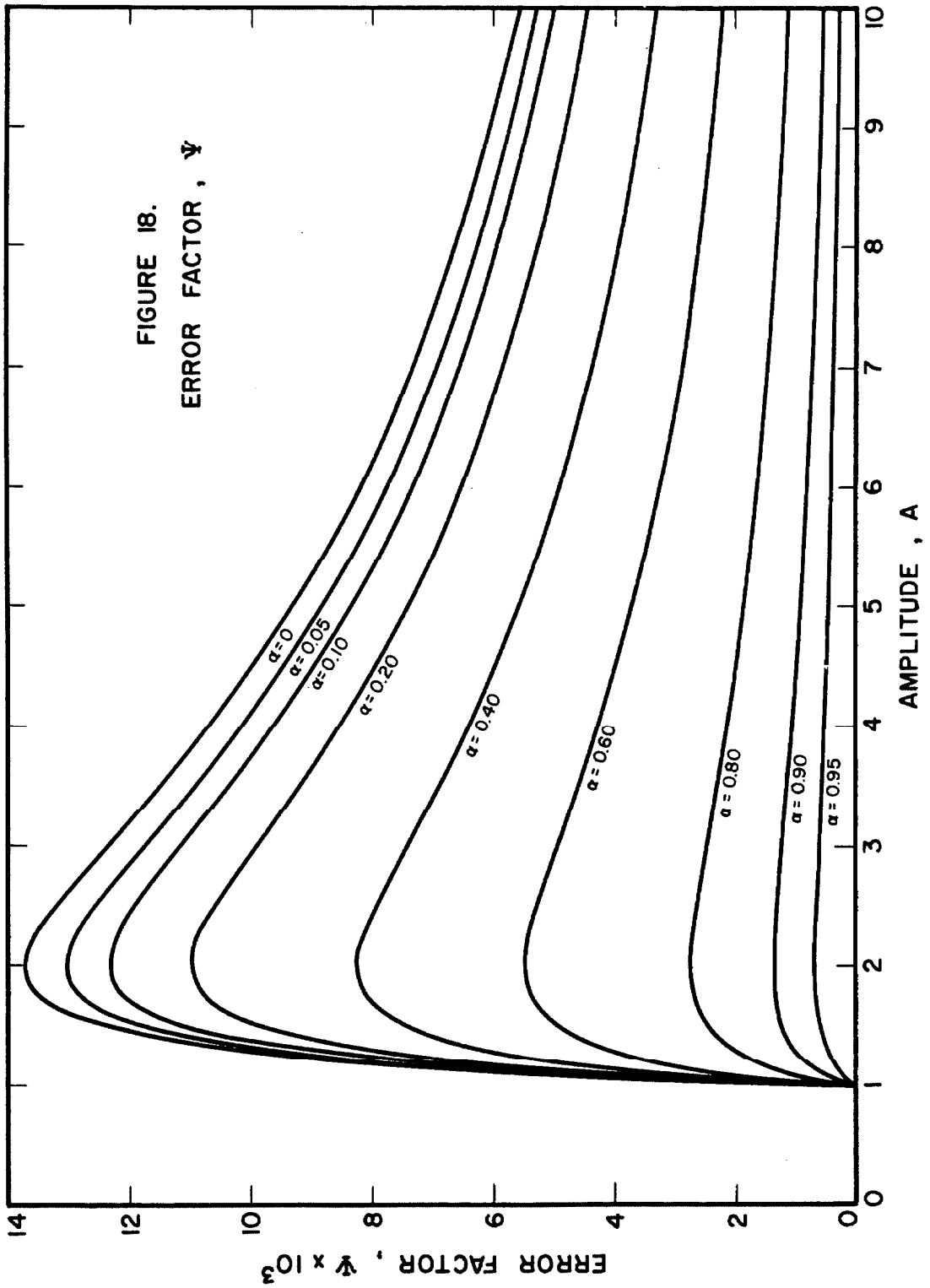
FIGURE 18.
ERROR FACTOR , Ψ
ERROR FACTOR , Ψ x 10³
AMPLITUDE , A
α=0
α=0.05
α=0.10
α=0.20
α=0.40
α=0.60
α=0.80
α=0.90
α=0.95
0
2
4
6
8
10
12
14
1
3
5
7
9

Locus of Peak Amplitude

The condition for peak amplitude of response will be that the two roots of the frequency equation (2.120) coalesce. Formally, this condition may be stated as

$$r = - S(A_p) \tag{2.133}$$

where the subscript p signifies the value corresponding to the peak response, and the negative sign is chosen because r has been defined as positive and $S(A_p)$ is inherently negative. Then, from (2.120) the equation for the locus of peak amplitude becomes

$$\omega_p^2 = C(A_p)/A_p. \tag{2.134}$$

Expanding $C(A_p)$ from equation (2.124a)

$$\omega_p^2 = \alpha + \frac{(1-\alpha)}{\pi} \left(\theta_p^* - \frac{1}{2} \sin 2\theta_p^* \right) \tag{2.135}$$

where

$$\theta_p^* = \cos^{-1} \left[\frac{(A_p - 2)}{A_p} \right] . \tag{2.136}$$

The locus of peak amplitude as obtained from (2.135) and (2.136) is shown by a dashed line in Fig. 17.

From equation (2.133) it is possible to obtain an expression relating the peak amplitude of response to the amplitude of excitation. Thus, substituting for $S(A_p)$ from (2.124b) it will be seen that

$$r = A_p \frac{(1-\alpha)}{\pi} \sin^2 \theta_p^* . \tag{2.137}$$

But θ_p^* may now be eliminated using equation (2.136). Therefore, rearranging terms it is found that

$$A_p = \frac{4(1-\alpha)/\pi}{4(1-\alpha)/\pi - r} . \tag{2.138}$$

Since A_p has been defined as positive, equation (2.138) implies that the system exhibits unbounded resonance if

$$r \geqslant 4(1-\alpha)/\pi. \tag{2.139}$$

From (2.135) and (2.136) the frequency at which this resonance first occurs will be

$$\omega = \sqrt{\alpha}. \tag{2.140}$$

Also, from (2.133) and (2.118b) it will be seen that at the point of peak response

$$\sin \phi_p = 1, \quad \phi_p = \pi/2. \tag{2.141}$$

Therefore, the approximate theory predicts precisely the same type of unbounded phase and amplitude resonance as was obtained by means of the exact theory in an earlier section. The underlying reason for this is, of course, that in the limit of extremely large amplitudes of oscillation the equation of motion actually becomes linear. Thus, in this limiting case the linearized treatment should be expected to be equivalent to the exact analysis.

Locus of Vertical Tangency

The condition that a frequency response curve have a point of vertical tangency may be stated as

$$\frac{\partial \omega}{\partial A} = 0. \tag{2.142}$$

Now, expanding equation (2.118a) by means of equation (2.124a) gives

$$\omega^2 = \frac{(1-\alpha)}{\pi}\theta^* + \alpha - (1-\alpha)\frac{\sin 2\theta^*}{2\pi} - \frac{r}{A}\cos\phi. \tag{2.143}$$

Thus, applying the vertical tangency condition (2.142),

$$2\omega\frac{\partial \omega}{\partial A} = 0 = \frac{(1-\alpha)}{\pi}(1-\cos 2\theta^*)\frac{\partial \theta^*}{\partial A} + \frac{r}{A^2}\cos\phi + \frac{r}{A}\sin\phi\frac{\partial \phi}{\partial A}. \tag{2.144}$$

But, from equations (2.118b) and (2.124b)

$$\frac{r}{A} \sin \phi = \frac{(1-\alpha)}{\pi} \sin^2 \theta^* , \tag{2.145}$$

and from equations (2.118a) and (2.134)

$$\frac{r}{A} \cos \phi = \omega_p^2 - \omega^2 . \tag{2.146}$$

Hence, differentiating (2.145) and using (2.146) to eliminate $\cos \phi$ it may be shown that

$$\frac{\partial \phi}{\partial A} = \frac{(1-\alpha)}{\pi} \frac{\frac{1}{A} \sin^2 \theta^* + \frac{\partial \theta^*}{\partial A} \sin 2\theta^*}{\omega_p^2 - \omega^2} . \tag{2.147}$$

Further, using equation (2.122), it will be seen that

$$\frac{\partial \theta^*}{\partial A} = \frac{-2}{A^2 \sin \theta^*} \tag{2.148}$$

and

$$\sin^2 \theta^* = \frac{4}{A^2} (A-1). \tag{2.149}$$

Therefore, equations (2.145) through (2.149) may be substituted into the vertical tangency equation (2.144) to give

$$(\omega_p^2 - \omega_v^2)^2 - 2\left[\frac{2(1-\alpha)}{A_v \pi} \sin \theta^* (A_v)\right](\omega_p^2 - \omega_v^2) + \left[\frac{2(1-\alpha)}{A_v \pi} \sin \theta^* (A_v)\right]^2 = 0 \tag{2.150}$$

where the subscript v signifies the value of the variable at the point of vertical tangency. Now the left hand side of (2.150) is a perfect square so the equation for the locus of vertical tangency becomes simply

$$\omega_v^2 = \omega_p^2 - \frac{2(1-\alpha)}{A_v \pi} \sin \theta^* (A_v). \tag{2.151}$$

Or, in expanded form this may be written as

$$\omega_v^2 = \frac{1}{\pi}\left[(1-\alpha)\,\theta^*(A_v) + \alpha\pi - (1-\alpha)\sin\theta^*(A_v)\right]. \qquad (2.152)$$

The locus of vertical tangency as obtained from equation (2.152) is shown by a dashed line in Fig. 17.

It will be noted that the present case there is only one locus of vertical tangency since the two roots of (2.150) were identical. This result enables one to make certain conclusions regarding the stability of steady state oscillations as will be discussed in the following subsection.

Stability

Derivation of the approximate system equations by the method of equivalent linearization does not lend itself to any direct investigation of stability. Therefore, the only observations which can be made relative to stability must be made on the basis of the general character of any loci of vertical tangency. In the present case, there is only one such locus. Thus, it may be concluded that the steady state frequency response curves are all single-valued, but beyond this, little can be said as to the actual stability of any particular portion of the frequency response curve. The stability problem was considered in some detail in the earlier mentioned work by Professor Caughey using the method of slowly varying parameters. There it was shown that the steady state response predicted by the first order theory is stable or marginally stable for all frequencies of excitation. A similar analysis of stability will be carried out later in the course of the present work for the hysteretic system with viscous damping.

Ultraharmonic Response

Assume that the displacement can be represented by

$$x(t) = A^{(1)} \cos \theta^{(1)} + A^{(3)} \cos \theta^{(3)} \tag{2.153}$$

where

$$\begin{aligned} \theta^{(1)} &= \omega t - \phi^{(1)} \\ \theta^{(3)} &= 3\omega t - \phi^{(3)} \end{aligned} \tag{2.154}$$

Then, the restoring force $f(x, \dot{x})$ may likewise be expressed in terms of the first two odd order terms of a Fourier series giving

$$f(x, \dot{x}) = C^{(1)} \cos \theta^{(1)} + S^{(1)} \sin \theta^{(1)} + C^{(3)} \cos \theta^{(3)} + S^{(3)} \sin \theta^{(3)} \tag{2.155}$$

where

$$C^{(j)} = \frac{1}{\pi} \int_0^{2\pi} f(x, \dot{x}) \cos \theta^{(j)} \, d\theta^{(1)} \; ; \; j = 1, 3 \tag{2.156a}$$

$$S^{(j)} = \frac{1}{\pi} \int_0^{2\pi} f(x, \dot{x}) \sin \theta^{(j)} \, d\theta^{(1)} \; ; \; j = 1, 3 \tag{2.156b}$$

But from (2.153)

$$\ddot{x} = -\omega^2 A^{(1)} \cos \theta^{(1)} - 9\omega^2 A^{(3)} \cos \theta^{(3)}. \tag{2.157}$$

Thus, substituting (2.155) and (2.157) into the differential equation of motion (2.4), for trigonometric excitation

$$\begin{aligned} -\omega^2 A^{(1)} \cos \theta^{(1)} - 9\omega^2 A^{(3)} \cos \theta^{(3)} + C^{(1)} \cos \theta^{(1)} + S^{(1)} \sin \theta^{(1)} \\ + C^{(3)} \cos \theta^{(3)} + S^{(3)} \sin \theta^{(3)} = r \cos (\theta^{(1)} + \phi^{(1)}). \end{aligned} \tag{2.158}$$

Collecting coefficients of like trigonometric terms then gives

$$\begin{aligned} -\omega^2 A^{(1)} + C^{(1)} &= r \cos \phi^{(1)} \\ S^{(1)} &= -r \sin \phi^{(1)} \\ -9\omega^2 A^{(3)} + C^{(3)} &= 0 \\ S^{(3)} &= 0 \end{aligned} \tag{2.159}$$

Hence, the problem of determining the steady state motion has been reduced to the solution of the four equations (2.159) for the four unknown quantities $A^{(1)}$, $A^{(3)}$, $\theta^{(1)}$ and $\theta^{(3)}$.

For a linear system $f(x, \dot{x})$ is equal to some linear combination of the displacement and velocity and it is readily seen from the last of equations (2.159) that $A_3 = 0$. However, for a non-linear system $S^{(3)}$ will in general be a function of both $A^{(1)}$ and $A^{(3)}$ in such a way that $A^{(3)}$ will not be identically zero for all ω and r. Therefore, in the case of the bilinear hysteretic system one would also expect to find that $A^{(3)}$ is finite.

Actual evaluation of the functions $C^{(1)}$, $S^{(1)}$, $C^{(3)}$, and $S^{(3)}$ for a particular case is complicated by the fact that the hysteresis loop may no longer have the simple shape of Fig. 2. Also, the problem of solving for the time angle at each point of slope change now becomes much more involved and it may be necessary to consider as many as three such points. Therefore, the analytic analysis of ultraharmonic response will be carried no further at this time. However, the entire problem will be taken up again later in connection with electric analog studies.

F. Addition of Viscous Damping

In this section the problem of the steady state response of the bilinear hysteretic system will be extended to include a viscous damping term. The method of solution will be the method of slowly varying parameters originally developed by Kryloff and Bogoliuboff (See Ref. 16) and used, as mentioned earlier, by T. K. Caughey[13] to investigate the case without viscous damping.

Formulation of the Governing Equations

The differential equation of motion with viscous damping may be written as

$$\ddot{x} + 2\beta x + f(x, \dot{x}) = r \cos \omega t \tag{2.160}$$

where $f(x, \dot{x})$ is again the bilinear hysteretic restoring force function and β is the coefficient of viscous damping.

Assume a solution of the form

$$x(t) = A \cos (\omega t - \phi) \tag{2.161}$$

where both the amplitude A and phase angle ϕ are slowly varying functions of t. Let

$$\theta = \omega t - \phi. \tag{2.162}$$

Then, differentiating (2.161) with respect to t,

$$\dot{x}(t) = - A \omega \sin \theta + A \dot{\phi} \sin \theta + \dot{A} \cos \theta. \tag{2.163}$$

But, by analogy to Lagrange's method of variation of a parameter one may set

$$\dot{A} \cos \theta + A \dot{\phi} \sin \theta = 0. \tag{2.164}$$

Thus,

$$\dot{x}(t) = - A \omega \sin \theta \tag{2.165}$$

and it will be seen that

$$\ddot{x}(t) = - A\omega^2 \cos \theta - \dot{A} \omega \sin\theta + A\omega \dot{\phi} \cos\theta. \tag{2.166}$$

Substituting equations (2.165) and (2.166) into the equation of motion (2.160) then gives

$$-A\omega^2 \cos\theta - \dot{A}\omega\sin\theta + A\omega\dot{\phi}\cos\theta - 2\beta A\omega\sin\theta + f(A,\theta) = r\cos(\theta+\phi). \tag{2.167}$$

Multiplying (2.164) by $\omega\sin\theta$, (2.167) by $\cos\theta$ and adding it is seen that

$$A\omega\dot{\phi} - A\omega^2\cos^2\theta - 2\beta A\omega\sin\theta\cos\theta + f(A,\theta)\cos\theta = r\cos(\theta+\phi)\cos\theta. \tag{2.168}$$

However, both A and ϕ have been assumed to be slowly varying functions of the time t. Therefore, within the limits of validity of this assumption one is justified in regarding A, ϕ, $\dot{A}$, and $\dot{\phi}$ as very nearly constant over any one cycle of θ. Hence, if equation (2.168) is averaged over one complete cycle of θ it will be found that

$$2A\omega\dot{\phi} - A\omega^2 + \frac{1}{\pi}\int_0^{2\pi} f(A,\theta)\cos\theta\, d\theta = r\cos\phi. \tag{2.169}$$

Multiplying (2.164) by $\omega\cos\theta$, (2.167) by $\sin\theta$ and subtracting, it is seen that

$$\dot{A}\omega\dot{\phi} + A\omega^2\cos\theta\sin\theta + 2\beta A\omega\sin^2\theta - f(A,\theta)\sin\theta = -r\cos(\theta+\phi)\sin\theta. \tag{2.170}$$

Thus, again averaging over one cycle of θ and regarding A, $\dot{A}$ and $\dot{\phi}$ as slowly varying, it will be found that

$$2\dot{A}\omega + 2\beta\omega A - \frac{1}{\pi}\int_0^{2\pi} f(A,\theta)\sin\theta\, d\theta = r\sin\phi. \tag{2.171}$$

As in the case of the system without viscous damping, it is convenient to introduce the two parameters C(A) and S(A) defined by

$$C(A) = \frac{1}{\pi}\int_0^{2\pi} f(A,\theta)\cos\theta\, d\theta$$

$$S(A) = \frac{1}{\pi}\int_0^{2\pi} f(A,\theta)\sin\theta\, d\theta \tag{2.172}$$

where it will be recalled that in terms of the hysteresis loop parameters

$$C(A) = \frac{A}{\pi}\left[(1-\alpha)\,\theta^* + \alpha\pi - \frac{(1-\alpha)}{2}\sin 2\theta^*\right]; \quad A > 1$$

$$S(A) = -\frac{A(1-\alpha)}{\pi}\sin^2\theta^* \qquad ; \quad A > 1 \qquad (2.173)$$

$$\theta^* = \cos^{-1}\left(1 - \frac{2}{A}\right)$$

Then equations (2.169) and (2.171) which govern the system motion may be written as

$$2A\omega\dot{\phi} - A\omega^2 + C(A) = r\cos\phi \qquad (2.174a)$$

$$2\dot{A}\omega + 2\beta\omega A - S(A) = r\sin\phi \qquad (2.174b)$$

Steady State Results

The equations for the steady state response will be obtained by setting $\dot{A}$ and $\dot{\phi}$ equal to zero in equations (2.174a and b). This then gives

$$-A_0\omega^2 + C(A_0) = r\cos\phi_0 \qquad (2.175a)$$

$$+2\beta\omega A_0 - S(A_0) = r\sin\phi_0. \qquad (2.175b)$$

where the subscript 0 signifies steady state values. Equations (2.175a and b) may now be used to obtain the steady state values of A and ϕ as a function of ω for given α, r, and β. This has been done for the case of $r = 4(1-\alpha)/\pi$ and the results are shown in Fig. 19. It will be noted from this figure that the major effect of the addition of viscous damping is, as one would expect, to reduce the peak amplitude of response. However, it is also seen that this amplitude reduction is accompanied by a marked decrease in the slope of the low frequency side of the response curve. Thus, even for moderate levels of viscous damping the frequency response curves lose nearly all of the asymmetric character of the purely hysteretic system and become more like the ordinary curves for a linear damped

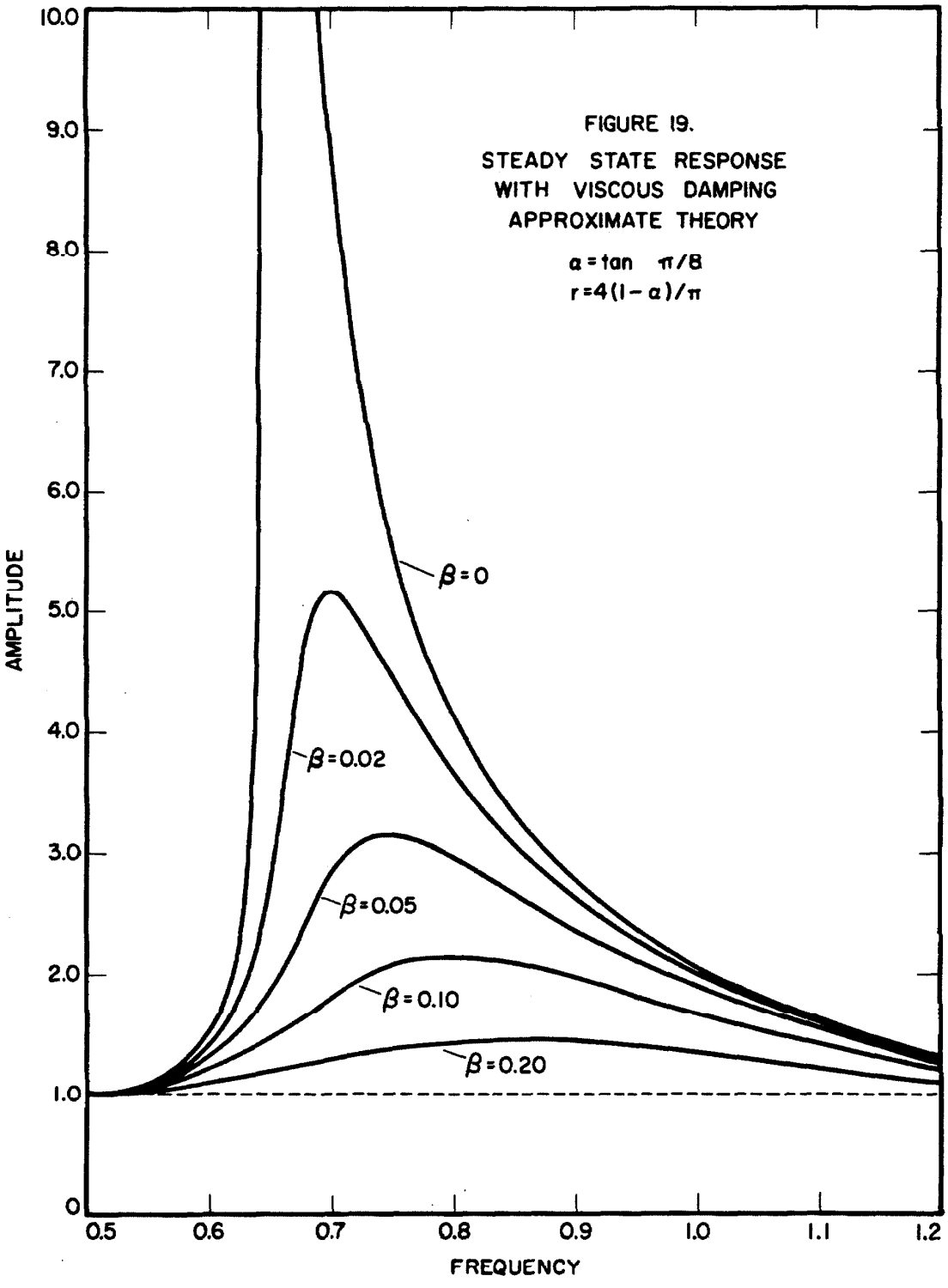
FIGURE 19.
STEADY STATE RESPONSE
WITH VISCOUS DAMPING
APPROXIMATE THEORY
α = tan π/8
r = 4(1 − α)/π
β = 0
β = 0.02
β = 0.05
β = 0.10
β = 0.20
AMPLITUDE
FREQUENCY
10.0
9.0
8.0
7.0
6.0
5.0
4.0
3.0
2.0
1.0
0
0.5
0.6
0.7
0.8
0.9
1.0
1.1
1.2

system. This is one reason why it is very difficult to recognize the existence of hysteretic behavior in most real physical systems.

Stability of the Steady State Response

Let

$$A = A_0 + \xi$$
$$\phi = \phi_0 + \psi \tag{2.176}$$

where ξ and ψ are small perturbations on the steady state values A_0 and ϕ_0. Then, substituting relations (2.176) into equations (2.174a and b) and using the steady state equations (2.175a and b)

$$2A_0\dot{\psi}\omega - \xi\omega^2 + \frac{\partial C}{\partial A}\xi = -r\psi\sin\phi_0$$
$$2\dot{\xi}\omega + 2\beta\omega\xi - \frac{\partial S}{\partial A}\xi = r\psi\cos\phi_0 \tag{2.177}$$

where it is to be understood that both S and C are functions of A and all partial derivatives are evaluated at the point $A = A_0$. Thus, using the steady state equations (2.175a and b) to eliminate $r\sin\phi_0$ and $r\cos\phi_0$ from (2.177), one obtains

$$2A_0\omega\dot{\psi} + \left[2\beta\omega A_0 - S(A_0)\right]\psi + \left(\frac{\partial C}{\partial A} - \omega^2\right)\xi = 0$$
$$2\omega\dot{\xi} + \left[\omega^2 A_0 - C(A_0)\right]\psi + \left(2\beta\omega - \frac{\partial S}{\partial A}\right)\xi = 0. \tag{2.178}$$

Now, let

$$\xi = \xi_0 e^{\lambda t}$$
$$\psi = \psi_0 e^{\lambda t}. \tag{2.179}$$

Then, substituting relations (2.179) into (2.178)

$$\left[2A_0\omega\lambda + 2A_0\omega\beta - S(A_0)\right]\psi_0 + \left(\frac{\partial C}{\partial A} - \omega^2\right)\xi_0 = 0$$
$$\left[\omega^2 A_0 - C(A_0)\right]\psi_0 + \left(2\omega\lambda + 2\omega\beta - \frac{\partial S}{\partial A}\right)\xi_0 = 0. \tag{2.180}$$

The frequency equation is obtained by setting the determinant of the coefficients of the set of equations (2.180) equal to zero. In this way it is found that

$$(2\omega\lambda)^2 + (2\omega\lambda)\left[4\beta\omega - \frac{S(A_0)}{A_0} - \frac{\partial S}{\partial A}\right] + \left[2\beta\omega - \frac{S(A_0)}{A_0}\right]\left[2\beta\omega - \frac{\partial S}{\partial A}\right]$$
$$+ \left[\frac{\partial C}{\partial A} - \omega^2\right]\left[\frac{C(A_0)}{A_0} - \omega^2\right] = 0. \tag{2.181}$$

From equations (2.173) it may be shown that

$$\frac{\partial C}{\partial A} = \frac{1}{\pi}\left[(1-\alpha)\theta_0^* + \alpha\pi + \frac{(1-\alpha)}{2}\sin 2\theta_0^* - 2(1-\alpha)\sin\theta_0^*\right]$$
$$\frac{\partial S}{\partial A} = -\frac{(1-\alpha)}{\pi}(2 - 2\cos\theta_0^* - \sin^2\theta_0^*). \tag{2.182}$$

Thus,

$$\left[2\beta\omega - \frac{S(A_0)}{A_0}\right]\left[2\beta\omega - \frac{\partial S}{\partial A}\right] + \left[\frac{\partial C}{\partial A} - \omega^2\right]\left[\frac{C(A_0)}{A_0} - \omega^2\right]$$
$$= \omega^2 - \frac{1}{\pi}\left[\alpha\pi + (1-\alpha)\theta^* - (1-\alpha)\sin\theta_0^*\right]^2 + 4\beta\omega\left[\beta\omega + \frac{(1-\alpha)}{\pi}(1-\cos\theta_0^*)\right] \tag{2.183}$$

But equations (2.173), (2.182) and (2.183) may now be substituted into the frequency equation (2.181) to give

$$(2\omega\lambda)^2 + 2(2\omega\lambda)\left[\frac{(1-\alpha)}{\pi}(1-\cos\theta_0^*) + 2\beta\omega\right] + 4\beta\omega\left[\beta\omega + \frac{(1-\alpha)}{\pi}(1-\cos\theta_0^*)\right]$$
$$+ \left[\omega^2 - \frac{1}{\pi}\left|\alpha\pi + (1-\alpha)\theta_0^* - (1-\alpha)\sin\theta_0^*\right|\right]^2 = 0 \tag{2.184}$$

Therefore,

$$(2\omega\lambda) = -\left[\frac{(1-\alpha)}{\pi}(1-\cos\theta_0^*) + 2\beta\omega\right] \pm \left\{4\beta\omega\left[\beta\omega + \frac{(1-\alpha)}{\pi}(1-\cos\theta_0^*)\right]\right.$$
$$\left. -\left[\omega^2 - \frac{1}{\pi}\left(\alpha\pi + (1-\alpha)\theta_0^* - (1-\alpha)\sin\theta_0^*\right)\right]^2 + \left[\frac{(1-\alpha)}{\pi}(1-\cos\theta_0^*) + 2\beta\omega\right]^2\right\}^{1/2} \tag{2.185}$$

and if β is finite,

$$\mathcal{R}(2\omega\lambda) < 0. \tag{2.186}$$

Thus, the steady state solution for the viscous damped bilinear hysteretic system is always stable.

It is also possible to consider the stability of the hysteretic system without viscous damping merely by letting β go to zero in equation (2.186). In this case

$$(2\omega\lambda) = -\left[\frac{(1-\alpha)}{\pi}(1-\cos\theta_0^*)\right] \pm \left\{\left[\frac{(1-\alpha)}{\pi}(1-\cos\theta_0^*)\right]^2\right.$$
$$\left. -\left[\omega^2 - \frac{1}{\pi}\left(\alpha\pi + (1-\alpha)\theta_0^* - (1-\alpha)\sin\theta_0^*\right)\right]^2\right\}^{1/2} \tag{2.187}$$

and it is apparent that

$$\mathcal{R}(2\omega\lambda) \leq 0 \tag{2.188}$$

for all A and ω. Thus, even in the absence of viscous damping the system is always stable or marginally stable. Points of marginal stability are defined as points where

$$(2\omega\lambda) = 0,$$

and in the present system this will be observed to be the case when

$$\omega^2 = \frac{1}{\pi}\left[\alpha\pi - (1-\alpha)\theta_0^* - (1-\alpha)\sin\theta_0^*\right]. \tag{2.189}$$

But this expression is recognized as being exactly the same as equation (2.152) for the locus of vertical tangency. Therefore, it is seen that the points of vertical

tangency are also the points of marginal stability.

Locus of Peak Amplitude

The steady state equations (2.175a and b) may just as well be written in the form

$$\omega^2 = \alpha + \frac{(1-\alpha)}{\pi}\left(\theta_0^* - \frac{1}{2}\sin 2\theta_0^*\right) - \frac{r}{A_0}\cos\phi_0 \tag{2.190a}$$

$$\omega = \frac{1}{2\beta}\left[\frac{r}{A_0}\sin\phi_0 - \frac{(1-\alpha)}{\pi}\sin^2\theta_0^*\right]. \tag{2.190b}$$

But now one may think of these two equations as being two separate functional relations giving ω in terms of ϕ_0 for fixed A_0 and r. In general, these two relations will have two points of intersection signifying the two roots of ω which exist for a given A_0 and r. However, at the point of peak response there will be only one root of ω and correspondingly only one point of intersection for the two relations. This condition may then be expressed as

$$\left.\frac{\partial\omega}{\partial\phi_0}\right|_a = \left.\frac{\partial\omega}{\partial\phi_0}\right|_b \tag{2.191}$$

where the subscript "a" denotes that the partial derivative is evaluated from equation (2.190a) and the subscript "b" has a similar meaning with regard to equation (2.190b). Carrying out the differentiations indicated in (2.191)

$$\left.\frac{\partial\omega}{\partial\phi_0}\right|_a = \frac{r}{2A_0\omega}\sin\phi_0$$

$$\left.\frac{\partial\omega}{\partial\phi_0}\right|_b = \frac{r}{2A_0\beta}\cos\phi_0. \tag{2.192}$$

Thus, from (2.191)

$$\sin\phi_0 = \frac{\omega}{\beta}\cos\phi_0. \tag{2.193}$$

The equation for the locus of peak amplitude may now be obtained by eliminating r between equations (2.190a and b) and using (2.193) to eliminate ϕ_0. This gives

$$\omega_p^3 + \left[2\beta^2 - \alpha - \frac{(1-\alpha)}{\pi}\theta_0^* - \frac{(1-\alpha)}{2}\sin 2\theta_0^*\right]\omega_p + \frac{\beta(1-\alpha)}{\pi}\sin^2\theta_0^* = 0 \tag{2.194}$$

where the subscript "p" denotes that the value is at the point of peak amplitude.

For large amplitudes A_0 it is seen from (2.173) that θ_0^* approaches zero. Therefore, equation (2.194) becomes

$$\omega_p^3 + (2\beta^2 - \alpha)\omega_p = 0$$

and

$$\omega_p \to 1/\sqrt{\alpha - 2\beta^2} \qquad \text{as } A_0 \to \infty. \tag{2.195}$$

For A_0 equal to one, θ_0^* equals π and (2.194) becomes

$$\omega_p^3 + (2\beta^2 - 1)\omega_p = 0.$$

Hence, in this limiting case of linear behavior

$$\omega_p = 1/\sqrt{1 - 2\beta^2} \quad , \; A_0 = 1. \tag{2.196}$$

Unbounded Resonance

Finally, consider equation (2.175b) eliminating θ_0^* by means of the last of equations (2.173). This gives

$$(2\beta\omega)\, A_0^2 + \left[r \sin\phi_0 - \frac{4(1-\alpha)}{\pi}\right] A_0 - \frac{4(1-\alpha)}{\pi} = 0 \tag{2.197}$$

But now for finite β and ω, this equation will have no infinite roots. Thus, the infinite amplitude resonance which was observed in the system without viscous damping will not be found in the present case with viscous damping included.

Locus of Vertical Tangency

It may be shown on a completely general basis (See Ref. 17) that the condition for a vertical tengency to the frequency response curve is that the constant term of the frequency equation of stability be identically zero. The frequency equation for infinitesimal stability in the present case is equation (2.184). Thus, the condition for a vertical tangency will be

$$\left[\omega^2 - \frac{1}{\pi}\left(\alpha\pi + (1-\alpha)\,\theta_0^* - (1-\alpha)\sin\theta_0^*\right)\right]^2 + 4\beta\omega\,\frac{(1-\alpha)}{\pi}(1-\cos\theta_0^*) + (2\beta\omega)^2 = 0 \tag{2.198}$$

But if both β and ω are non-zero, it is seen that condition (2.198) can never be satisfied. Therefore, no locus of vertical tangency exists for the bilinear hysteretic system with viscous damping.

G. Transient Response

Due to the inapplicability of the principle of superposition, a completely general treatment of the transient response of hysteretic systems is not feasible. Instead, each new problem must be treated as a special case using some method of graphic, numeric, or piece-wise analytic integration of the equation of motion. Although such methods may become quite involved, they have been used recently by several workers to study the response of the bilinear hysteretic system to various forms of transient excitation. L. S. Jacobsen[1,2] has considered the transient response to pulse and step function excitation, G. Berg[10] has investigated the problem of earthquake excitation, and N. Ando[12] has solved for the initial transient oscillations of a system which is suddenly subjected to sinusoidal excitation.

One of the more important questions which arises in connection with the transient response of the general hysteretic system concerns the nature of the final state of the system upon completion of the excitation. In some cases it will be found that the system develops a certain permanent offset, while in others the system returns to oscillate about its original point of zero displacement*. If the excitation is reasonably symmetric and of low enough level that the response is due primarily to resonance effects or, if the excitation is of very short duration, any final offset will most likely result from the behavior of the system after the excitation has ceased. Thus, in order to better understand the mechanism by which such an offset may occur, it is instructive to actually follow the motion of a

---

* If there is no viscous damping in the system, the final state will in general be oscillatory.

hysteretic system during the period from the end of the excitation until a steady state condition is reached. This will be done below for the bilinear hysteretic system.

Analytic Considerations

Let the first maxima of the displacement after the excitation has ceased be denoted by x_1 and for the present assume that x_1 is positive*. Then, from (2.3) the subsequent motion of the system will initially be governed by the homogeneous differential equation

$$\ddot{x} + x - (x_1-1)(1-\alpha) = 0. \; ; \; (x_1-2) < x < x_1. \tag{2.199}$$

This equation will remain valid until the system reaches the point at which the restoring force diagram first changes slope. Letting the system displacement and time at this point be x' and t', it is seen from the general solution of (2.199) that

$$x' = \left[x_1 - (x_1-1)(1-\alpha)\right] \cos t' + (x_1-1)(1-\alpha) \tag{2.200}$$

and

$$\dot{x}' = -\left[x_1 - (x_1-1)(1-\alpha)\right] \sin t'. \tag{2.201}$$

But from the normalization of the hysteresis loop, it will be recalled that

$$x' = x_1 - 2. \tag{2.202}$$

---

* A "maxima of the displacement" will herein be taken to mean any displacement x_i which satisfies the conditions

$$\dot{x}_i = 0 \; , \; |x_i| > 1$$

and

$$|f(x_i, 0)| = \alpha|x_i| + (1-\alpha).$$

Thus, from (2.200)

$$\cos t' = \frac{x_1 - 2 - (x_1-1)(1-\alpha)}{x_1 - (x_1-1)(1-\alpha)} . \tag{2.203}$$

Using this result in equation (2.201) for $\dot{x}'$, it may then be shown that

$$\dot{x}' = -2\left[\alpha(x_1-1)\right]^{1/2}, \tag{2.204}$$

where it will be noted that $\dot{x}'$ is real only if

$$x_1 > 1. \tag{2.205}$$

Having determined both x' and $\dot{x}'$, these values may now be used as initial conditions for the motion which proceeds along the restoring force segment of slope α. From (2.3) the differential equation of motion in this regime will be

$$\ddot{x} + \alpha x - (1-\alpha) = 0. \tag{2.206}$$

This equation will govern the system behavior until the velocity becomes zero. If the displacement at the point of zero velocity is denoted by x_2 and the time interval between points x' and x_2 is t_2, then

$$x_2 = (\dot{x}'/\sqrt{\alpha}) \sin \sqrt{\alpha} t_2 + \left[x' - (1-\alpha)/\alpha\right] \cos \sqrt{\alpha} t_2 + (1-\alpha)/\alpha \tag{2.207}$$

and

$$\dot{x}_2 = 0 = \dot{x}' \cos \sqrt{\alpha} t_2 - \sqrt{\alpha}\left[x' - (1-\alpha)/\alpha\right] \sin \sqrt{\alpha} t_2. \tag{2.208}$$

But, from (2.208)

$$\sqrt{\alpha} t_2 = \tan^{-1}\left\{\frac{\dot{x}'}{\sqrt{\alpha}\left[x' - (1-\alpha)/\alpha\right]}\right\} \tag{2.209}$$

Therefore, substituting relations (2.202), (2.204), and (2.209) into equation (2.207)

$$x_2 = -\left[(x_1 - 1 - 1/\alpha)^2 + 4(x_1-1)\right]^{1/2} + (1-\alpha)/\alpha \tag{2.210}$$

where x_2 is now the second maxima of the displacement (in this case a minimum).

Equation (2.210) has been derived by assuming that x_1 is the first maxima of the displacement, that this maxima is positive, and also that x_1 satisfies the condition (2.205). However, the first two of these assumptions were made only as a matter of convenience and it is readily seen that the same type of analysis could be used to find the relation between any two successive maxima regardless of whether they are positive or negative. Thus, with only minor changes of notation, equation (2.210) may be generalized so as to give the value of the $(i+1)^{th}$ maxima of displacement solely in terms of the i^{th} maxima and the hysteresis loop parameter α. This generalized relation will be

$$x_{i+1} = (\operatorname{sgn} x_i)\left\{ -\left[(|x_i| - 1 - 1/\alpha)^2 + 4(|x_i| - 1)\right]^{1/2} + (1-\alpha)/\alpha \right\} \qquad (2.211)$$

and condition (2.205) becomes

$$-x_i (\operatorname{sgn} x_{i+1}) > 1 \qquad (2.212)$$

where

$$|x_1| > 1. \qquad (2.213)$$

Using equation (2.211), the course of the system motion upon completion of the excitation may be followed from maxima to maxima until condition (2.212) is no longer satisfied. At this point equation (2.211) becomes invalid and the system merely oscillates along the restoring force segment of unity slope being energetically unable to move into a region of slope α. These residual oscillations will be undamped linear oscillations and will take place about some mean displacement δ_s given by

$$\delta_s = (1-\alpha)\left[(\operatorname{sgn} x_{k-1}) + x_k \right] \qquad (2.214)$$

where x_k is the last maxima which can be obtained by means of equation (2.211).

Graphical Interpretation

The information contained in equation (2.211) and condition (2.212) may be interpreted graphically as shown in Fig. 20. This figure gives a family of curves which may be used to obtain the $(i + 1)^{th}$ maxima of the displacement in terms of the i^{th} maxima for various values of the parameter α. If, for a particular maxima x_j, the point (x_{j+1}, x_j) lies within the cross-hatched area of the figure, then x_j is the last maxima which will satisfy condition (2.212). Hence, in this case x_{j+1} equals x_k and subsequent motion of the system will take place along a single unity slope segment of the restoring force diagram with an offset δ_s given by (2.214). Thus, for a given initial maxima x_1 one may easily determine each successive maxima up to and including the final maxima x_k which may then be used to calculate the resultant offset.

Maximum Absolute Offset

It will be noted from Fig. 20 that the absolute offset $|\delta_s|$ has a definite upper bound which depends only on the value of the hysteresis loop parameter α. In general, this upper bound may be obtained by setting

$$\frac{dx_k}{dx_{k-1}} = 0 \tag{2.215}$$

where from (2.211)

$$x_k = (\operatorname{sgn} x_{k-1})\left\{-\left[(|x_{k-1}| - 1 - 1/\alpha)^2 + 4(|x_{k-1}| - 1)\right]^{1/2} + (1-\alpha)/\alpha\right\}. \tag{2.216}$$

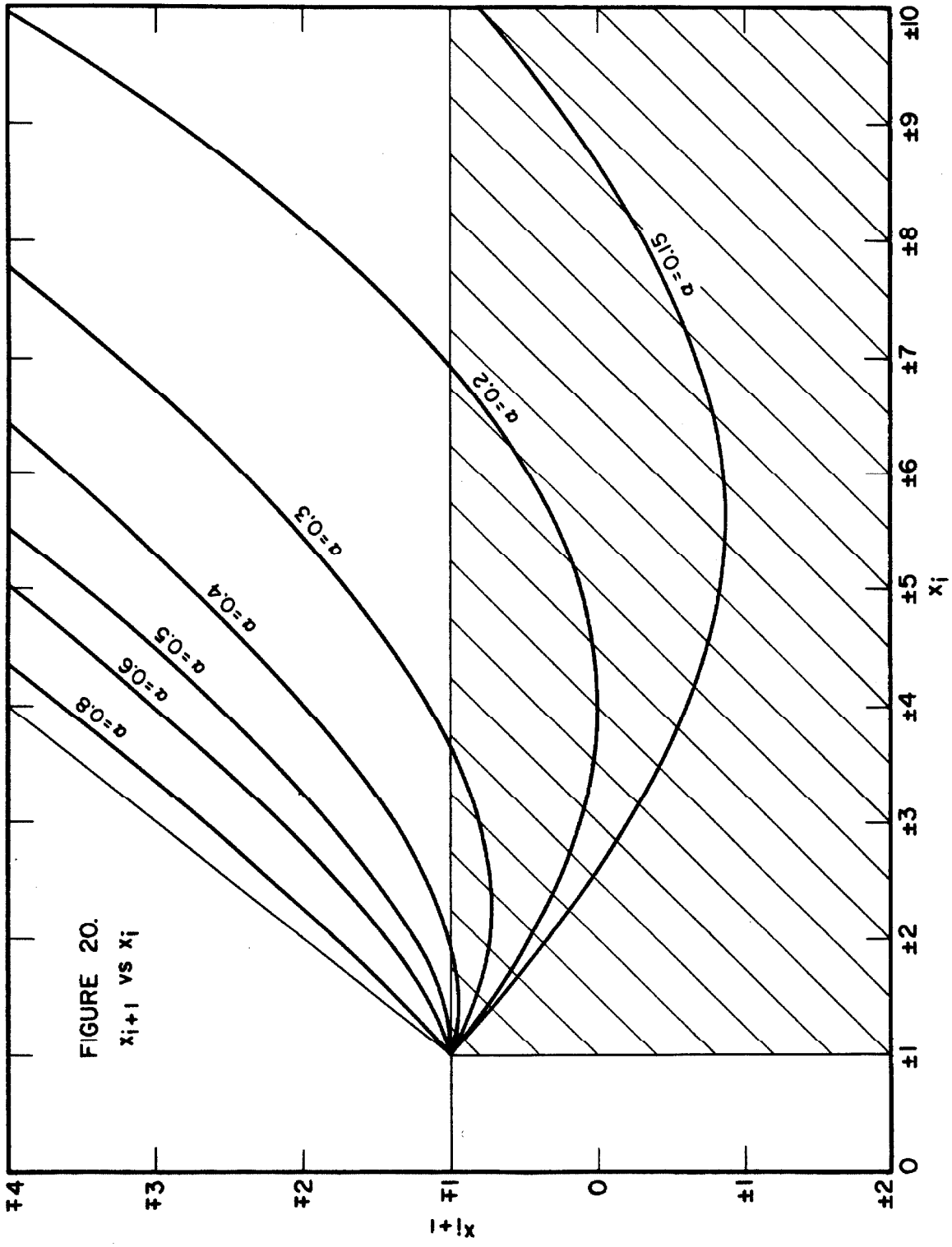

FIGURE 20.
x_{i+1} vs x_i

Thus, differentiating equation (2.216) and setting the resulting expression equal to zero, it may be shown that

$$|x_{k-1}| \left(\frac{dx_k}{dx_{k-1}}\right) = 0 \quad = (1-\alpha)/\alpha . \tag{2.217}$$

However, there can be no solution for x_k if $|x_{k-1}| < 1$. Therefore, if the value of $|x_{k-1}|$ which is predicted by (2.217) is less than one, the maximum of $|\delta_s|$ will actually occur at the point $|x_{k-1}| = 1$. Now, from (2.217)

$$|x_{k-1}| \left(\frac{dx_k}{dx_{k-1}}\right) = 0 \quad < 1, \text{ implies that } \alpha > 1/2. \tag{2.218}$$

Thus, it will be seen that

$$\left|x_{k-1}^{(m)}\right| = \begin{cases} (1-\alpha)/\alpha & ; \ \alpha \leqslant 1/2 \\ 1 & ; \ \alpha \geqslant 1/2 \end{cases} \tag{2.219}$$

where the superscript (m) denotes the value which makes $|\delta_s|$ a maximum. Substituting (2.219) into (2.216) then gives

$$x_k^{(m)} = \begin{cases} (\operatorname{sgn} x_{k-1}^{(m)}) \left\{ (1-\alpha)/\alpha - 2 \left[(1-\alpha)/\alpha \right]^{1/2} \right\} & ; \ \alpha \leqslant 1/2 \\ (\operatorname{sgn} x_{k-1}^{(m)}) \left\{ -1 \right\} & ; \ \alpha \geqslant 1/2 \end{cases} \tag{2.220}$$

and from equation (2.214)

$$|\delta_s|_{max} = \begin{cases} (1-\alpha) \left\{ 1/\alpha - 2 \left[(1-\alpha)/\alpha \right]^{1/2} \right\} & ; \ \alpha \leqslant 1/2 \\ 0 & ; \ \alpha \geqslant 1/2 \end{cases} \tag{2.221}$$

Conclusions

Based on the above analysis which presupposes only the existence of a "maxima of the displacement" after completion of the excitation, it may be

concluded that the maximum offset $|\delta_s|$ resulting from an arbitrary transient oscillation will be bounded for all $\alpha > 0$ and may become unbounded only if $\alpha = 0$. In particular, if $\alpha \geq 1/2$, it has been shown that there can be no permanent offset regardless of the value of the initial maxima x_1 so long as $|x_1| > 1$.

III. TWO DEGREE OF FREEDOM SYSTEM

A. Approximate Steady State Theory

The problem of the steady state response of a two degree of freedom bilinear hysteretic system will now be considered using the method of slowly varying parameters which was so highly successful in the treatment of the single degree of freedom system.

Equations of Motion

In order to simplify the problem mathematically, it will be assumed that the system has the configuration shown schematically in Figs. 21 and 22 with equal unity masses and identical normalized hysteresis loop properties. Let the displacement of the first mass with respect to the moving base be denoted by x_1 and let x_2 be the relative displacement between the first and second masses. Then, for trigonometric excitation of amplitude r and frequency ω the differential equations of motion may be written as

$$\ddot{x}_1 + f(x_1, \dot{x}_1) - f(x_2, \dot{x}_2) = r \cos \omega t \tag{3.1}$$

$$\ddot{x}_2 + 2f(x_2, \dot{x}_2) - f(x_1, \dot{x}_1) = 0 \tag{3.2}$$

where the dot denotes differentiation with respect to the time t.

Formulation of the Approximate Steady State Theory

Assume that the solutions to equations (3.1) and (3.2) may be approximated by

$$\begin{aligned} x_1 &= A_1 \cos \theta_1 \\ x_2 &= A_2 \cos \theta_2 \end{aligned} \tag{3.3}$$

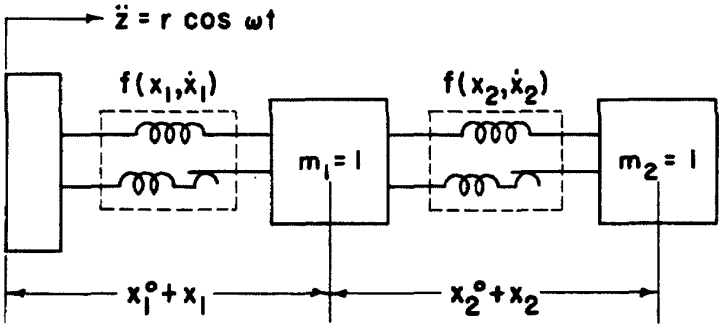

x_1° and x_2° = static displacements

FIGURE 21. TWO DEGREE OF FREEDOM BILINEAR HYSTERETIC SYSTEM

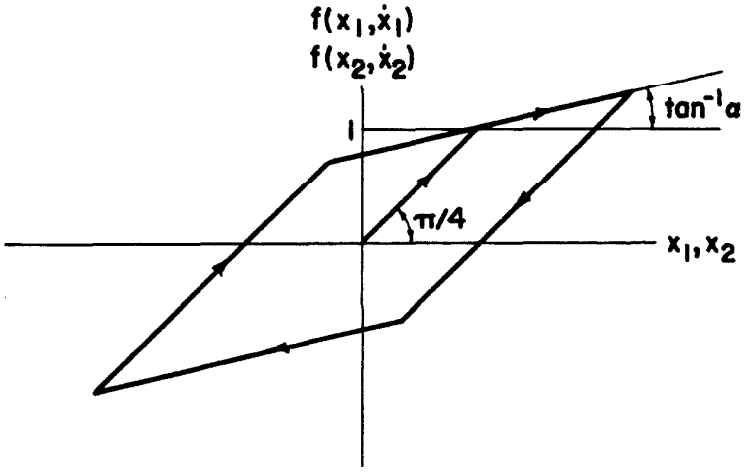

FIGURE 22. NORMALIZED HYSTERETIC RESTORING FORCE

where

$$\theta_1 = \omega t - \phi_1$$
$$\theta_2 = \theta_1 - \phi_2 \tag{3.4}$$

and where A_1, A_2, ϕ_1, and ϕ_2 are all slowly varying functions of the time t. Then

$$\dot{x}_1 = -\omega A_1 \sin\theta_1 + \dot{A}_1 \cos\theta_1 + A_1\dot{\phi}_1 \sin\theta_1$$
$$\dot{x}_2 = -\omega A_2 \sin\theta_2 + \dot{A}_2 \cos\theta_2 + A_2\dot{\phi}_2 \sin\theta_2 . \tag{3.5}$$

But by analogy to Lagrange's method of variation of a parameter, it is permissible to set

$$\dot{A}_1 \cos\theta_1 + A_1\dot{\phi}_1 \sin\theta_1 = 0 \tag{3.6a}$$

$$\dot{A}_2 \cos\theta_2 + A_2\dot{\phi}_2 \sin\theta_2 = 0. \tag{3.6b}$$

Thus,

$$\ddot{x}_1 = -\omega^2 A_1 \cos\theta_1 - \omega\dot{A}_1 \sin\theta_1 + \omega A_1\dot{\phi}_1 \cos\theta_1$$
$$\ddot{x}_2 = -\omega^2 A_2 \cos\theta_2 - \omega\dot{A}_2 \sin\theta_2 + \omega A_2\dot{\phi}_2 \cos\theta_2. \tag{3.7}$$

Substituting equation (3.7) into the equations of motion (3.1) and (3.2) then gives

$$-\omega^2 A_1 \cos\theta_1 - \omega\dot{A}_1 \sin\theta_1 + \omega A_1\dot{\phi}_1 \cos\theta_1 + f(A_1, \theta_1) - f(A_2, \theta_2) = r\cos(\theta_1 + \phi_1) \tag{3.8}$$

$$-\omega^2 A_2 \cos\theta_2 - \omega\dot{A}_2 \sin\theta_2 + \omega A_2\dot{\phi}_2 \cos\theta_2 + 2f(A_2, \theta_2) - f(A_1, \theta_1) = 0 \tag{3.9}$$

Multiplying (3.6a) by $\omega\cos\theta_1$, (3.8) by $\sin\theta_1$, and subtracting it will be seen

that

$$-\omega^2 A_1 \sin\theta_1 \cos\theta_1 - \omega\dot{A}_1 + f(A_1, \theta_1)\sin\theta_1 - f(A_2, \theta_2)\sin(\theta_2 + \phi_2) = r \sin\theta_1 \cos(\theta_1 + \phi_1). \quad (3.10)$$

But now due to their assumed slowly varying character, the variables A_1, A_2, ϕ_1, and ϕ_2 will remain essentially constant over one cycle of θ_1. Thus, equation (3.10) may be averaged over a cycle of θ_1 giving

$$-\omega\dot{A}_1 + \frac{1}{2\pi}\int_0^{2\pi} f(A_1, \theta_1)\sin\theta_1 \, d\theta_1 - \sin\phi_2 \frac{1}{2\pi}\int_0^{2\pi} f(A_2, \theta_2)\cos\theta_2 \, d\theta_2 - \cos\phi_2 \frac{1}{2\pi}\int_0^{2\pi} f(A_2, \theta_2)\sin\theta_2 \, d\theta_2 = -\frac{r}{2}\sin\phi_1 \quad (3.11)$$

where strictly speaking the A's and ϕ's now represent mean values of the functions over the cycle in question. Multiplying (3.6a) by $\omega\sin\theta_1$, (3.8) by $\cos\theta_1$ and adding

$$-\omega^2 A_1 \cos^2\theta_1 + \omega A_1\dot{\phi}_1 + f(A_1, \theta_1)\cos\theta_1 - f(A_2, \theta_2)\cos(\theta_2 + \phi_2) = r\cos\theta_1\cos(\theta_1 + \phi_1). \quad (3.12)$$

Therefore, averaging (3.12) over one cycle of θ_1

$$-\frac{\omega^2 A_1}{2} + \frac{1}{2\pi}\int_0^{2\pi} f(A_1, \theta_1)\cos\theta_1 \, d\theta_1 - \cos\phi_2 \frac{1}{2\pi}\int_0^{2\pi} f(A_2, \theta_2)\cos\theta_2 \, d\theta_2 + \omega A_1\dot{\phi}_1 + \sin\phi_2 \frac{1}{2\pi}\int_0^{2\pi} f(A_2, \theta_2)\sin\theta_2 \, d\theta_2 = r\cos\phi_1. \quad (3.13)$$

Similarly, multiplying (3.6b) by $\omega\cos\theta_2$, (3.9) by $\sin\theta_2$, subtracting, and averaging, it may be shown that

$$-\omega\dot{A}_2 + 2\frac{1}{2\pi}\int_0^{2\pi} f(A_2, \theta_2)\sin\theta_2 \, d\theta_2 - \cos\phi_2 \frac{1}{2\pi}\int_0^{2\pi} f(A_1, \theta_1)\sin\theta_1 \, d\theta_1 - \sin\phi_2 \frac{1}{2\pi}\int_0^{2\pi} f(A_1, \theta_1)\cos\theta_1 \, d\theta_1 = 0. \quad (3.14)$$

Finally, multiplying (3.6b) by $\omega \sin \theta_2$, (3.9) by $\cos \theta_2$, adding, and averaging gives

$$-\frac{\omega^2 A_2}{2} + 2\frac{1}{2\pi}\int_0^{2\pi} f(A_2, \theta_2)\sin\theta_2 \, d\theta_2 - \cos\phi_2 \frac{1}{2\pi}\int_0^{2\pi} f(A_1, \theta_1)\cos\theta_1 \, d\theta_1$$

$$+ \omega A_2 \dot{\phi}_2 - \sin\phi_2 \frac{1}{2\pi}\int_0^{2\pi} f(A_1, \theta_1)\sin\theta_1 \, d\theta_1 = 0 \qquad (3.15)$$

In order to simplify the notation, let

$$C_i(A_i) = \frac{1}{\pi}\int_0^{2\pi} f(A_i, \theta_i)\cos\theta_i \, d\theta_i \qquad i = 1, 2 \qquad (3.16)$$

$$S_i(A_i) = \frac{1}{\pi}\int_0^{2\pi} f(A_i, \theta_i)\sin\theta_i \, d\theta_i \qquad i = 1, 2 \qquad (3.17)$$

Then equations (3.11), (3.13), (3.14), and (3.15) may be written as

$$-2\omega\dot{A}_1 + S_1(A_1) - C_2(A_2)\sin\phi_2 - S_2(A_2)\cos\phi_2 = -r\sin\phi_1 \qquad (3.18)$$

$$-\omega^2 A_1 + 2\omega A_1 \dot{\phi}_1 + C_1(A_1) - C_2(A_2)\cos\phi_2 + S_2(A_2)\sin\phi_2 = r\cos\phi_1 \qquad (3.19)$$

$$-2\omega\dot{A}_2 + 2S_2(A_2) - S_1(A_1)\cos\phi_2 + C_1(A_1)\sin\phi_2 = 0 \qquad (3.20)$$

$$-\omega^2 A_2 + 2\omega A_2 \dot{\phi}_2 + 2C_2(A_2) - C_1(A_1)\cos\phi_2 - S_1(A_1)\sin\phi_2 = 0. \qquad (3.21)$$

Within the range of applicability of the approximate analysis, the four equations (3.18) through (3.21) may now be regarded as a complete statement of the problem in terms of the four variables A_1, A_2, ϕ_1, and ϕ_2.

Evaluation of $C_i(A_i)$ and $S_i(A_i)$

Except for the subscript notation used here, the functions $C_i(A_i)$ and $S_i(A_i)$ will have precisely the same form as the functions C(A) and S(A) defined earlier

in connection with the formulation of the single degree of freedom approximate theory. Thus, from equations (2.124a and b) it will be seen that

$$C_i(A_i) = \begin{cases} \frac{A_i}{\pi}\left[(1-\alpha)\,\theta_i^* + \alpha\pi - \frac{(1-\alpha)}{2}\sin 2\,\theta_i^*\right] & ;\ A_i > 1 \\ A_i & ;\ A_i < 1 \end{cases} \qquad i = 1,2 \qquad (3.22)$$

$$S_i(A_i) = \begin{cases} -\frac{A_i}{\pi}(1-\alpha)\sin^2\theta_i^* & ;\ A_i > 1 \\ 0 & ;\ A_i < 1 \end{cases} \qquad i = 1,2 \qquad (3.23)$$

where

$$\theta_i^* = \cos^{-1}\left(\frac{A_i - 2}{A_i}\right) \qquad i = 1,2\,. \qquad (3.24)$$

Approximation of $C_i(A_i)$ and $S_i(A_i)$ for Large A_i

In much of the work to follow it will be advantageous to have approximations for $C_i(A_i)$ and $S_i(A_i)$ which are valid for large amplitudes A_i. Using equation (3.24), it may be seen that for large A_i

$$\theta_i^* = \sin\theta_i^* + \frac{1}{6}\sin^3\theta_i^* \quad \ldots \qquad \text{(See Ref. 18)}$$

$$= \frac{2}{A_i}(A_i - 1)^{1/2} + \frac{1}{6}\,\frac{8}{A_i^3}(A_i - 1)^{3/2} \quad \ldots$$

$$= \frac{2}{A_i^{1/2}} + \frac{1}{3}\,\frac{1}{A_i^{3/2}} + 0\left(\frac{1}{A_i^{5/2}}\right)\,. \qquad (3.25)$$

Thus, substituting (3.25) into expression (3.22) for $C_i(A_i)$

$$C_i(A_i) = \frac{A_i}{\pi}\left[(1-\alpha)\left(\frac{2}{A_i^{1/2}} + \frac{1}{3A_i^{3/2}}\right) + \alpha\pi - (1-\alpha)\,\frac{2}{A_i^{1/2}}\left(1 - \frac{2}{A_i}\right)\left(1 - \frac{1}{2A_i}\right) + 0\left(\frac{1}{A_i^{5/2}}\right)\right]$$

$$= A_i\alpha + \frac{16(1-\alpha)}{3\pi}\,\frac{1}{A_i^{1/2}} + 0\left(\frac{1}{A_i^{3/2}}\right)\,. \qquad (3.26)$$

In the case of $S_i(A_i)$ the function may be evaluated exactly in terms A_i giving

$$S_i(A_i) = -\frac{4(1-\alpha)}{\pi}\left(1 - \frac{1}{A_i}\right) . \tag{3.27}$$

Approximation of $C_i(A_i)$ and $S_i(A_i)$ for $A_i = 1 + \nu$, $\nu << 1$

Consider the limiting case in which

$$A_i = 1 + \nu, \quad \nu << 1. \tag{3.28}$$

Then, from equation (3.24)

$$\theta_i^* = \pi - \left(\sin\theta_i^* + \frac{1}{6}\sin^3\theta_i^* + \ldots\right)$$

$$= \pi - 2\nu^{1/2} - \frac{2}{3}\nu^{3/2} + 0(\nu^{5/2}). \tag{3.29}$$

But now, using (3.29) in expression (3.22)

$$C_i(A_i) = \frac{(1\ \nu)}{\pi}\left[(1-\alpha)(\pi - 2\nu^{1/2} - \frac{2}{3}\nu^{3/2}\right] + \alpha\pi - \frac{2(1-\alpha)}{(1+\nu)}\nu^{1/2}\ (-1+2\nu) + 0(\nu^2)$$

$$= 1 + \nu - \frac{16(1-\alpha)}{3\pi}\nu^{3/2} + 0(\nu^{5/2}) \tag{3.30}$$

In the same manner, it may also be shown that

$$\frac{\partial C_i(A_i)}{\partial A_i} = 1 - \frac{8(1-\alpha)}{\pi}\nu^{1/2} + \frac{32}{3}\nu^{3/2} + 0(\nu^{5/2}) \tag{3.31}$$

$$S_i(A_i) = -\frac{4(1-\alpha)}{\pi}\nu + 0(\nu^2) \tag{3.32}$$

and

$$\frac{\partial S_i(A_i)}{\partial A_i} = -\frac{4(1-\alpha)}{\pi}(1-2\nu) + 0(\nu^2). \tag{3.33}$$

All of these relations will be referred to later in the course of the analysis.

Steady State Equations

The steady state equations may be obtained by setting $\dot{A}_1$, $\dot{A}_2$, $\dot{\phi}_1$ and $\dot{\phi}_2$ equal to zero in equations (3.18) through (3.21). In this way it will be seen that

$$S_1(A_1^0) - C_2(A_2^0) \sin \phi_2^0 - S_2(A_2^0) \cos \phi_2^0 = - r \sin \phi_1^0 \tag{3.34}$$

$$-\omega^2 A_1^0 + C_1(A_1^0) - C_2(A_2^0) \cos \phi_2^0 + S_2(A_2^0) \sin \phi_2^0 = r \cos \phi_1^0 \tag{3.35}$$

$$2 S_2(A_2^0) - S_1(A_1^0) \cos \phi_2^0 + C_1(A_1^0) \sin \phi_2^0 = 0 \tag{3.36}$$

$$-\omega^2 A_2^0 + 2 C_2(A_2^0) - C_1(A_1^0) \cos \phi_2^0 - S_1(A_1^0) \sin \phi_2^0 = 0 \tag{3.37}$$

where the superscript 0 denotes the steady state value. The variable ϕ_1^0 may now be eliminated from this set of equations by squaring and adding equations (3.34) and (3.35). This gives

$$\left[-\omega^2 A_1^0 + C_1^0 - C_2^0 \cos \phi_2^0 + S_2^0 \sin \phi_2^0\right]^2 + \left[S_1^0 - C_2^0 \sin \phi_2^0 - S_2^0 \cos \phi_2^0\right]^2 = r^2 \tag{3.38}$$

where for convenience the functional notation for C_i and S_i has been dropped. Expanding equation (3.38) and using equations (3.36) and (3.37), it may then be shown that

$$-\omega^2 A_2^0(-\omega^2 A_1^0 + C_1^0/2) \cos \phi_2^0 - (\omega^2 A_2^0 S_1^0/2) \sin \phi_2^0 + (-\omega^2 A_2 + C_1^0/2)^2 + (\omega^2 A_2^0)^2/4 + (S_1^0)^2/4 = r^2 \tag{3.39}$$

But, from equations (3.36) and (3.37)

$$\sin \phi_2^0 = \left[-2 C_1^0 S_2^0 + S_1^0(-\omega^2 A_2^0 + 2 C_2^0)\right] \Big/ \left[(C_1^0)^2 + (S_1^0)^2\right] \tag{3.40}$$

$$\cos \phi_2^0 = \left[C_1^0(-\omega^2 A_2^0 + 2 C_2^0) + 2 S_1^0 S_2^0\right] \Big/ \left[(C_1^0)^2 + (S_1^0)^2\right] \tag{3.41}$$

Thus substituting (3.40) and (3.41) into equation (3.39) and rearranging

$$(-\omega^2 A_1^0 + C_1^0/2)^2 + (-\omega^2 A_2^0 + 2C_2^0)\left[\frac{\omega^4 A_1^0 A_2^0 C_1^0}{(C_1^0)^2+(S_1^0)^2} - \frac{\omega^2 A_2^0}{2}\right] + \omega^4 A_1^0 A_2^0 \frac{2S_1^0 S_2^0}{(C_1^0)^2+(S_1^0)^2}$$

$$+ \frac{(\omega^2 A_2^0)^2}{4} + \frac{(S_1^0)^2}{4} = r^2 \qquad (3.42)$$

A second equation containing only the variables A_1^0 and A_2^0 may be obtained by squaring and adding equations (3.40) and (3.41). This gives

$$(-\omega^2 A_2^0 + 2\, C_2^0)^2 = (C_1^0)^2 + (S_1^0)^2 - 4(S_2^0)^2 \qquad (3.43)$$

from which

$$\omega^2 = 2\, C_2^0/A_2^0 \mp \left[(C_1^0)^2 + (S_1^0)^2 - 4(S_2^0)^2\right]^{1/2}/A_2^0. \qquad (3.44)$$

Thus, the statement of the steady state problem has been reduced to a set of two simultaneous equations, (3.42) and (3.44) in terms of the two unknown amplitudes A_1 and A_2. A method for the solution of these equations is considered in the next subsection.

Numerical Determination of the Steady State Response

Due to the highly transcendental character of equations (3.42) and (3.44), explicit determination of A_1 and A_2 in terms of ω and r is not practical. Thus, one is forced to consider numerical techniques as an alternate means of obtaining the desired solution of the steady state response. A method of solution which is particularly suited to high speed numerical computation is outlined in the following paragraph.

Using equation (3.44), ω^2 may be eliminated from equation (3.42) giving a new equation in A_1, A_2, and the parameter r. Thus, if r is given and A_2 is select-

ed arbitrarily, one may obtain A_1 by solving for the roots of this newly formulated equation. In general there will be several such roots each of which may then be used along with A_2 to calculate a value of ω from equation (3.44). If the ω obtained thereby is real, the particular solution for A_1 and A_2 is valid, if not, the solution is rejected. After checking the validity of all of the roots for an assumed A_2, the procedure is begun anew using a new value of A_2. In this way it is possible to calculate a complete response curve for any given level of excitation r.

Discussion of Results

Digital computer solutions of the steady state response have been obtained using the general approach outlined above and the results are shown in Figs. 23, 24, and 25. It will be noted that these response curves are similar in many respects to those of a linear two degree of freedom system. However, at the same time there are some very definite differences. The low-frequency peaks for both x_1 and x_2 resemble the response curves for the single degree of freedom bilinear hysteresic system and are typical of "soft" type resonance; i.e. the response curves appear to lean toward lower frequency and the peak response moves to a lower frequency as the level of excitation is increased. On the other hand, the high-frequency response peaks behave in a somewhat different manner. The upper peak for x_2 has the typical soft character but that for x_1 appears to lean in the opposite direction. This observation may at first seem contradictory but it is not at all unreasonable in the light of the complex nature of the forces resulting from non-linearities in both of the system restoring forces. Also, it should be noted that there is a very steep slope on the low-frequency side of the upper x_1 peak even though the peak itself leans toward higher frequency.

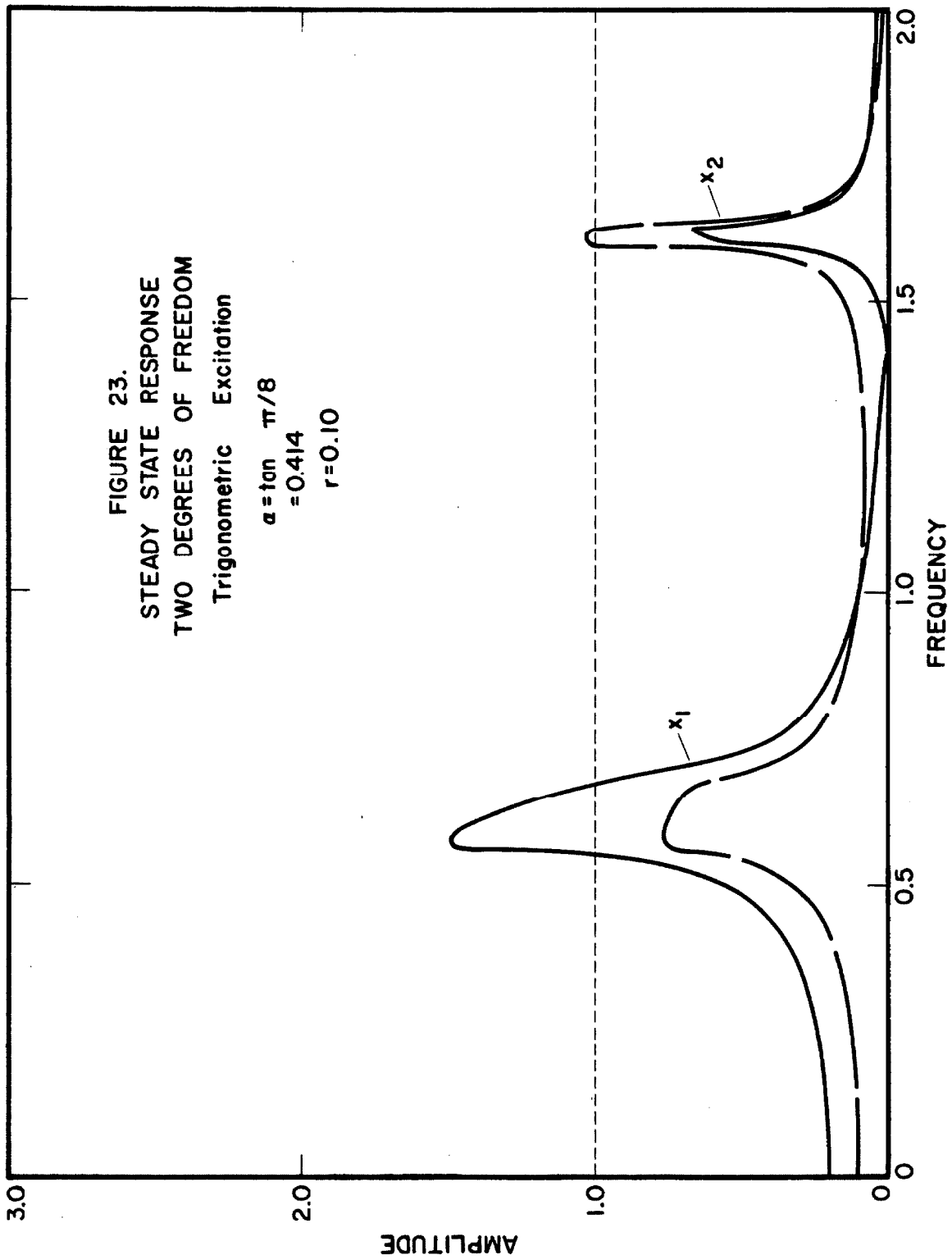
FIGURE 23.
STEADY STATE RESPONSE
TWO DEGREES OF FREEDOM
Trigonometric Excitation
α = tan π/8
= 0.414
r = 0.10
AMPLITUDE
FREQUENCY
3.0
2.0
1.0
0
0.5
1.0
1.5
2.0
x1
x2

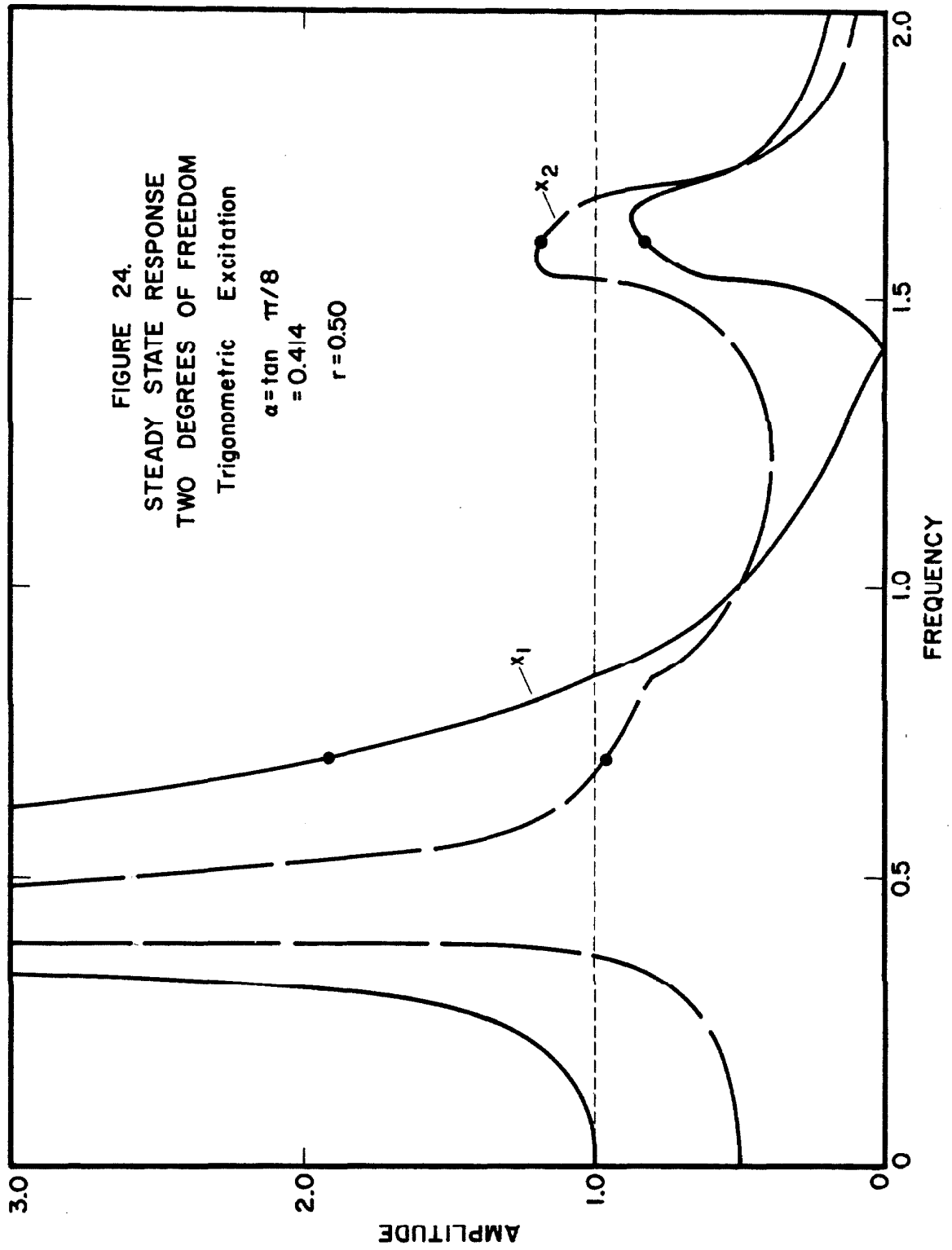
FIGURE 24.
STEADY STATE RESPONSE
TWO DEGREES OF FREEDOM
Trigonometric Excitation
α = tan π/8
= 0.414
r = 0.50
x_1
x_2
AMPLITUDE
FREQUENCY
0
1.0
2.0
3.0
0
0.5
1.0
1.5
2.0

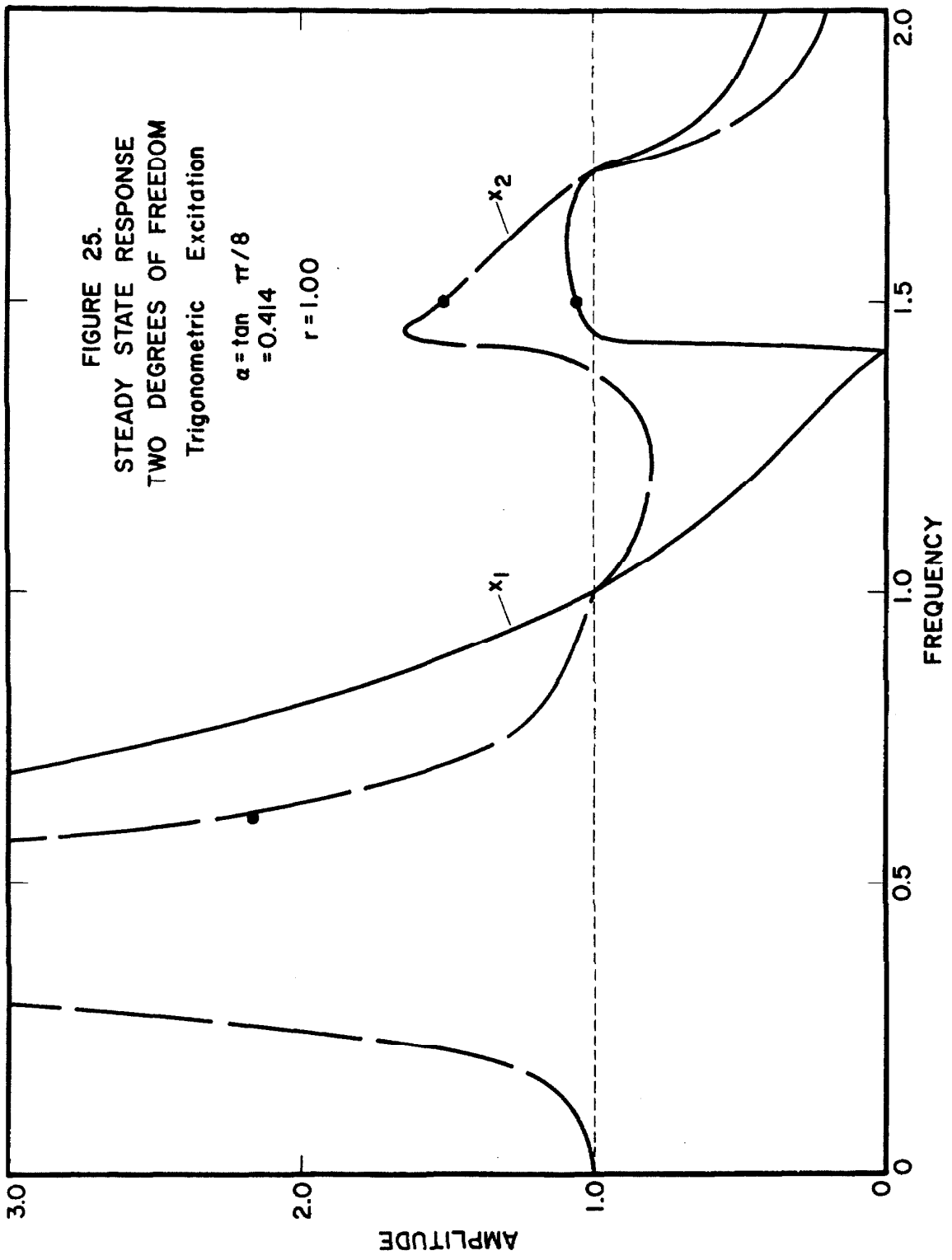
FIGURE 25.
STEADY STATE RESPONSE
TWO DEGREES OF FREEDOM
Trigonometric Excitation
α = tan π/8
=0.414
r = 1.00
x1
x2
AMPLITUDE
FREQUENCY
3.0
2.0
1.0
0
0.5
1.0
1.5
2.0

Although certain portions of the response curves will be seen to have very steep slopes, all of the curves appear to be single valued thus implying that the system does not possess any of the "jumps" which are often associated with soft systems. This is consistent with the analogous conclusion which is arrived at for the single degree of freedom system. Whether or not the resemblance between the one and two degree of freedom systems also carries over into the existence of a critical force level for unbounded resonance is not apparent from the figures and must be treated separately as a special problem.

Large Amplitude Steady State Behavior

Assume that A_1^0 and A_2^0 both become very large but that the ratio of A_1^0 to A_2^0 remains finite. Then substituting the large amplitude approximations (3.26) and (3.27) into the steady state equation (3.44), it will be seen that

$$\omega^2 = 2\left(\alpha + \frac{4}{3}\frac{\sigma}{A_2^{3/2}}\right) \mp \left[\left(A_1\alpha + \frac{4}{3}\frac{\sigma}{A_1^{1/2}}\right)^2 + \sigma^2\left(\frac{1}{A_1} - 1\right)^2 - 4\sigma^2\left(\frac{1}{A_2} - 1\right)^2\right]^{1/2} + 0\left(\frac{1}{A_2^{5/2}}\right) \tag{3.45}$$

where it is understood that A_1 and A_2 refer to steady state values and where

$$\sigma = 4(1-\alpha)/\pi . \tag{3.46}$$

Expanding equation (3.45) and introducing the new variable

$$N = A_1/A_2, \tag{3.47}$$

it may then be shown that

$$\omega^2 = \alpha(2 \mp N) + \frac{4}{3}\sigma\left(2 \mp \frac{1}{N^{1/2}}\right)\frac{1}{A_2^{3/2}} \pm \frac{3}{2}\frac{\sigma^2}{\alpha}\left(\frac{1}{N}\right)\frac{1}{A_2^2} + 0\left(\frac{1}{A_2^{5/2}}\right). \tag{3.48}$$

Making a similar large amplitude approximation in the remaining steady

state equation (3.42), it will be seen that

$$r^2 = \left(-\omega^2 A_1 + \frac{\alpha A_1}{2} + \frac{2}{3}\frac{\sigma}{A_1^{1/2}}\right)^2 + \omega^4 A_1 A_2 \frac{2\sigma^2\left(1-\frac{1}{A_1}\right)\left(1-\frac{1}{A_2}\right)}{\left(\alpha A_1 + \frac{4}{3}\frac{\sigma}{A_1^{1/2}}\right)^2 + \sigma^2\left(1-\frac{1}{A_1}\right)^2} + \frac{\omega^4 A_2^2}{4}$$

$$+ \left(-\omega^2 A_2 + 2\alpha A_2 + \frac{8}{3}\frac{\sigma}{A_2^{1/2}}\right)\left[\frac{\omega^4 A_1 A_2\left(\alpha A_1 + \frac{4}{3}\frac{\sigma}{A_1^{1/2}}\right)}{\left(\alpha A_1 + \frac{4}{3}\frac{\sigma}{A_1^{1/2}}\right)^2 + \sigma^2\left(1-\frac{1}{A_1}\right)^2} - \frac{\omega^2 A_2}{2}\right]$$

$$+ \frac{1}{4}\sigma^2\left(1-\frac{1}{A_1}\right)^2 + 0\left(\frac{1}{A_2^{3/2}}\right) . \qquad (3.49)$$

Thus, expanding and using equation (3.47)

$$r^2 = A_2^2\left[N^2(-\omega^2 + \frac{\alpha}{2})^2 + \omega^2(-\omega^2 + 2\alpha)(\frac{\omega^2}{\alpha} - \frac{1}{2}) + \frac{\omega^4}{4}\right]$$

$$+ \frac{4\sigma}{3\alpha} A_2^{1/2}\left[-\frac{\omega^4}{\alpha N^{3/2}}(-\omega^2 + 2\alpha) + 2\omega^4 + \frac{\alpha^2 N^{1/2}}{2} - \alpha\omega^2(N^{1/2} + 1)\right]$$

$$+ \frac{\sigma^2}{\alpha^2}\left[\frac{2\omega^4}{N} - \frac{\omega^4}{\alpha N^2}(-\omega^2 + 2\alpha) + \frac{\alpha^2}{4}\right] + 0\left(\frac{1}{A_2^{1/2}}\right) . \qquad (3.50)$$

Consider now the special case where N has a fixed value N_0 defined by

$$N_0 = \lim_{A_1, A_2 \to \infty} A_1/A_2. \qquad (3.51)$$

Then, equation (3.45) may be used to eliminate ω^2 from equation (3.50) giving

$$r^2 = \alpha^2 A_2^2 (N_0^4 \mp 2N_0^3 - N_0^2 \pm 2N_0 + 1)$$

$$+ \frac{8\alpha\sigma}{3} A_2^{1/2}\left[(\mp 2N_0^3 + N_0^2 \pm 3N_0 + 1) + \frac{1}{N_0^{1/2}}(N_0^3 - 2N_0 \mp 1)\right]$$

$$+ \sigma^2\left[\frac{3}{4N_0}(-4N_0^3 + 13N_0 \mp 4) + \frac{1}{N_0}(2 \mp 1)(2 \mp N_0)^2 + \frac{1}{4}\right] + 0\left(\frac{1}{A_2^{1/2}}\right) . \qquad (3.52)$$

For r finite, equation (3.52) indicates that there can be an unbounded resonant solution (A_1 and A_2 infinite) if and only if the coefficients of both the A_2^2 and $A_2^{1/2}$ terms vanish identically. Thus, the conditions for unbounded resonance with finite excitation may be stated as

$$(N_0^4 \mp 2N_0^3 - N_0^2 \pm 2N_0 + 1) = 0 \tag{3.53}$$

$$\left[(\mp 2N_0^3 + N_0^2 \pm 3N_0 + 1) + \frac{1}{N_0^{1/2}} (N_0^3 - 2N_0 \mp 1)\right] = 0. \tag{3.54}$$

Now, from (3.53) it is seen that

$$(N_0^2 \mp N_0 - 1)^2 = 0. \tag{3.55}$$

Hence,

$$N_0 = \frac{1}{2} (\sqrt{5} \pm 1). \tag{3.56}$$

But, it may then be shown that

$$\begin{aligned} &(\mp 2N_0^3 + N_0^2 \pm 3N_0 + 1) = 0 \\ &(N_0^3 - 2N_0 \mp 1) = 0. \end{aligned} \tag{3.57}$$

Therefore, the value of N_0 which satisfies (3.53) simultaneously satisfies (3.48) and the coefficients of A_2^2 and $A_2^{1/2}$ in equation (3.52) may both be made to vanish identically by the same value of N_0. This then implies the existence of an unbounded amplitude solution in which both N and r remain finite.

The limiting excitation level for unbounded resonance may now be obtained from the constant term of equation (3.52). After simplification by means of (3.55), this yields

$$r_c = \sigma \frac{(N_0 + 1)}{(2N_0 \pm 1)} \tag{3.58}$$

where the subscript c denotes that this value of r has the nature of a critical system parameter. The frequency which corresponds to unbounded resonance may be found from equation (3.49) and is easily seen to be

$$\omega_0^2 = \alpha(2 \mp N_0) =$$

$$= \frac{\alpha}{2}(3 \mp \sqrt{5}). \tag{3.59}$$

Making the large amplitude approximations in equation (3.41), it may be shown that

$$\cos \phi_2 = \pm 1 + \frac{\sigma^2}{2\alpha^2}(4 \mp 5)\frac{1}{A_1^2} + 0\left(\frac{1}{A_1^{5/2}}\right)$$

and hence that

$$\phi_2 \to 0, \pi \text{ as } A_1,\ A_2 \to \infty. \tag{3.60}$$

Similarly, from equation (3.35)

$$\cos \phi_1 = \pm \frac{\alpha A_2}{r}(N_0^2 \mp N_0 - 1) + 0\left(\frac{1}{A_2^{1/2}}\right)$$

$$= 0\left(\frac{1}{A_2^{1/2}}\right);$$

from which it will be seen that

$$\phi_1 \to \pi/2 \text{ as } A_1,\ A_2 \to \infty. \tag{3.61}$$

Thus, the unbounded resonance described above has much the same character as an ordinary linear undamped amplitude and phase resonance. This of course is completely reasonable since it will be seen that the bilinear hysteretic system actually approaches linearity in the limit of large amplitude oscillations.

By means of the above analysis it has therefore been possible to demonstrate the existence of two unbounded amplitude and phase resonances which occur for finite values of the excitation parameter r. In this respect then the two degree of freedom bilinear hysteretic system exhibits precisely the same type of response behavior as the one degree of freedom system considered earlier.

General Infinitesimal Stability of the Steady State Solution

Let

$$A_i = A_i^0 + \xi_i \qquad i = 1,2$$
$$\phi_i = \phi_i^0 + \psi_i \qquad i = 1,2 \tag{3.62}$$

where ξ_i and ψ_i are small perturbations on the steady state values A_i^0 and ϕ_i^0. Then, substituting relations (3.62) into equations (3.18) through (3.21) and neglecting all terms of higher order than unity in ξ_i and ψ_i, it may be shown that

$$-2\omega\dot{\xi}_1 + S_1\xi_1 - \xi_2(C_2'\sin\phi_2^0 + S_2'\cos\phi_2^0) - \psi_2\left[C_2(A_2^0)\cos\phi_2^0 - S_2(A_2^0)\sin\phi_2^0\right] = -r\psi_1\cos\phi_1^0 \tag{3.63}$$

$$-\omega^2\xi_1 + 2\omega A_1^0\dot{\psi}_1 + C_1'\xi_1 - \xi_2(C_2'\cos\phi_2^0 - S_2'\sin\phi_2^0) + \psi_2\left[C_2(A_2^0)\sin\phi_2^0 + S_2(A_2^0)\cos\phi_2^0\right] = -r\psi_1\sin\phi_1^0 \tag{3.64}$$

$$-2\omega\dot{\xi}_2 + 2S_2'\xi_2 + \xi_1(C_1'\sin\phi_2^0 - S_1'\cos\phi_2^0) + \psi_2\left[S_1(A_1^0)\sin\phi_2^0 + C_1(A_1^0)\cos\phi_2^0\right] = 0 \tag{3.65}$$

$$-\omega^2\xi_2 + 2\omega A_2^0(\dot{\psi}_1 + \dot{\psi}_2) + 2C_2'\xi_2 - \xi_1(C_1'\cos\phi_2^0 + S_1'\sin\phi_2^0) + \psi_2\left[C_1(A_1^0)\sin\phi_2^0 - S_1(A_1^0)\cos\phi_2^0\right] = 0 \tag{3.66}$$

where

$$C_i' = \left.\frac{\partial C_i}{\partial A_i}\right|_{A_i = A_i^0} \qquad i = 1,2$$

$$S_i' = \left.\frac{\partial S_i}{\partial A_i}\right|_{A_i = A_i^0} \qquad i = 1,2 \tag{3.67}$$

The first two steady state equations (3.34) and (3.35) may now be used to eliminate $r \cos \phi_1^0$ and $r \sin \phi_1^0$ from (3.63) and (3.64), and the remaining steady state equations (3.36) and (3.37) may be used to simplify the form of (3.65) and (3.66). This gives

$$\left.\begin{aligned}
&-2\omega\dot{\xi}_1 + S_1'\xi_1 - \xi_2(C_2' \sin\phi_2 + S_2' \cos\phi_2) - (\omega^2 A_1 - C_1)\psi_1 \\
&\qquad - (\psi_1 + \psi_2)(C_2 \cos\phi_2 - S_2 \sin\phi_2) = 0 \\
&-\omega^2\dot{\xi}_1 + 2\omega A_1\dot{\psi}_1 + C_1'\xi_1 - \xi_2(C_2' \cos\phi_2 - S_2' \sin\phi_2) - \psi_1 S_1 \\
&\qquad (\psi_1 + \psi_2)(C_2 \sin\phi_2 + S_2 \cos\phi_2) = 0 \\
&-2\omega\dot{\xi}_2 + 2S_2'\xi_2 + \xi_1(C_1' \sin\phi_2 - S_1' \cos\phi_2) + \psi_2(-\omega^2 A_2 + 2C_2) = 0 \\
&-\omega^2\xi_2 + 2\omega A_2(\dot{\psi}_1 + \dot{\psi}_2) + 2C_2'\xi_2 - \xi_1(C_1' \cos\phi_2 + S_1' \sin\phi_2) \\
&\qquad -2\psi_2 S_2 = 0
\end{aligned}\right\} \tag{3.68}$$

where it is understood that all A_i, C_i, and S_i refer to steady state values even

though the functional notation and superscripts have been set aside for the sake of brevity.

In order to examine the time behavior of the small perturbations ξ_i and ψ_i, let

$$\xi_i = \overline{\xi}_i e^{\lambda t}$$
$$\psi_i = \overline{\psi}_i e^{\lambda t}. \tag{3.69}$$

Then, substituting relations (3.69) into the stability equations (3.68), one obtains

$$\left.\begin{aligned}
&(2\omega\lambda - S_1')\overline{\xi}_1 + (C_2' \sin\phi_2 + S_2' \cos\phi_2)\overline{\xi}_2 + (C_2 \cos\phi_2 - S_2 \sin\phi_2 + \omega^2 A_1 - C_1)\overline{\psi}_1 \\
&\qquad + (C_2 \cos\phi_2 - S_2 \sin\phi_2)\overline{\psi}_2 = 0 \\
&(-\omega^2 C_1')\overline{\xi}_1 - (C_2' \cos\phi_2 - S_2' \sin\phi_2)\overline{\xi}_2 + (C_2 \sin\phi_2 + S_2 \cos\phi_2 + 2\omega A_1\lambda - S_1)\overline{\psi}_1 \\
&\qquad + (C_2 \sin\phi_2 + S_2 \cos\phi_2)\overline{\psi}_2 = 0 \\
&(C_1' \sin\phi_2 - S_1' \cos\phi_2)\overline{\xi}_1 - (2\omega\lambda - 2S_2')\overline{\xi}_2 + (-\omega^2 A_2 + 2C_2)\overline{\psi}_2 = 0 \\
&(C_1' \cos\phi_2 + S_1' \sin\phi_2)\overline{\xi}_1 + (\omega^2 - 2C_2')\overline{\xi}_2 + (-2\omega A_2\lambda)\overline{\psi}_1 + (-2\omega A_2\lambda + 2S_2)\overline{\psi}_2 = 0
\end{aligned}\right\} \tag{3.70}$$

The frequency equation is obtained by setting the determinant of the coefficients

of equation (3.70) equal to zero and may be written as

$$(2\omega\lambda)^4 + (2\omega\lambda)^3 a_3 + (2\omega\lambda)^2 a_2 + (2\omega\lambda) a_1 + a_0 = 0 \tag{3.71}$$

where

$$a_3 = \frac{1}{A_1 A_2}\left\{ -2A_1S_2 - 2A_1A_2S_2' - A_2S_1 - A_1A_2S_1' \right\} \tag{3.72}$$

$$a_2 = \frac{1}{A_1 A_2}\left\{ \begin{array}{l} -S_1'(2A_1S_2 - A_2S_1 - 2A_1A_2S_2') + 4A_1S_2S_2 + 2A_2S_1S_2' - 2S_2(①) \\ +2S_1S_2 + A_2(C_1 - \omega^2 A_1)(-\omega^2 + C_1') + (\omega^2 A_2 - 2C_2)\left[A_2(②) + A_1(\omega^2 - 2C_2')\right] \\ +A_1A_2(③)(④) + A_1(⑤)(⑥) \end{array} \right\} \tag{3.73}$$

$$a_1 = \frac{1}{A_1 A_2}\left\{ \begin{array}{l} -S_1'\left\{4A_1S_2S_2' + 2A_2S_1S_2' - 2S_2(①) + 2S_1S_2 + (\omega^2 A_2 - 2C_2)\left[A_2(②)\right.\right. \\ \left.\left. +A_1(\omega^2 - 2C_2')\right]\right\} + 4S_2'S_2(①) - 4S_1S_2S_2' - S_1(\omega^2 A_2 - 2C_2)(\omega^2 - 2C_2') \\ +(\omega^2 A_2 - 2C_2)(\omega^2 - 2C_2')(①) - (③)\left\{(④)(2A_1S_2 + A_2S_1) + (\omega^2 A_2 - 2C_2)\right. \\ \left.\left[A_1(⑥) + A_2(-\omega^2 + C_1')\right]\right\} - (C_1 - \omega^2 A_1)\left[-A_2(④)(②) + 2S_2'A_2(-\omega^2 + C_1')\right. \\ \left. +2S_2(-\omega^2 + C_1') - (⑥)(①)\right] - (⑤)\left[-A_1(④)(\omega^2 - 2C_2') - 2S_2(-\omega^2 + C_1')\right. \\ \left. +(S_1 + 2A_1S_2')(⑥)\right] \end{array} \right\} \tag{3.74}$$

$$a_0 = \frac{1}{A_1 A_2}\left\{ \begin{array}{l} -S_1'\left[4S_1'S_2(①) - 4S_1S_2S_1' - S_1(\omega^2 A_2 - 2C_2)(\omega^2 - 2C_2') + (\omega^2 A_2 - 2C_2)\right. \\ \left.(\omega^2 - 2C_2')(①)\right] - (③)\left[2S_2(④)(①) - 2S_1S_2(④) - S_1(\omega^2 A_2 - 2C_2)(⑥)\right. \\ \left. +(\omega^2 A_2 - 2C_2)(⑥)(①)\right] - (C_1 - \omega^2 A_1)\left\{(④)\left[2S_2(②) - (\omega^2 - 2C_2')(①)\right]\right. \\ -2S_2'\left[2S_2(-\omega^2 + C_1') - (⑥)(①)\right] + (-\omega^2 A_2 + 2C_2)\left[(-\omega^2 + C_1')(\omega^2 - 2C_2')\right. \\ \left.\left. -(⑥)(②)\right]\right\} - (⑤)\left\{(④)\left[S_1(\omega^2 - 2C_2') - 2S_2(②)\right] - 2S_2'\left[S_1(⑥)\right.\right. \\ \left.\left. -2S_2(-\omega^2 + C_1')\right] + (\omega^2 A_2 - 2C_2)\left[(-\omega^2 + C_1')(\omega^2 - 2C_2') - (⑥)(②)\right]\right\} \end{array} \right\} \tag{3.75}$$

and where

$$\begin{aligned}
① &= C_2 \sin \phi_2 + S_2 \cos \phi_2 \\
② &= S_2' \sin \phi_2 - C_2' \cos \phi_2 \\
③ &= C_2' \sin \phi_2 + S_2' \cos \phi_2 \\
④ &= C_1' \sin \phi_2 - S_1' \cos \phi_2 \\
⑤ &= C_2 \cos \phi_2 - S_2 \sin \phi_2 \\
⑥ &= C_1' \cos \phi_2 + S_1' \sin \phi_2 .
\end{aligned} \tag{3.76}$$

Thus, from the Routh-Hurwitz stability criteria the system will be stable if

$$a_j > 0 \qquad j = 0, 1, 2, 3 \tag{3.77}$$

and if

$$a_1 a_2 a_3 > a_1^2 + a_0 a_3^2 . \tag{3.78}$$

It may be shown on a completely general basis that a_3 is always greater than zero for A_1 and A_2 finite. However, the complicated nature of the a_0, a_1, and a_2 terms precludes any such general treatment for these coefficients. Therefore, one must be content with making detailed studies of stability only for those limiting cases which will lead to a substantial simplification of the frequency equation. Two such cases will now be considered.

Stability of Small Amplitude Solutions

For cases in which both A_1 and A_2 are less than unity, the normalized bilinear hysteretic system behaves exactly like an undamped linear system and

it is easily shown that the steady state solutions are marginally stable $\left(\mathcal{R}(\lambda) = 0\right)$. However, such cases of purely linear response are not at all typical of the general system behavior. Therefore, as a means of observing the effect of hysteresis on the system stability, it is instructive to consider the case where one of the system displacements has an amplitude somewhat greater than unity while the other has an amplitude which is less than unity.

Case 1) $A_2 < 1$; $A_1 = 1 + \nu$, $\nu << 1$.

Consider the case in which A_1 is slightly greater than unity and A_2 is less than unity. Then,

$$C_2/A_2 = C_2' = 1$$
$$S_2 = S_2' = 0, \tag{3.79}$$

and using relations (3.28) through (3.33) in equations (3.66) through (3.69) gives

$$a_3 = \sigma + 0(\nu) > 0$$
$$a_2 = (2N^2 - 2N + 3) + 0(\nu^{1/2}) > 0 \text{ for all N}$$
$$a_1 = \sigma(N^2 - 2N + 2) + 0(\nu^{1/2}) > 0 \text{ for all N} \tag{3.80}$$
$$a_0 = (N^2 - N - 1)^2 + 0(\nu^{1/2}) > 0 \text{ for all } N \neq \frac{1}{2}(\sqrt{5}+1).$$

For the present case, the particular amplitude ratio $N = \frac{1}{2}(\sqrt{5}+1)$ corresponds to the limiting steady state solution as r approaches zero. Thus, for r finite a_0, a_1, a_2, and a_3 are all positive and the first stability condition (3.77) is satisfied.

From equations (3.80) it may now be shown that

$$a_1 a_2 a_3 - a_1^2 - a_0 a_3^2 = \sigma^2 (2N - 1)^2 \; ; \tag{3.81}$$

and thereby that

$$a_1 a_2 a_3 > a_1^2 + a_0 a_3^2 \text{ for all } N \neq 1/2.$$

However, by supposition $N > 1$. Therefore, the second stability condition (3.78) is also satisfied, and the system is stable.

Case 2) $A_1 < 1$; $A_2 = 1 + \nu$, $\nu << 1$.

Now, consider the case where A_2 is slightly greater than unity and A_1 is less than unity. In this case then

$$\begin{aligned} C_1/A_1 &= C_1' = 1 \\ S_1 &= S_1' = 0, \end{aligned} \tag{3.82}$$

and expansion of equations (3.66) through (3.69) in powers of ν yields

$$\begin{aligned} a_3 &= 2\sigma + 0(\nu) > 0 \\ a_2 &= (2N^2 + 2N + 3) + 0(\nu^{1/2}) > 0 \quad \text{for all } N \\ a_1 &= \sigma (2N^2 + 6N + 5) + 0(\nu^{1/2}) > 0 \quad \text{for all } N \\ a_0 &= (N^2 + N - 1)^2 + 0(\nu^{1/2}) > 0 \quad \text{for all } N \neq \tfrac{1}{2} (\sqrt{5} - 1). \end{aligned} \tag{3.83}$$

where here, as before, the particular amplitude ratio which causes a_0 to vanish corresponds to the limiting steady state solution as r approaches zero. Thus, for r finite a_0, a_1, a_2, and a_3 are again all positive and condition (3.77) is satisfied.

But now from equations (3.83) it may further be shown that

$$a_1 a_2 a_3 - a_1^2 - a_0 a_3^2 = \sigma^2 (2N+1)^2 \qquad (3.84)$$
$$> 0 \quad \text{for all N.}$$

Therefore, the stability condition (3.78) is also satisfied and it is once again found that the system is stable.

Stability of Large Amplitude Solutions

Assume that A_1 and A_2 become very large and that the ratio of A_1 to A_2 remains finite. Then, using the large amplitude approximations of equations (3.26), (3.27), and (3.48), it may, with some effort, be shown that

$$\begin{aligned}
a_3 &= \sigma (1 + 2N) \frac{1}{A_1} \quad > 0 \quad \text{for all } N > 0 \\
a_2 &= \alpha^2 (2N^2 \mp 2N + 3) + 0\left(\frac{1}{A_1^{3/2}}\right) > 0 \quad \text{for all N} \\
a_1 &= \sigma \alpha^2 \left[2N^3 + (1 \mp 6) N^2 + (5 \mp 2) N + 2\right] \frac{1}{A_1} + 0\left(\frac{1}{A_1^2}\right) > 0 \quad \text{for all N} \\
a_0 &= \alpha^4 (N^2 \mp N - 1) + 0\left(\frac{1}{A_1^{3/2}}\right) \geqslant 0 \quad \text{for all N near } N_0.
\end{aligned} \qquad (3.85)$$

Thus, for all but the limiting case of infinite amplitudes a_0, a_1, a_2, and a_3 are all positive and the first stability condition (3.77) is satisfied. In the limiting case where A_1 is actually infinite (unbounded resonance) a_0, a_1, and a_3 approach zero and the system is marginally stable ($\lambda = 0$).

From equations (3.85) it may now be shown that

$$a_1 a_2 a_3 - a_1^2 - a_0 a_3^2 = \sigma^2 \alpha^4 \left\{ \left[2N^3 + (1 \mp 6)N^2 + (5 \mp 2)N + 2\right] \left[2N^3 + (1 \pm 2)N^2 + N + 1\right] - (1 + 2N)(N^2 \mp N - 1) \right\} \frac{1}{A_1^2} + 0\left(\frac{1}{A_1^3}\right). \qquad (3.86)$$

But for large amplitude oscillation

$$N = N_0 + 0\left(\frac{1}{A^k}\right) \quad k > 0 \tag{3.87}$$

Therefore, substituting (3.87) into (3.86) and using relation (3.56),

$$a_1 a_2 a_3 - a_1^2 - a_0 a_3^2 = \sigma^2 \alpha^4 (28 \mp 25) \frac{1}{A_1^2} + 0\left(\frac{1}{A_1^{2+m}}\right) \quad m > 0$$

$$> 0 \text{ for all } A_1 \text{ large but finite.} \tag{3.88}$$

Hence, the second stability condition (3.78) is also satisfied and it is concluded that the system is stable for all A_1 and A_2 large becoming marginally stable in the limit of infinite amplitudes.

By way of summary, Fig. 26 shows those regions of the response curve which the above analysis has shown to be either stable or marginally stable.

Loci of Vertical Tangency

It can be shown on a completely general basis (See Ref. 17) that

$$\frac{\partial A_i}{\partial \omega} \to \infty \text{ if and only if } a_0 \to 0. \tag{3.89}$$

Thus, in the present case the loci of vertical tangency, if such exist, may be obtained by setting expression (3.75) equal to zero. However, to do this for the entire range of variables A_i would lead to such a complicated relationship for the loci that practically speaking the problem cannot be solved. Therefore, as in the treatment of stability, one must resort to an analysis which is valid only in certain limiting cases thereby demonstrating the existence (or non existence) of loci of vertical tangency without actually obtaining their detailed character.

Case 1) $A_2 < 1$; $A_1 = 1 + \nu_1$, $\nu_1 << 1$.

Let A_1 be slightly greater than unity and A_2 be less than unity. Then, expanding equation (3.75) by means of relations (3.79) and (3.28) through (3.33), it may be shown that

$$a_0 = \left[\omega^4 - (3 - 2\sigma\nu_1^{1/2})\omega^2 + (1 - 2\sigma\nu_1^{1/2})\right](\omega^4 - 3\omega^2 + 1) + 0(\nu_1). \quad (3.90)$$

But, from (3.89) the condition for a vertical tangency is

$$a_0 = 0. \quad (3.91)$$

Therefore, to order $\nu_1^{1/2}$ the locus of vertical tangency will be given by

$$\omega_v^4 - (3 - 2\sigma\nu_1^{1/2})\omega_v^2 + (1 - 2\sigma\nu_1^{1/2}) = 0. \quad (3.92)$$

where the subscript "v" denotes the value at the point of vertical tangency. Solving equation (3.92) for ω_v with the stipulation that $A_1 > A_2$ then gives

$$\omega_v^2 = \frac{1}{2}(3 - \sqrt{5}) - \sigma\nu_1^{1/2}(1 - \sqrt{5}/5), \quad \nu_1 > 0. \quad (3.93)$$

The existence of at least one locus of vertical tangency has thereby been demonstrated and it is seen that this locus originates at the point $\omega^2 = \frac{1}{2}(3 - \sqrt{5})$, $A_1 = 1$, and moves toward lower frequency as A_1 increases.

The above result was derived in terms of the amplitude A_1, however, since there is a definite steady state functional relationship between A_1 and A_2 for all ω, precisely the same type of analysis could have been applied using A_2. Thus, a vertical tangency for A_1 directly implies the existence of a vertical tangency for A_2 and vice versa. From equation (3.44) and relations (3.30) and (3.32) it is seen that in the present limiting case

$$A_2 = -\frac{1}{\omega^2 - 2}\left[C_1^2 + S_1^2\right]^{1/2}$$

$$= -\frac{1}{\omega^2 - 2}(1 + \nu_1) + 0(\nu_1^{3/2}). \quad (3.94)$$

But at the point of vertical tangency $\omega^2 = \omega_v^2$ and using (3.93)

$$A_2 = \frac{2}{(1+\sqrt{5})} - 4\sigma \nu_1^{1/2} \frac{(1-\sqrt{5}/2)}{(1+\sqrt{5})^2} + 0(\nu_1). \tag{3.95}$$

Thus, letting

$$A_2 = \frac{2}{(1+\sqrt{5})} + \nu_2, \tag{3.96}$$

equation (3.95) gives

$$\nu_2 = -4\sigma \nu_1^{1/2} \cdot \frac{(1-\sqrt{5}/2)}{(1+\sqrt{5})^2} + 0(\nu_1) \tag{3.97}$$

and thereby,

$$\nu_1^{1/2} = -\frac{(1+\sqrt{5})^2}{4\sigma(1-\sqrt{5}/2)} \nu_2 + 0(\nu_2^2). \tag{3.98}$$

Hence, from (3.93) the locus of vertical tangency for A_2 may be written as

$$\omega_v^2 = \frac{1}{2}(3-\sqrt{5}) + \frac{1}{4}(1+\sqrt{5})^2 \nu_2 + 0(\nu_2^2) \tag{3.99}$$

where from (3.97), $\nu_2 < 0$. It will be noted that the above locus for A_2 originates at the point $\omega^2 = \frac{1}{2}(3-\sqrt{5})$, $A_2 = \frac{1}{2}(\sqrt{5}-1)$ and unlike the corresponding locus for A_1, moves initially downward from its point of origin.

Case 2) $A_1 < 1$, $A_2 = 1 + \nu_2$, $\nu_2 << 1$

Next, consider the case where A_2 is slightly greater than unity while A_1 is less than unity. Expanding (3.75) in powers of ν_2 for this case, it may be shown that

$$a_0 = \left[\omega^4 - (3-4\sigma\nu_2^{1/2})\omega^2 + (1-2\sigma\nu_2^{1/2})\right](\omega^4 - 3\omega^2 + 1) + 0(\nu_2). \tag{3.100}$$

Thus, to order $\nu_2^{1/2}$ the equation for the locus of vertical tangency becomes

$$\omega_v^4 - (3-4\sigma\nu_2^{1/2})\omega_v^2 + (1-2\sigma\nu_2^{1/2}) = 0 \tag{3.101}$$

where again the subscript denotes that the variable is evaluated at the point of vertical tangency. Solving equation (3.101) and stipulating that $A_1 < A_2$ then gives

$$\omega_v^2 = \frac{1}{2}(3 + \sqrt{5}) - 2\sigma \nu_2^{1/2}(1 + 2\sqrt{5}/5), \quad \nu_2 > 1. \tag{3.102}$$

Equation (3.102) therefore represents a locus of vertical tangency for A_2 which originates at the point $\omega^2 = \frac{1}{2}(3 + \sqrt{5})$, $A_2 = 1$ and moves away from this point in the direction of increasing amplitude and decreasing frequency.

As pointed out earlier, the existence of a locus of vertical tangency for A_2 implies the existence of a corresponding locus for A_1 and this latter locus may be obtained directly from (3.102) if the functional relationship between A_1 and A_2 is known. Now, from equation (3.44) and relations (3.30) and (3.32)

$$A_1^2 = C_1^2 = (A_2\omega^2 - 2C_2)^2 + 4S_2^2$$

$$= \left\{\omega^2(1 + \nu_2) - 2\left[1 + \nu_2 + 0(\nu_2^{3/2})\right]\right\}^2 + 0(\nu_2^2). \tag{3.103}$$

Thus,

$$A_1 = (\omega^2 - 2) + 2(\omega^2 - 2)\nu_2 + 0(\nu_2^{3/2}). \tag{3.104}$$

But at the point of vertical tangency $\omega^2 = \omega_v^2$ so using equation (3.102)

$$A_1 = \frac{1}{2}(\sqrt{5}-1) - 2\sigma\nu_2^{1/2}(1 + 2\sqrt{5}/5) + 0(\nu_2). \tag{3.105}$$

Hence, letting

$$A_1 = \frac{1}{2}(\sqrt{5}-1) + \nu_1 \tag{3.106}$$

it is seen that

$$\nu_1 = -2\sigma\nu_2^{1/2}(1 + 2\sqrt{5}/5) + 0(\nu_2). \tag{3.107}$$

where it is required that $\nu_1 < 0$ within the range of validity of the present approximation for $0 < \nu_2 < 1$. The locus of equation (3.107) therefore moves towards

decreasing amplitude and frequency from an origin at the point $\omega^2 = \frac{1}{2}(3 + \sqrt{5})$, $A_1 = \frac{1}{2}(\sqrt{5}-1)$.

On the basis of the above analysis and information obtained from the steady state response curves, the probable configurations of the known loci of vertical tangency have been sketched schematically in Fig. 27.

Summary

The results of the preceeding analysis of the two degree of freedom bilinear hysteretic system may be summarized as follows:

(1) The low-frequency response peaks for both x_1 and x_2 are typical of soft type resonance in that the response curves appear to lean toward lower frequency and the peak response moves to a lower frequency as the level of excitation is increased. On the other hand, the high-frequency response peaks behave somewhat differently with x_2 having typical soft character but x_1 appearing to lean in the opposite direction for at least two of the cases considered. All of the resonance peaks regardless of their general shape have very steep slopes on the low-frequency side of the peak response.

(2) Associated with the steep sloped portions of the response curves are four loci of vertical tangency having the probable configurations shown schematically in Fig. 27.

(3) For all of the specific cases investigated here the response curves were single-valued indicating that "jumps" between multiple stable branches are not present within the range of the present analysis.

(4) There are two critical levels of excitation above which the system exhibits unbounded amplitude and phase resonance. The lowest critical level

corresponds to unbounded resonance of the low frequency response peak ($A_1 > A_2$), and the highest corresponds to a similar behavior of the high frequency peak ($A_2 > A_1$). For the present normalized problem the values of the critical excitation levels are $\sigma(\sqrt{5}-1)/2$ and $\sigma(3\sqrt{5}+7)/2$ where $\sigma = 4(1-\alpha)/\pi$.

(5) The system has been shown to be stable or marginally stable for the regions of response shown schematically in Fig. 26.

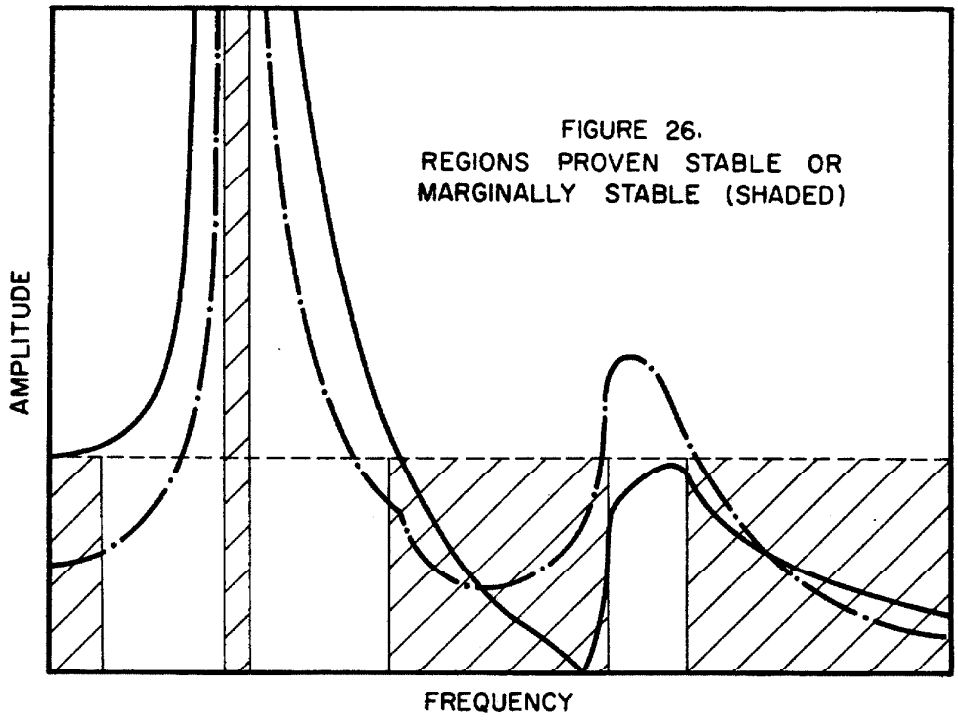

FIGURE 26.
REGIONS PROVEN STABLE OR MARGINALLY STABLE (SHADED)

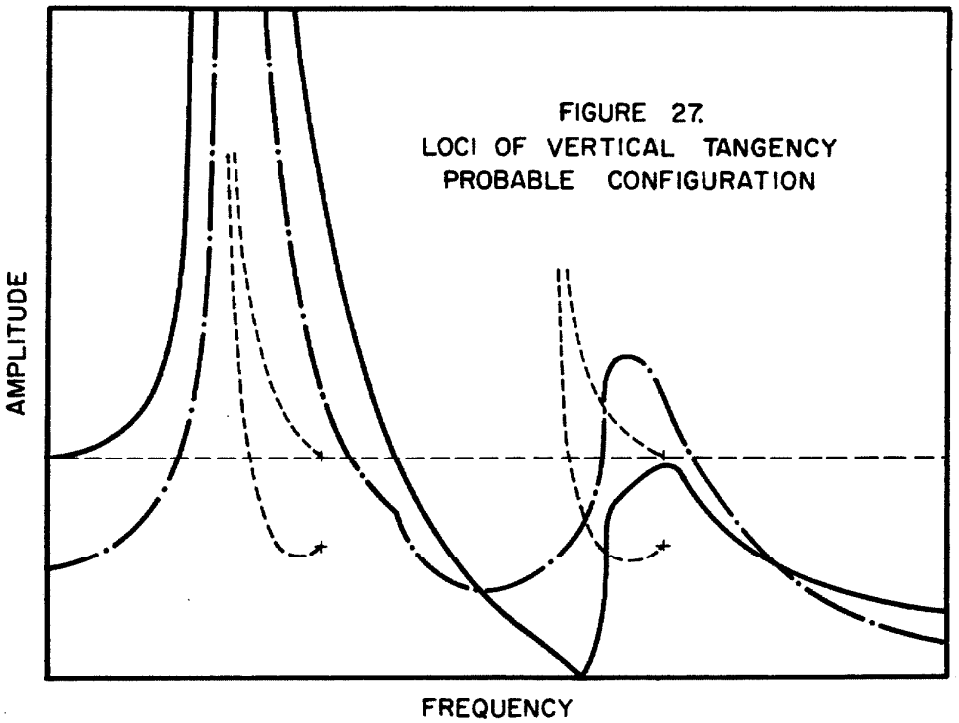

FIGURE 27.
LOCI OF VERTICAL TANGENCY PROBABLE CONFIGURATION

B. Numerical Integration of the Equations of Motion

As a means of checking the approximate steady state theory, one may solve for the system motion by direct numerical integration of the equations of motion. This procedure will now be discussed.

Steady State Solutions

Steady state solutions have been obtained for a number of specific cases using a fifth order Runge-Kutta numerical integration technique (See Ref. 19) with the approximate theory results as initial conditions. These solutions have been denoted by dots on the response curves of Figs. 24 and 25. It will be noted that for all of the cases checked the amplitude as predicted by the approximate and numerical solutions is in quite close agreement.

Harmonic Content

In the linearized treatment of steady state motion, it is assumed that the displacement contains a single harmonic component with a frequency equal to the frequency of excitation. However, unless both amplitudes are less than unity this assumption will be violated due to the presence of higher order harmonic terms in the real system. Thus, a good indication of the overall merit of the approximate theory will be obtained from the harmonic content of the true displacement wave forms as calculated by numerical integration.

Let $\Delta(t)$ be the difference between the actual displacement $x(t)$ and the fundamental Fourier component of this displacement. Then

$$\Delta(t) = x(t) - (a_1 \sin \omega t + b_1 \cos \omega t), \tag{3.108}$$

where

$$x(t) = \sum_{n=1}^{\infty} (a_n \sin n\omega t + b_n \cos n\omega t \tag{3.109}$$

and

$$a_n = \frac{1}{\pi}\int_0^{2\pi} x(t) \sin n\omega t \, d(\omega t)$$

$$b_n = \frac{1}{\pi}\int_0^{2\pi} x(t) \cos n\omega t \, d(\omega t). \tag{3.110}$$

But now from (3.109) and (3.110)

$$\Delta(t) = \sum_{n=2}^{\infty} (a_n \sin n\omega t + b_n \cos n\omega t), \tag{3.111}$$

and using the orthogonality conditions for the trigonometric functions

$$\overline{\Delta(t)^2} = \frac{1}{2\pi}\int_0^{2\pi} \left[\Delta(t)\right]^2 d(\omega t)$$

$$= \frac{1}{2}\sum_{n=2}^{\infty} (a_n^2 + b_n^2) \tag{3.112}$$

Thus, one may define a measure of the harmonic content as

$$\chi \equiv \left[\frac{\sum_{n=2}^{\infty} (a_n^2 + b_n^2)}{(a_1^2 + b_1^2)}\right]^{1/2}$$

$$= \left[\frac{2\,\overline{\Delta(t)^2}}{(a_1^2 + b_1^2)}\right]^{1/2}. \tag{3.113}$$

Table II gives the values of χ which correspond to the numerical integration solutions denoted in Figs. 24 and 25. The steady state displacement wave forms

TABLE II

α	r	ω	Harmonic Content, χ	
			for x_1	for x_2
tan $\pi/8$	0.50 (Fig. 26)	0.706	0.025	0.063
		1.600	0.003	0.004
	1.00 (Fig. 27)	0.611	0.026	0.083
		1.500	0.003	0.006

for the four cases of Table II are shown in Figs. 28 and 29, and velocity wave forms for two representative cases are shown in Fig. 30.

It will be noted that the harmonic content of the true displacement wave forms is quite low (1-3%) for small amplitude solutions but becomes significant (~8%) when the amplitude of one or both displacements is moderately large. On the other hand, the actual values of the steady state amplitude of response as predicted by the approximate theory agree very well with the numerical results over the entire range of amplitudes considered.

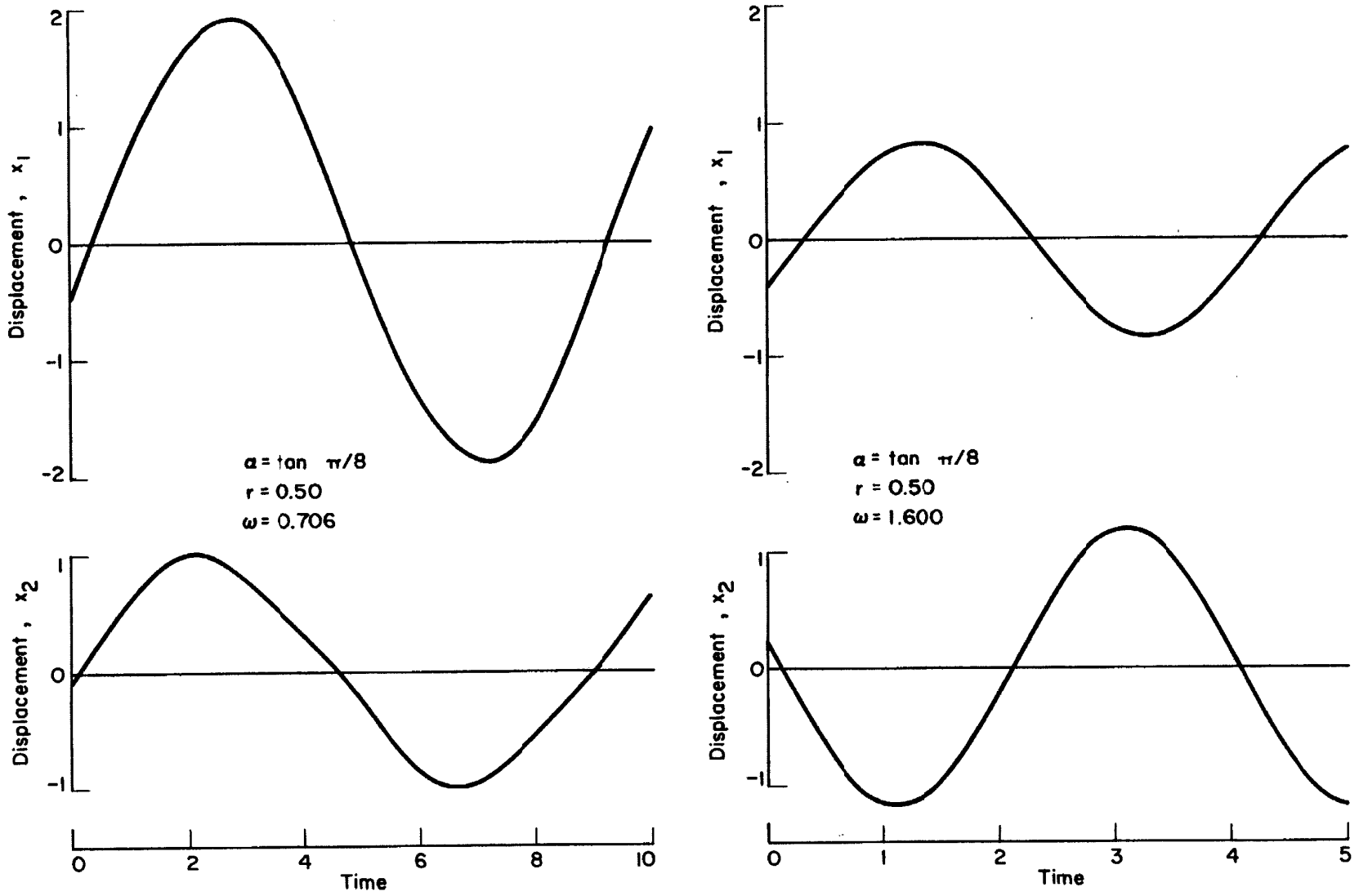

FIGURE 28. DISPLACEMENT WAVE FORMS

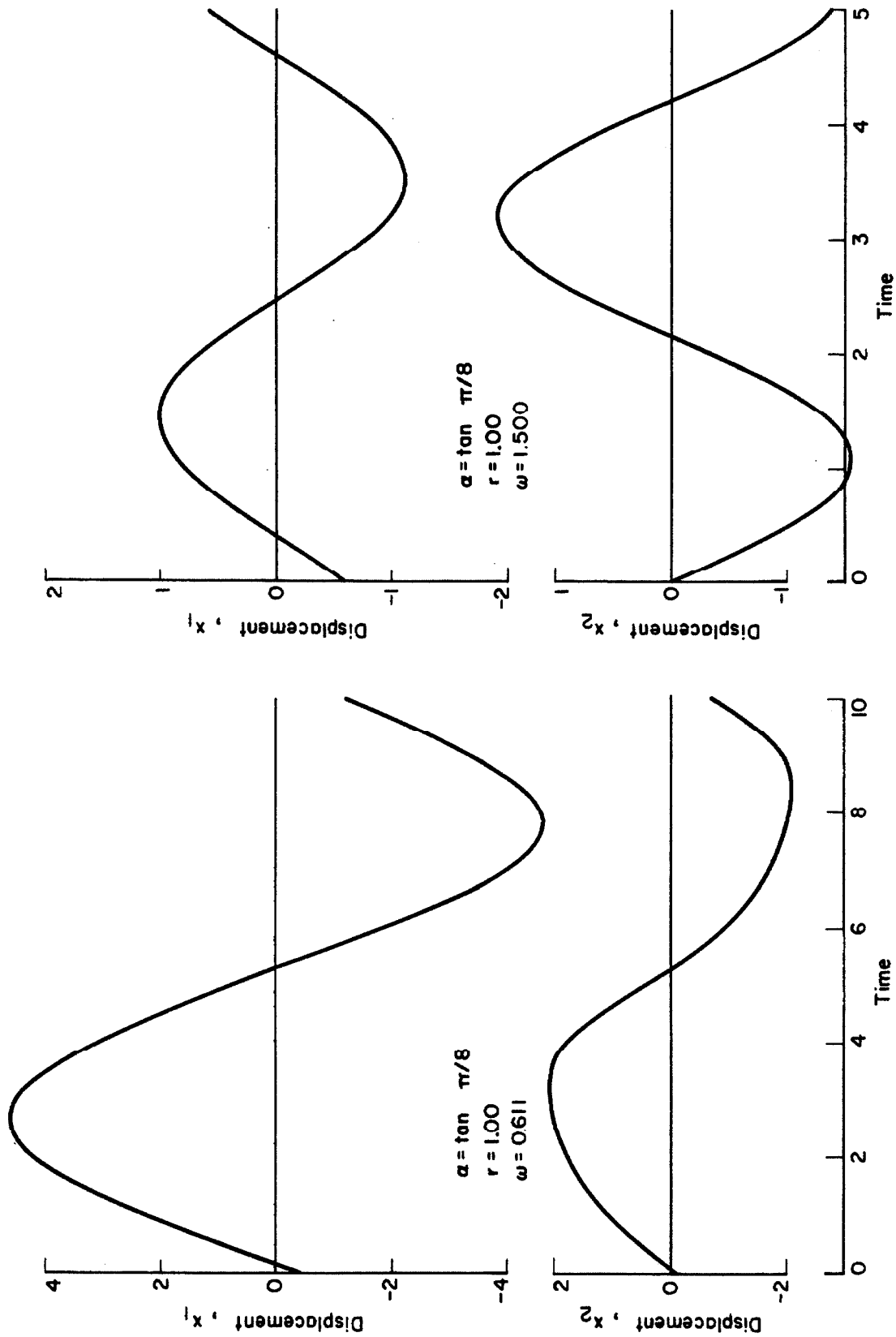

FIGURE 29. DISPLACEMENT WAVE FORMS

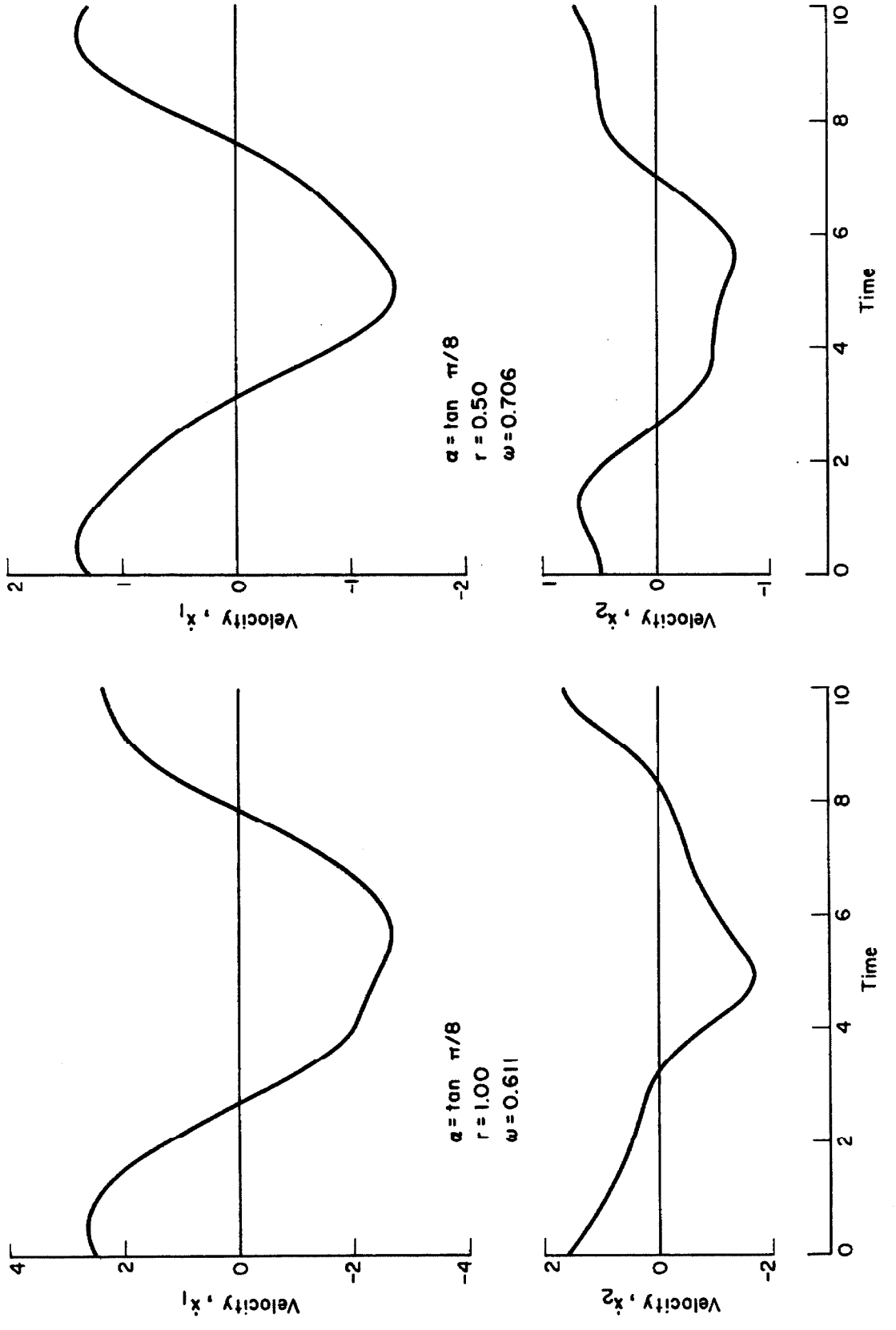

FIGURE 30. VELOCITY WAVE FORMS

IV. ELECTRIC ANALOG STUDIES OF THE ONE DEGREE OF FREEDOM SYSTEM

Introduction

All of the approaches thus far considered involve some degree of numerical calculation in order to obtain a steady state solution. Indeed, in some cases these calculations have tended to become so involved that they have obscured much of the real character of the solutions which they represent. It is therefore desirable to construct an analog capable of providing rapid cursory checks of analytic procedures while giving a feeling for the overall nature of the system response. Both electrical and mechanical analogs could be used but in general the electric analog provides greater flexibility and closer control of system parameters. Thus, the remainder of the present discussion will be limited to this type of analog.

In the case of piece-wise linear systems and specifically in the case of the bilinear hysteretic system, at least two general methods of electrical simulation have been employed. One method uses high speed switching circuitry to alternately activate separate linear sub-circuits corresponding to different system regimes while the other uses inherently nonlinear circuit elements whose characteristics may be utilized directly to generate the desired piece-wise linear function. The first method has been employed rather successfully by W. T. Thompson[8] to represent a bilinear hysteretic system subjected to a unidirectional force excitation. However, the overall complexity of this method makes it somewhat impractical when applied to the steady state problem. In this case the potential physical simplicity of the second method may be used to advantage.

T. K. Caughey[13] has generated the bilinear hysteretic function by means of a parallel network consisting of two oppositely biased conventional diodes and a capacitor. In this configuration the biased diodes act to limit the voltage which

may appear across the capacitor thereby causing a discontinuity in the slope of the charge-voltage characteristic of the network which is exactly analogous to the slope discontinuity of the restoring force in the mechanical system. Studies of the steady state response of the bilinear system using this network in conjunction with an electric differential analyzer gave results which agreed quite favorably with theoretical predictions over a fairly wide range of parameters.

The method used to simulate the bilinear hysteretic function in the present study is basically just a modification of the technique employed by Professor Caughey. However, in the present case use has been made of certain recent developments in the field of semiconductor devices which enable further simplification of the required circuitry along with improvement in the overall performance of the analog. This will now be discussed in some detail.

Function Generation for Systems Having Some Form of Coulomb Damping

As a semiconductor diode is more and more strongly reverse biased, a point is reached where the resulting electric field in the semiconductor is strong enough to pull electrons from the lattice structure of the material thereby causing a sudden onset of conduction. Once this conduction has begun, it increases rapidly with increased reverse bias giving rise to a sharp knee in the current-voltage characteristic of the diode. The transition between conduction and non-conduction is much more abrupt than that associated with the usual forward diode characteristic, and the resistance during conduction is extremely low. The voltage at which this so called Zener breakdown first occurs is strongly dependent on the impurity concentration or "doping" of the semiconductor and can be rather closely controlled.

In order to provide a limiting or clipping device, two of these Zener diodes having very nearly the same doping may be manufactured as a single unit in a back

to back or cathode to cathode configuration. These "Double-Anode" Zener Diodes have remarkably symmetric current-voltage characteristics with a general shape similar to that shown schematically in Fig. 31. It will be noted that except for an interchange of the coordinate axes, this characteristic is very nearly the same as the force-velocity relationship of a Coulomb damper. For this reason, the "Double-Anode" Zener Diode is an extremely useful tool in the electrical simulation of systems which can be realized physically by the introduction of Coulomb damping. The bilinear hysteretic system is such a system.

Idealized Analog Circuit for Bilinear Hysteresis

The mechanical model of Fig. 32 is an example of a physical system which has a bilinear hysteretic restoring force characteristic. Therefore, making use of this model and the Coulomb damping character of Fig. 31, it is a straight forward matter to construct an electrical analog which is governed by a differential equation of the desired form. The direct passive analog obtained in this way is shown in Fig. 33.

In order to understand the manner in which the hysteretic restoring force is generated, consider the voltage-charge characteristic of the portion of the circuit between points a and c. The operation of this portion of the circuit is best understood using Fig. 34 and can be explained as follows: For simplicity assume that the initial current and charge is zero in both branches of the circuit. Then, when a positive voltage e_{ac} is first applied and current begins to flow, the voltage e_{ab} across the Zener diode will be insufficient for conduction and the diode will act as an open circuit. Voltages therefore appear across the two capacitors in proportion to the time integral of the current in the loop and operation is in the range 0 to 1 of Fig. 34 where the voltage-charge characteristic has a slope

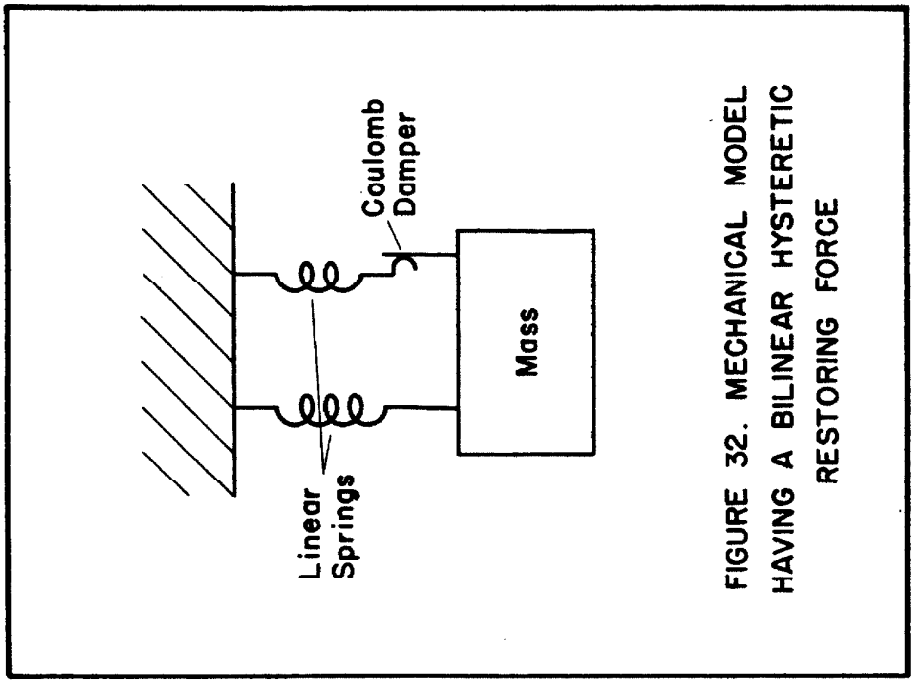

FIGURE 32. MECHANICAL MODEL HAVING A BILINEAR HYSTERETIC RESTORING FORCE

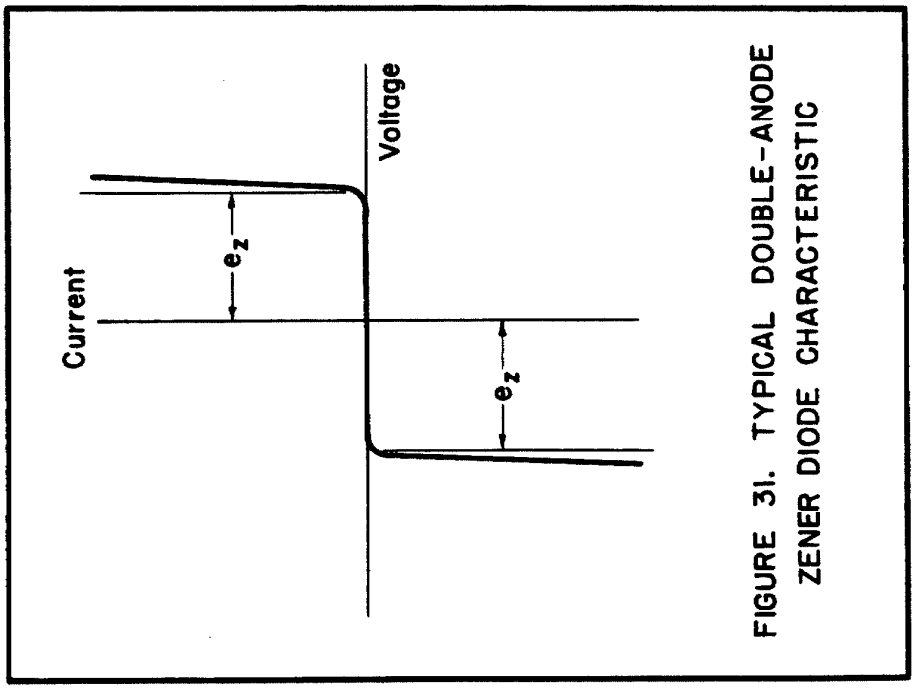

FIGURE 31. TYPICAL DOUBLE-ANODE ZENER DIODE CHARACTERISTIC

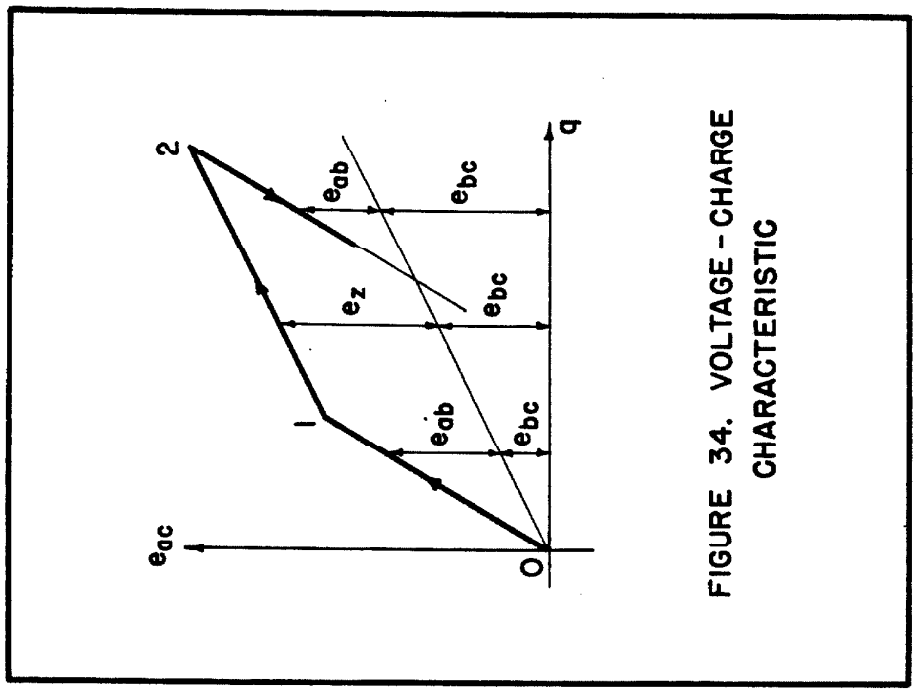

FIGURE 34. VOLTAGE - CHARGE CHARACTERISTIC

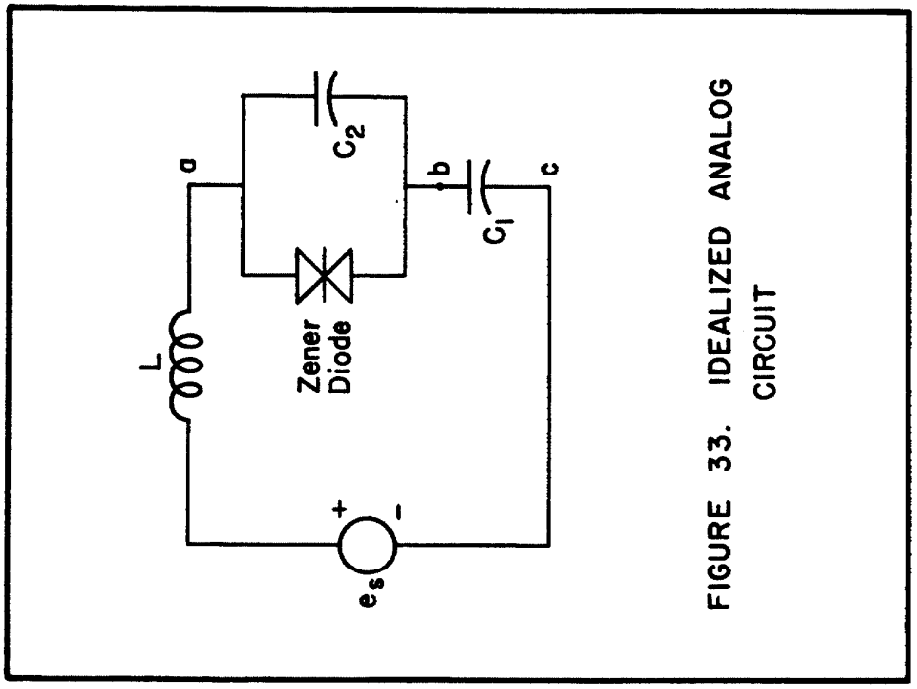

FIGURE 33. IDEALIZED ANALOG CIRCUIT

$1/C_0 = 1/C_1 + 1/C_2$. If the voltage e_{ac} becomes sufficiently large, the voltage e_{ab} across capacitor C_2 will reach the Zener breakdown voltage e_z, and the diode then acts as a short circuit device having a fixed voltage drop. Any further charge storage must therefore be accommodated by C_1 alone and the slope of the voltage-charge characteristic becomes $1/C_1$. As e_{ac} reaches the maximum denoted by point 2 in Fig. 34 and is then decreased, the current reverses direction and both C_1 and C_2 begin to discharge. But, as C_2 discharges, its voltage drops below the Zener voltage e_z, and the diode ceases to conduct. Thus, the voltage-charge characteristic will once again be determined by the series combination of C_1 and C_2, and the voltages e_{ab} and e_{bc} will again decrease in proportion to the charge until the current becomes zero or until e_{ab} equals $-e_z$ and the diode again conducts.

Since the circuit of Fig. 33 is a direct current-velocity analog, charge corresponds to displacement in the mechanical system and voltage corresponds to force. Thus, the voltage-charge characteristic of the circuit between points a and c is seen to be exactly analogus to the bilinear hysteretic restoring force characteristic of the mechanical model.

Equivalence of the Electrical and Mechanical Systems

The normalized differential equations describing the behavior of the system are equations (2.3a) and (2.3b). If the system is subjected to a sinusoidal force excitation of frequency ω and amplitude r these equations become;

$$\frac{d^2x}{dt^2} + x = r \sin\omega t - \left(\operatorname{sgn}\frac{dx}{dt}\right)(|x_m| - 1)(1-\alpha);\ (|x_m| - 2) < -\left(\operatorname{sgn}\frac{dx}{dt}\right)x < |x_m| \tag{4.1}$$

$$\frac{d^2x}{dt^2} + \alpha x = r \sin\omega t - \left(\operatorname{sgn}\frac{dx}{dt}\right)(1-\alpha) \quad ;\ -\left(\operatorname{sgn}\frac{dx}{dt}\right)x < (|x_m| - 2)$$

where the natural frequency for the limiting linear case is normalized to unity and α is the slope of the second linear regime of the restoring force characteristic. From Fig. 33, the electrical system equations which correspond to equations (4.1) are:

$$\frac{d^2q}{d\tau^2} + \frac{1}{LC_0} q = \frac{E_0}{L} \sin \omega_a \tau - (\operatorname{sgn} \frac{dq}{d\tau}) \left[\frac{q_m}{LC_0} \left(1 - \frac{C_0}{C_1}\right) - \frac{e_z}{L} \right]$$

$$\frac{d^2q}{d\tau^2} + \frac{1}{LC_1} q = \frac{E_0}{L} \sin \omega_a \tau - (\operatorname{sgn} \frac{dq}{d\tau}) \frac{e_z}{L} \qquad (4.2)$$

where in these equations q is the charge, C_0 is the series capacitance of C_1 and C_2, ω_a is the excitation frequency in the analog system and τ is the analog time. The two systems represented by equations (4.1) and (4.2) will be equivalent if the following relations are satisfied:

$$x = \frac{(1-\alpha)}{C_0 e_z} q \qquad (4.3a)$$

$$\alpha = C_0/C_1 = C_2/(C_1 + C_2) \qquad (4.3b)$$

$$\omega = \sqrt{LC_0}\, \omega_a = \omega_a/\omega_0 \qquad (4.3c)$$

$$r = \frac{E_0}{e_z}(1-\alpha). \qquad (4.3d)$$

If α is greater than zero, C_1 will be finite and the simplest means of measuring the charge q is to measure the voltage drop e_{bc} across C_1. Then,

$$x = \frac{(1-\alpha)}{\alpha} \frac{e_{bc}}{e_z} .$$

However, in the limiting case of elasto-plastic behavior, α approaches zero which requires that C_1 become infinite (assuming a finite C_0 and thereby finite x and ω). Therefore, direct measurement of q is impossible in this case and special

circuit techniques must be employed.

Practical Circuit Considerations

In the above idealized treatment of the analog circuit all parasitic elements and the effects which they cause have been neglected. However, in practice such elements certainly exist and their presence must be reckoned with. In general, there are two ways of doing this; 1) an estimate of the effect of the parasitic elements may be incorporated into a correction factor which is applied to the results of actual measurements, or 2) an attempt may be made to directly compensate for the effect of such elements within the analog itself. Where feasible, the second of these approaches is felt to be the best and is the one used in the present work.

Fig. 35 shows the analog circuit with major parasitic elements included; these are the resistive impedance of the source R_S, the series resistance of the inductor R_L, and the equivalent series resistance of the diode R_Z. As all of these elements are resistive in nature, it would appear possible to eliminate their effect by simply introducing an equivalent negative resistance at some convenient point in the circuit. Basically, this is correct but certain other steps must also be taken. Since in normal operation the diode conducts during only a portion of each cycle, its series resistance R_Z is likewise in the circuit for only a portion of each cycle. The total main loop resistance is therefore a discontinuous function of time and cannot be accurately approximated by any single negative impedance device. This problem can be overcome by introducing a resistance R_C in series with the capacitor C_2 where R_C is equal to R_Z over the desired range of operation. Then, either R_Z or R_C will be in the circuit at any given time and a negative impedance device may be used which has an effective resistance $-R = -(R_S + R_L + R_Z)$. The negative resistance device used in the present study consists of a resistance shunting the

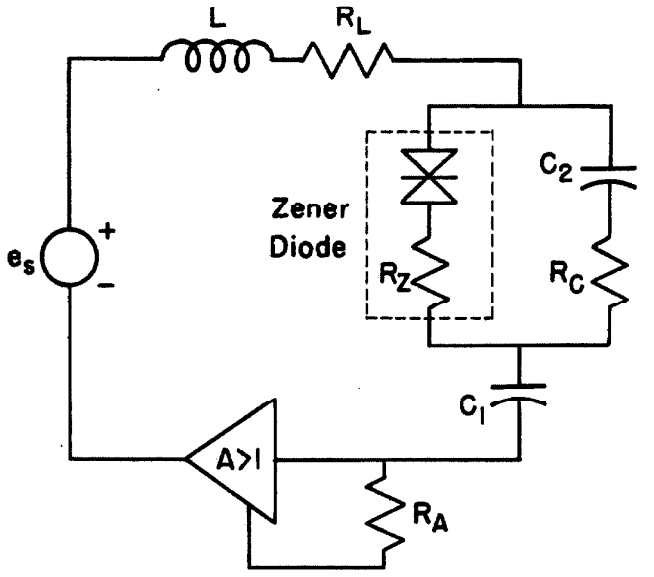

FIGURE 35. ACTUAL ANALOG CIRCUIT

input of a greater than unity gain "floating" amplifier as shown schematically in Fig. 35.

A parasitic element which has been ignored in the above discussion is the internal shunt resistance of the two capacitors C_1 and C_2. For good polystyrene capacitors, this resistance will generally be of the order of 1×10^8 ohms as compared with a nominal operating impedance of $5 - 6 \times 10^3$ ohms for the capacitors. Thus, any effects due purely to the existence of an additional current path in the circuit should be quite small. The time constant for such capacitors will be approximately 1 - 10 seconds which is sufficiently long that steady state operation in the 200-600 cps range should not be significantly affected by capacitor self-discharge. However, for transient operation the effect of discharge may become significant as the length of time for which information is desired approaches the time constant of the capacitors. This fact should be kept in mind when establishing the duration of any transient measurements.

Discussion of Results —— Fundamental Frequency Range

The measured response of the analog circuit to inputs of varying frequency and amplitude is shown in Figs. 36 and 37 along with the corresponding exact solutions obtained by numerical techniques. It is seen that over the range of variables considered, the agreement is quite good. The only noticeable difference between the analog and exact solutions occurs for values of response which are only slightly larger than unity. This is to be expected, however, since it is in this range that the Zener diode is operating near the knee of its current-voltage characteristic where the effects of rounding may be significant.

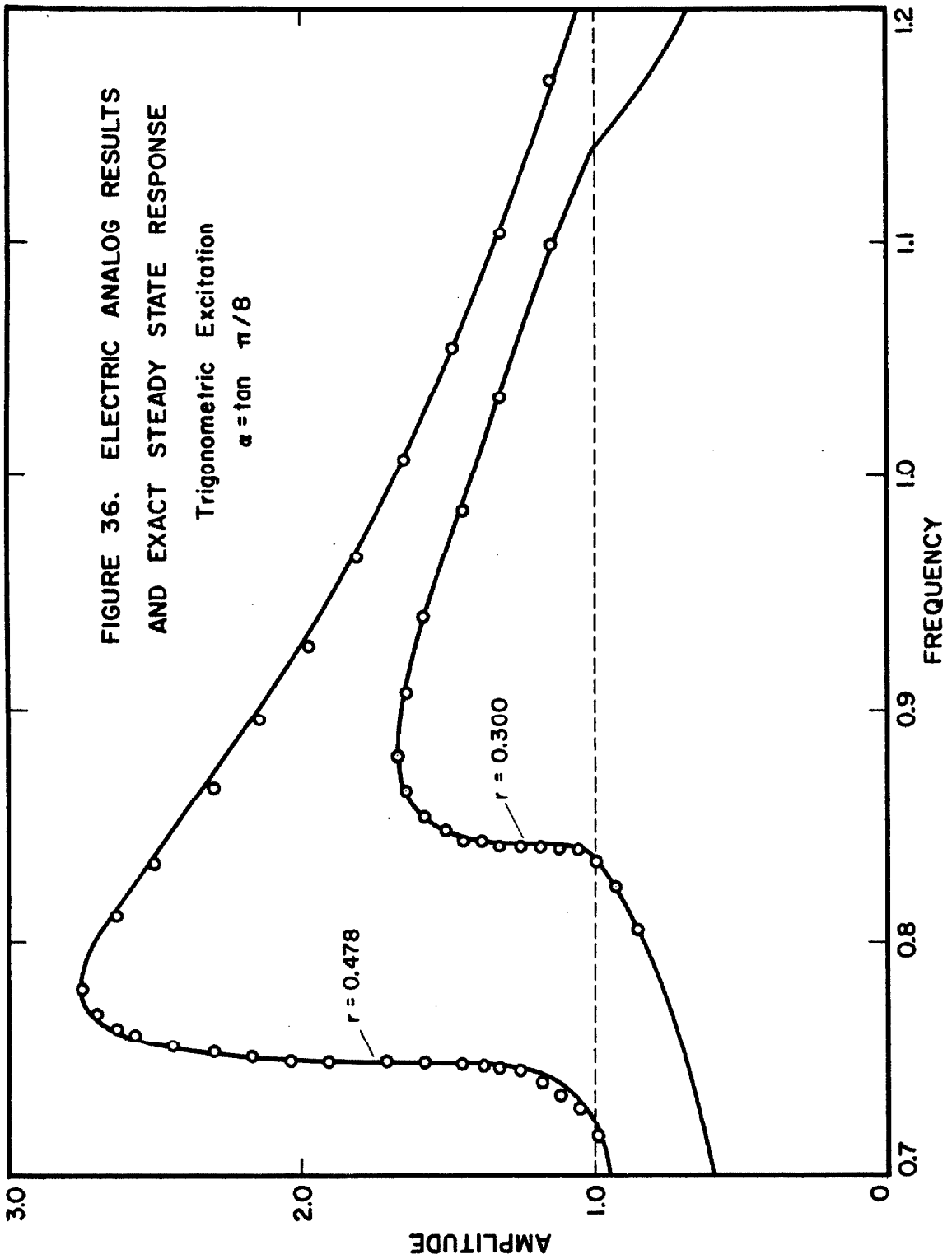
FIGURE 36. ELECTRIC ANALOG RESULTS
AND EXACT STEADY STATE RESPONSE
Trigonometric Excitation
α = tan π/8
r = 0.478
r = 0.300
AMPLITUDE
FREQUENCY
3.0
2.0
1.0
0
0.7
0.8
0.9
1.0
1.1
1.2

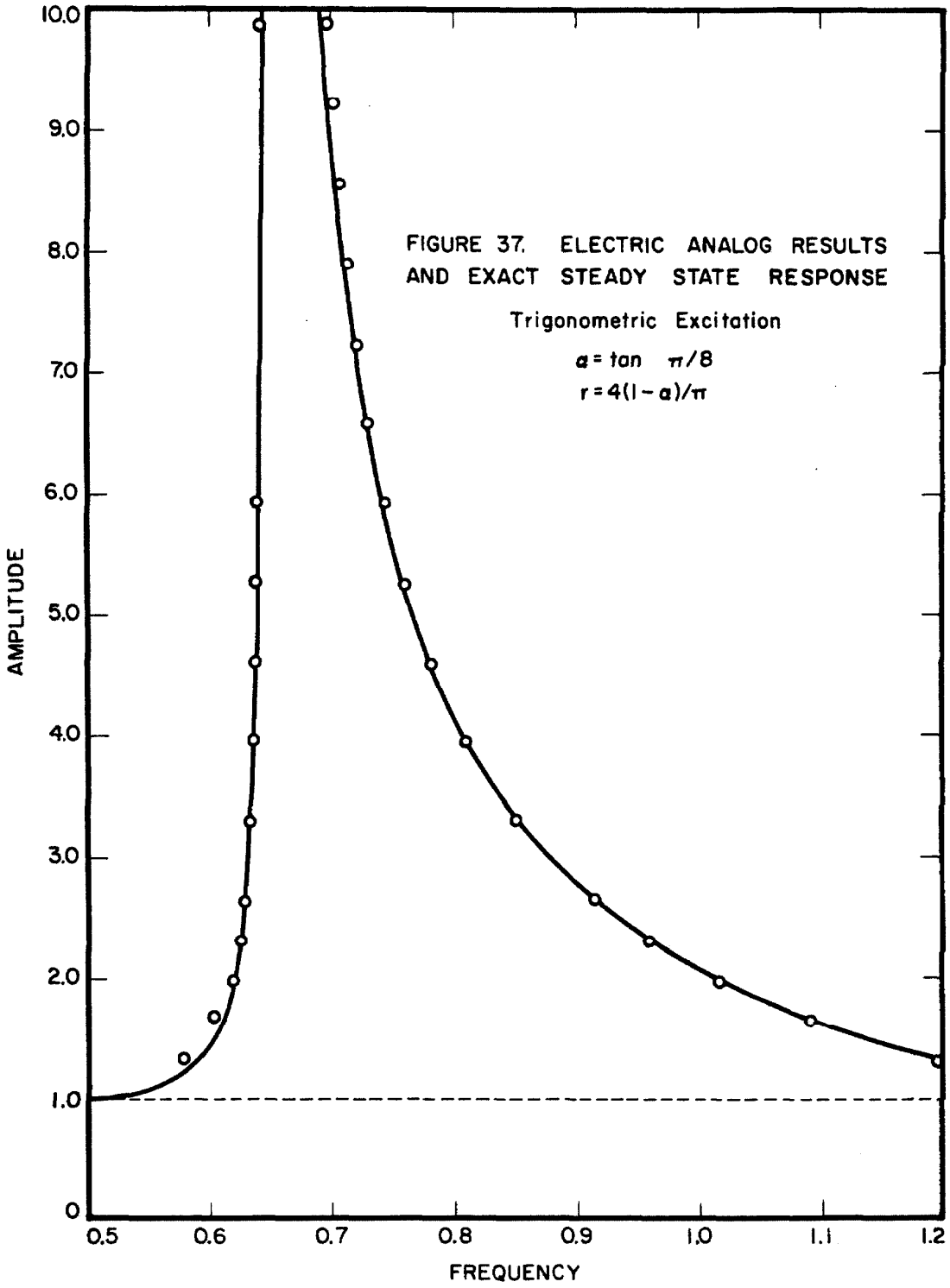

FIGURE 37. ELECTRIC ANALOG RESULTS AND EXACT STEADY STATE RESPONSE

Trigonometric Excitation

$\alpha = \tan \pi/8$

$r = 4(1-\alpha)/\pi$

Ultraharmonic Response

The existence of ultraharmonic behavior in the bilinear hysteretic system was discussed in a previous section of this thesis. However, due to the analytic complexity of the problem no information was obtained regarding the detailed character of this behavior. It is now possible to complete this earlier discussion and to show the nature of the ultraharmonic response by means of the electric analog described above.

Fig. 38 shows a family of response curves where the frequency range and amplitude of excitation have been chosen so as to allow for the appearance of ultraharmonic response peaks. Due to low frequency limitations on the physical circuitry, only ultraharmonic response peaks of order 3, 5, and 7 are shown. However, this does not in any way indicate that ultraharmonics of higher order do not also exist.

It is noted from the figure that the ultraharmonic response peaks clearly exhibit a tendency to lean towards lower frequencies as is typical of soft systems in general and the bilinear hysteretic system in particular. However, it is not possible on the basis of these results to either confirm of deny the existence of a locus of vertical tangency for the ultraharmonic peaks.

Fig. 39 is a reproduction of oscilloscope records showing the displacement as a function of time and the hysteretic restoring force as a function of displacement for frequencies at or near the ultraharmonic response peaks. The presence of the relevant ultraharmonic is clearly visible in the displacement and leads to the successive doubling back exhibited in the hysteresis loop. As mentioned earlier, this doubling back along certain segments of the hysteresis loop is one of the primary causes of difficulty in treating ultraharmonic behavior by means of any exact or approximate analytic techniques.

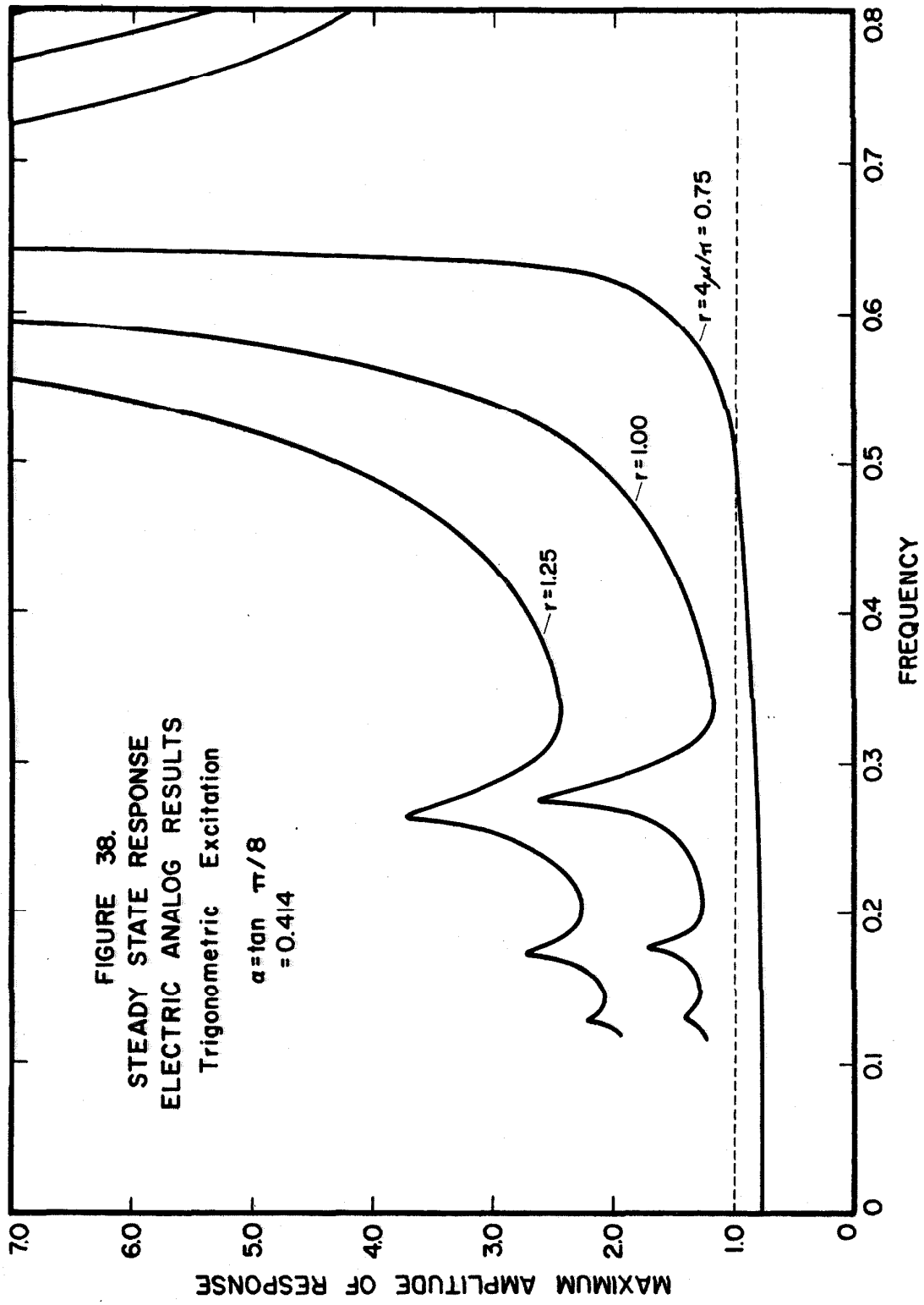

FIGURE 38.
STEADY STATE RESPONSE
ELECTRIC ANALOG RESULTS
Trigonometric Excitation
$\alpha = \tan \pi/8 = 0.414$

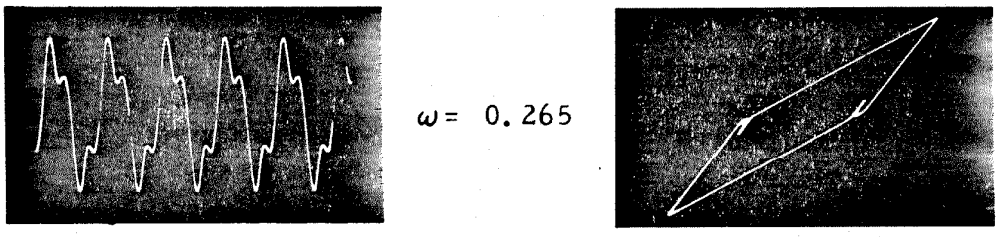

(a) Ultraharmonic of Order Three

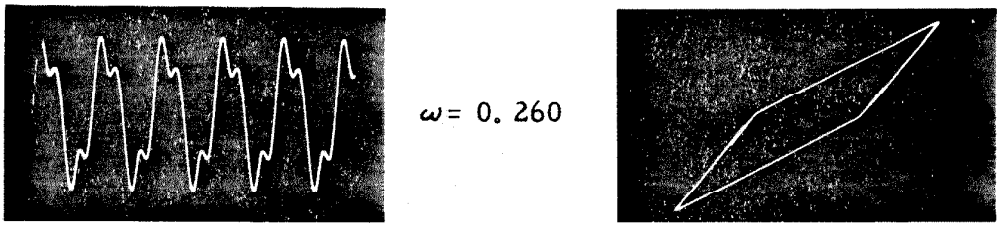

(b) Ultraharmonic of Order Three

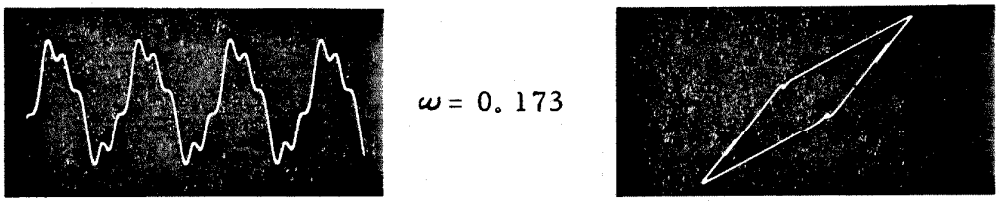

(c) Ultraharmonic of Order Five

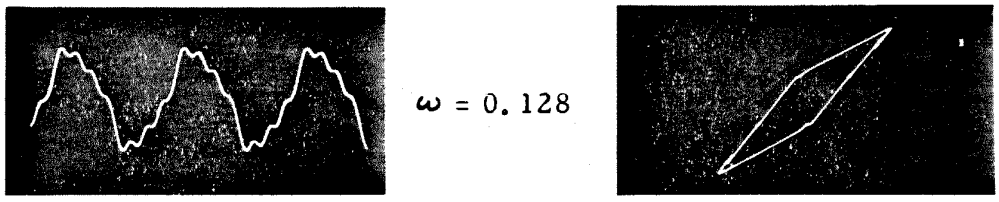

(d) Ultraharmonic of Order Seven

Figure 39. Displacement Wave Forms and Hysteresis Loop Configurations in Regions of Ultraharmonic Response.

$\alpha = \tan \pi/8$, $r = 1.25$

V. SUMMARY AND CONCLUSIONS

On the basis of the present investigation it has been possible to make certain observations and conclusions about the dynamic response of one and two degree of freedom bilinear hysteretic systems. These observations and conclusions are summarized in the following paragraphs.

One Degree of Freedom System

From the exact steady state solutions for square wave and trigonometric excitation it is concluded that the one degree of freedom system exhibits a typical soft type resonance with the peak response moving to a lower frequency as the level of excitation is increased. All of the response curves are apparently single valued but their general shape is noticeably asymmetric having a very steep slope on the low-frequency side of the peak response. For amplitudes of excitation greater than or equal to $(1-\alpha)$ in the case of square wave excitation and $4(1-\alpha)/\pi$ in the case of trigonometric excitation, the system displays unbounded resonance which first occurs at a frequency of $\omega = \sqrt{\alpha}$. An examination of the steady state displacement wave forms for trigonometric excitation shows that these are very nearly sinusoidal with a harmonic content in general less than 4%.

Approximate theories based on either the method of equivalent linearization or the method of slowly varying parameters prove quite adequate in predicting the steady state system response to trigonometric excitation even for relatively small values of α*. Both of these theories indicate the existence of an unbounded resonant solution with finite excitation and both indicate the existence of a single

---

* $\alpha = 0$ corresponds to the limiting case of elasto-plastic behavior.

point of vertical tangency on the low-frequency side of each response peak. The method of slowly varying parameters further indicates that the system is stable or marginally stable for all frequencies of excitation.

If viscous damping is introduced into the system the steady state response curves lose much of their asymmetric character and become more like those for a linear damped system. Application of the method of slowly varying parameters in this case indicates that the peak response remains finite for all finite levels of excitation, that there are no loci of vertical tangency, and that the system is stable for all frequencies of excitation.

Electric analog studies of the system without viscous damping show the existence of ultraharmonic response peaks under certain conditions of excitation. These peaks appear to have much the same character as the harmonic peaks described earlier but the nature of the analog method precludes detailed examination of such features as loci of vertical tangency.

For transient excitation of finite duration where at least one maxima of the displacement* occurs after the excitation has ceased, it has been shown that there will be no resultant permanent offset if $\alpha \geq 1/2$; i.e. the final motion of the system will be oscillatory with zero average displacement. This conclusion is particularly applicable when the system response is due primarily to resonance effects as in short duration shock and pulse excitation or low level random excitation.

---

* A "maxima of the displacement" is defined as any displacement x satisfying the conditions

$$\dot{x} = 0, \quad |x| > 1$$
$$|f(x, 0)| = \alpha |x| + (1 - \alpha).$$

Two Degree of Freedom System

In the case of the two degree of freedom system an approximate analysis by the method of slowly varying parameters gives modified soft type response curves which are single valued within the range of the investigation but which are definitely asymmetric and have very steep slopes on the low-frequency sides of each peak. Associated with the steep sloped portions of the response curves are at least four loci of vertical tangency occuring in such a way that there is one locus corresponding each peak of the two system displacements. There are two critical levels of excitation above which the system will exhibit unbounded amplitude and phase resonance. For the normalized system these critical excitation levels are $r = 4(1-\alpha)(\sqrt{5}-1)/2\pi$ for unbounded resonance of the low-frequency response peaks and $r = 4(1-\alpha)(3\sqrt{5}+7)/2\pi$ for a similar behavior of the high-frequency peaks. The stability of the system has been examined only in certain limiting cases but in each of these the steady state motion was found to be stable or marginally stable.

No exact steady state response solution is available for the two degree of freedom system but the equations of motion can be integrated numerically for specific cases in order to provide a spot check of the approximate theory. In the case of $\alpha = \tan \pi/8$, examination of the true steady state displacement wave forms obtained in this way indicates that the harmonic content is quite low (1-3%) for amplitudes only slightly greater than unity but may become significant ($\sim$8%) for moderately large amplitudes*. Similarly, the steady state amplitude

---

* For very large displacement amplitudes the system approaches linearity and the harmonic content thereby approaches zero.

of response as predicted by the approximate theory is in very close agreement with the numerical results for low amplitudes and disagrees somewhat only for moderately large amplitude solutions. Strictly speaking, the approximate theory can be considered accurate only for the nearly linear cases of $\alpha \approx 1$. However, on the basis of the present analysis it is concluded that the theory will actually give quite good results over a fairly wide range of α if interested is restricted to lower displacement amplitudes as α is decreased.

VI. REFERENCES

1. Jacobsen, L.S. "On a General Method of Solving Second Order Ordinary Differential Equations by Phase-Plane Displacements", Journal of Applied Mechanics, vol. 19, No. 4, (1952) pp. 543-553.

2. Jacobsen, L.S. and Ayre, R.S. Engineering Vibrations McGraw-Hill Book Company, Inc., New York, N.Y., (1958).

3. Jacobsen, L.S. "Dynamic Behavior of Simplified Structures up to the Point of Collapse", Symposium on Earthquake and Blast Effects on Structures (1952) pp. 112-113.

4. Goodman, L.E. and Klumpp, J.H. "Analysis of Slip Damping With Reference to Turbine-Blade Vibration", Journal of Applied Mechanics, vol. 23, Trans. ASME, vol. 78, (1956), pp. 421-429.

5. Goodman, L.E. and Klumpp, J.H. "Analysis of Slip Damping With Reference to Turbine-Blade Vibration", WADC Technical note 55-232, (June 1955).

6. Tanabashi, R. "Studies on the Non-Linear Vibrations of Structures Subjected to Destructive Earthquakes", World Conference on Earthquake Engineering, (1956).

7. Tanabashi, R. "Nonlinear Transient Vibration of Structures", Second World Conference on Earthquake Engineering, (1960)

8. Thompson, W.T. "Analog Computer for Nonlinear System With Hysteresis", Journal of Applied Mechanics, vol. 24, Trans. ASME, vol. 79, (1957) pp. 245-247.

9. Ruzicka, J.E. "Forced Vibrations in Systems with Elastically Supported Dampers", MSc. Thesis, Massechusetts Institute of Technology, (1957).

10. Berg, G.V. "The Analysis of Structural Response to Earthquake Forces", Report of the Industry Program of the College of Engineering, University of Michigan, Ann Arbor, (1958).

11. Kobori, T. and Minai, R. "Study on Unstationary Vibration of Building Structure with Plastic Deformation of Substructure", Second World Conference on Earthquake Engineering, (1960).

12. Ando, N. "Nonlinear Vibrations of Building Structures", Second World Conference on Earthquake Engineering, (1960).

~~13~~ 14. Caughey, T.K. "Sinusoidal Excitation of a System With Bilinear Hysteresis", Journal of Applied Mechanics, vol. 27, No. 4, (1960), pp. 640-643.

15 ~~14~~. Caughey, T.K. "Forced Oscillations of a Semi-Infinite Rod Exhibiting Weak Bilinear Hysteresis", Journal of Applied Mechanics, vol. 27, No. 4, (1960), pp. 644-648.

16 ~~15~~. Caughey, T.K. "Random Excitation of a System With Bilinear Hysteresis", Journal of Applied Mechanics, vol. 27, No. 4, (1960), pp. 649-652.

out ~~16. Minorsky, N. Non-Linear Mechanics, J.W. Edwards, Ann Arbor, Mich.,~~ (1947).

17. Caughey, T.K. "The Existence and Stability of Periodic Motions in Forced Non-Linear Oscillations", Ph.D. Thesis, California Institute of Technology, (1954), pp. 8-10.

out 18. Standard Mathematical Tables, Chemical Rubber Publishing Co., Cleveland, Ohio, (1954), p. 320.

19. Hildebrand, F.B. Introduction to Numerical Analysis, McGraw-Hill Book Company, Inc., (1956), pp. 236-239.